Kidney Tumor

1

Maria Tretiakova and Sean R. Williamson

Evaluating a Renal Epithelial Tumor in a Biopsy Specimen

In many institutions, renal mass biopsy is used conservatively, since most renal neoplasms will be treated with partial or radical nephrectomy. However, renal mass biopsy is often undertaken when the results may influence clinical management. Some goals of renal mass biopsy include distinguishing primary renal cell neoplasms from other tumors that would necessitate different treatment, particularly metastases, lymphoma, urothelial carcinoma, or rare variants (medullary, collecting duct, or sarcomatoid carcinomas). Secondly, subclassification and grading of primary renal epithelial neoplasms may lead to differences in management. For example, elderly patients with multiple comorbidities may be candidates for surveillance or ablation of nonaggressive tumor subtypes.

- Benign tumor types that can be recognized by biopsy include oncocytoma and angiomyolipoma, among other rarer entities (metanephric adenoma, mixed epithelial and stromal tumor).
- Lower-risk primary renal epithelial tumors include oncocytic neoplasms (possible or definite oncocytomas) and chromophobe renal cell carcinoma (RCC; particularly eosinophilic variant).
- Of note, some pathologists are unwilling to diagnose oncocytoma in a biopsy sample, instead giving a diagnosis of "oncocytic neoplasm" or "oncocytic tumor" with a comment that the features would be compatible with oncocytoma if representative of the entire tumor (since distinguishing eosinophilic chromophobe from oncocytoma remains challenging).

Table 1.1 shows clues to well-differentiated "clear cell tumors" in renal mass biopsy, and Table 1.2 shows high-grade carcinomas in renal mass biopsy (see also Fig. 1.1).

References: [1–9].

Effectively Sampling a Renal Mass in a Resection Specimen

Sampling a renal mass and determining the pathologic stage are among the most critical steps to determine patient prognosis. RCCs often invade structures (renal sinus or veins) with subtle, finger-like outpouchings that are relatively easy to miss if the individual performing gross examination is not familiar with the usual growth patterns of tumors, especially clear cell RCC.

- The renal sinus is the central fat compartment that surrounds the hilar structures (renal pelvis, arteries, and veins).
- With increasing tumor size, the likelihood of clear cell RCC invading the renal sinus increases dramatically, to the point that >90% of tumors over 7 cm invade the renal sinus (Fig. 1.2a), making pT2 clear cell RCC rare.
- For tumors larger than 4–5 cm, the likelihood of renal sinus invasion increases to over 50%. Histologic assessment of the entire tumor-sinus interface should be strongly considered.
- Any deviation from a well-circumscribed, spherical tumor shape should be viewed with great suspicion for extension into a vein branch or tributary (Fig. 1.2b).
- Changes to the 2016 American Joint Commission on Cancer (AJCC) staging system include removal of the requirements that vein invasion be recognized grossly and that the vein wall contain muscle microscopically.

M. Tretiakova (✉)
Department of Pathology, University of Washington, Seattle, WA, USA
e-mail: mariast@uw.edu

S. R. Williamson
Department of Pathology, Cleveland Clinic, Cleveland, OH, USA

X. J. Yang, M. Zhou (eds.), *Practical Genitourinary Pathology*, Practical Anatomic Pathology,
https://doi.org/10.1007/978-3-030-57141-2_1

Table 1.1 Clues to well-differentiated "clear cell tumors" in renal mass biopsy

	Frequency in adult renal tumors	Clues	Helpful immunohistochemistry
Clear cell RCC	>50–60%	Solid, nested, alveolar growth patterns; often purely clear cytoplasm (less often vacuolated; Fig. 1.1a–d)	PAX8 positive, carbonic anhydrase IX diffuse membrane positive, cytokeratin 7 and high molecular weight cytokeratin usually focal/limited, alpha-methylacyl-CoA racemase (AMACR) variable
Papillary RCC with clear cell change	15% (overall incidence, of which up to 39% may have clear cell change)	Vacuolated cytoplasm, foamy macrophages, hemosiderin	AMACR diffuse/strong, cytokeratin 7 positive in type 1 tumors, carbonic anhydrase IX negative or minimal (except with necrosis/ischemia)
Clear cell papillary RCC	3–4%	Branched glandular configuration, nuclear alignment	PAX8 positive, carbonic anhydrase IX "cup-shaped" pattern, cytokeratin 7 diffuse, high molecular weight cytokeratin frequently positive, GATA3 frequently positive, CD10 negative, AMACR negative/minimal
Adrenal rest/adrenal-renal fusion	Rare	Vacuolated cytoplasm	PAX8 negative, inhibin positive, Melan-A positive
Hemangioblastoma	Rare	Solid, foamy cytoplasm, lack of glandular structures	Inhibin positive, neuron-specific enolase (NSE) positive, S100 positive, keratin negative (note: PAX8 may be unexpectedly positive in primary renal hemangioblastoma)
Hemangioma	Rare, increased incidence in end-stage renal disease	No epithelial component, often requiring immunohistochemical verification; anastomosing subtype often contains hematopoiesis and hyaline globules	CD31/CD34/ERG positive; keratin, carbonic anhydrase IX, PAX8 negative

Table 1.2 High-grade carcinomas in renal mass biopsy

	Helpful immunohistochemistry	Notes
High-grade clear cell RCC (Fig. 1.1e)	PAX8 positive, carbonic anhydrase IX positive (usually maintained in high-grade tumors), cytokeratin 7 usually minimal/negative	PAX8 and GATA3 are not always perfect for distinguishing RCC from urothelial carcinoma in the upper urinary tract
Urothelial carcinoma	GATA3 positive, p63 positive, high molecular weight cytokeratin positive	PAX8 and GATA3 are not always perfect for distinguishing RCC from urothelial carcinoma in the upper urinary tract
Metastatic carcinoma of another origin	Organ-specific markers (TTF1, etc.)	Lung cancer is among the more common metastases to the kidney and may mimic a primary tumor
Medullary carcinoma	OCT3/4 often positive, INI-1 loss	Sickle cell trait essentially a requirement (without sickle trait = "RCC unclassified with medullary phenotype")
Fumarate hydratase (FH)-deficient RCC	Abnormal negative FH immunohistochemistry, positive 2-succino-cysteine	If germline, hereditary leiomyomatosis and RCC (HLRCC) syndrome; or FH-deficient if unknown germline status
Collecting duct carcinoma	PAX8 positive	Diagnosis of exclusion if medullary and FH-deficient carcinoma excluded

- Invasion of the renal pelvis has been added as a route to pT3a for RCC in the AJCC system.
- Invasion of the perinephric fat is less common than renal sinus or vein branch invasion in RCC, but qualifies for pT3a.
- In modern practice, surgeons usually attempt to spare the adrenal gland; however, pathologic assessment of adrenal involvement, when present, should aim to discern direct invasion (pT4) from metastatic involvement (pM1).
- Gerota fascia involvement (pT4) is quite rare but usually occurs in the context of RCC extending to the soft tissue surface of a radical nephrectomy, in conjunction with clinical/intraoperative impression of Gerota fascia involvement.
- RCC tumors can extend into the main renal vein and rarely follow the inferior vena cava (pT3b–pT3c) to the level of the heart.
- RCC tumor may be protruding from the vein margin; however, consensus among urologic pathologists is

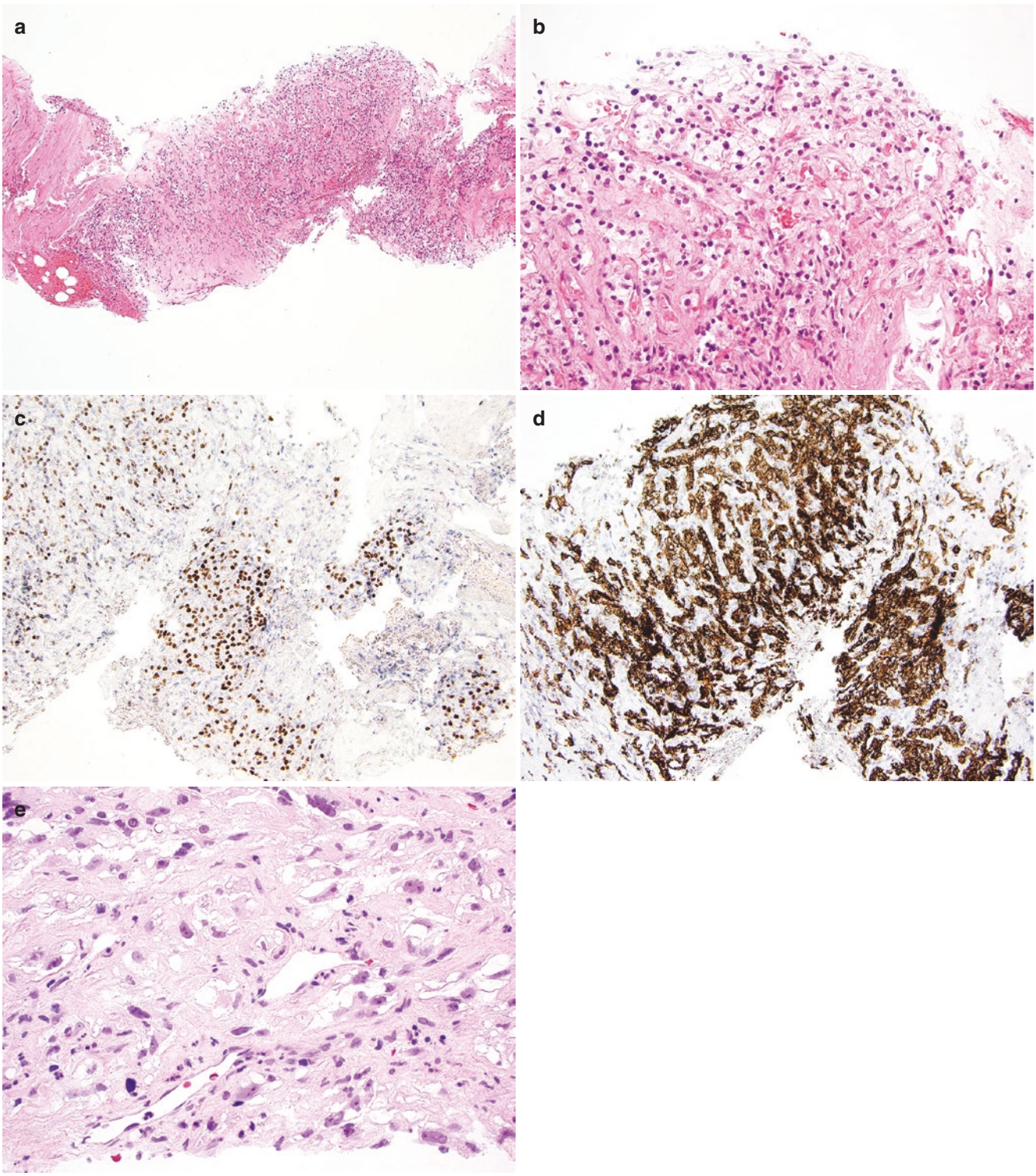

Fig. 1.1 (**a**) Clear cell renal cell carcinoma in renal mass biopsy is composed of fibrosis and bland epithelial cells. (**b**) Higher magnification demonstrates cells with clear cytoplasm. (**c**) Positive PAX8 immunohistochemistry supports a primary renal cell neoplasm and argues against an adrenal rest or non-renal lesion. (**d**) Diffuse membrane staining for carbonic anhydrase IX supports clear cell subtype. (**e**) A different case of high-grade clear cell renal cell carcinoma in renal mass biopsy shows clusters of cells with clear cytoplasm in fibrous stroma with marked nuclear atypia

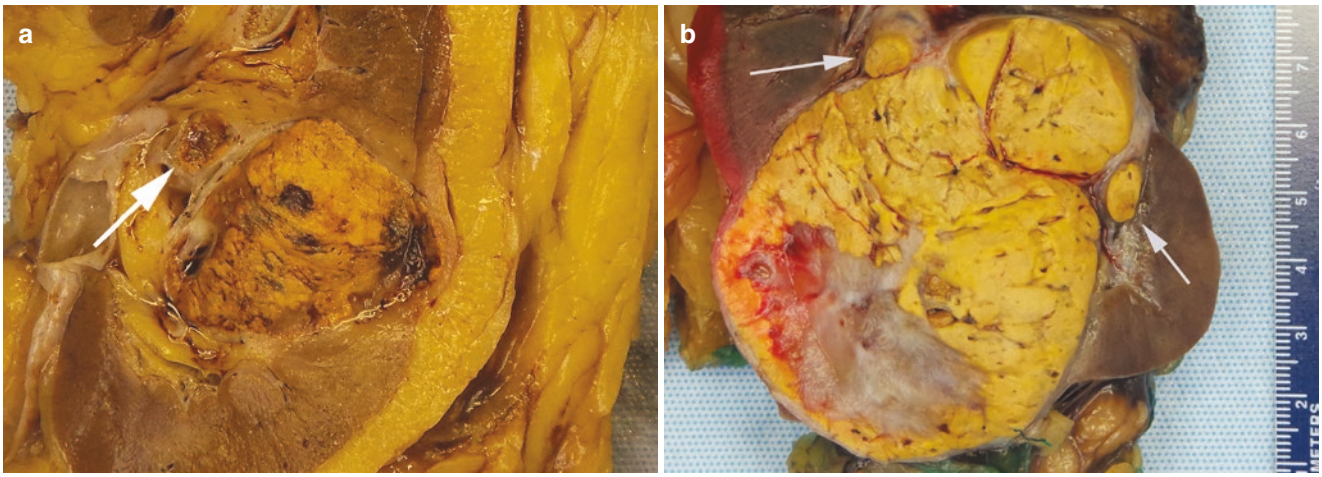

Fig. 1.2 (**a**) This clear cell renal cell carcinoma abuts the renal sinus (the fatty compartment containing the renal pelvis and vasculature) with an outpouching (arrow), concerning for renal sinus invasion. (**b**) This clear cell renal cell carcinoma has multiple outpouchings (arrows) that likely represent extension of the tumor into renal vein branches, which would qualify for pT3a

that this only constitutes a positive margin if the tumor is confirmed histologically to be adherent to or invading the vein wall at the margin (as the surgeon would not have necessarily transected tumor when freely mobile).

- Separately submitted vena cava "thrombus" should be examined histologically (at least 2–3 sections) to evaluate for adherent/invaded vein wall, which defines pT3c.
- In some cases (5–8%), RCC extending into the main renal vein subsequently spreads backwards into tributary veins, creating multiple nodules in the kidney (retrograde venous invasion). This can be misinterpreted as multiple tumors or a multinodular tumor by those unfamiliar with the phenomenon.

Table 1.3 shows recommended sampling of renal epithelial tumor specimens.

References: [10–16].

Table 1.3 Recommended sampling of renal epithelial tumor specimens

Normal kidney	1–2 sections away from the tumor, if possible
Hilar margins	1 or more cassettes containing: Artery, vein*, and ureter margins (there may be more than one artery or vein) *Vein with tumor can be sampled by trimming the vein wall circumferentially (if freely mobile from the tumor) or cutting a complete cross section of vein containing tumor (to assess for microscopic adherence)
Tumor to renal sinus	2–3 sections routinely; consider entire interface if tumor is larger than 4–5 cm
Tumor to perinephric fat	1–2 sections routinely; more if gross impression of invasion
Secondary tumors	International Society of Urological Pathology (ISUP) guidelines recommend measuring and sampling at least the 5 largest tumors
Other	Any finger-like outpouching of the tumor, to assess for possible vein branch invasion

What Are the Typical Gross Features of Renal Tumors?

Gross examination is an important part of the pathology of renal tumors for two major reasons: (1) Staging of RCC, as discussed in question 1.2, and (2) differential diagnosis of renal neoplasms. In general, RCC tumors and other renal neoplasms are predominantly spherical, and deviation from this round shape should be viewed with caution for invasion of structures, as discussed previously. Tumors can bulge well beyond the contour of the normal kidney, markedly distorting its shape, which does not necessarily indicate invasion. Gross "necrosis" should be confirmed histologically to be coagulative tumor necrosis, as large zones of hemorrhage and fibrosis are relatively common and do not have the same prognostic implications as true necrosis. The significance of necrosis in papillary RCC is less clear, perhaps due to an increased tendency of the fragile papillary structures to undergo necrosis.

Table 1.4 shows gross features of renal neoplasms (see also Fig. 1.3).

References: [10, 14, 17–24].

Table 1.4 Gross features of renal neoplasms

	Classic gross appearance	Variations	Notes
Clear cell RCC	Golden-yellow to orange, heterogeneous (Fig. 1.3a)	White or tan (fibrotic areas or sarcomatoid dedifferentiation), red-brown (hemorrhage), cystic	Sampling of any golden-yellow areas may be helpful to verify a low-grade clear cell component for poorly differentiated tumors
Papillary RCC	Variable, tan, yellow, or red-brown	Yellow (with abundant foamy cells), red-brown (with abundant hemosiderin)	A granular cut surface can sometimes be appreciated as a clue to the papillary architecture; necrosis is common
Chromophobe RCC	Pale tan	Red-brown resembling oncocytoma for eosinophilic variant	Can have central scar resembling oncocytoma
Clear cell papillary RCC	Tan-white, fibrous, solid and cystic		Usually does not have golden-yellow/orange cut surface of clear cell RCC, despite histologic similarity
Oncocytoma	Red-brown ("mahogany"; Fig. 1.3b)	Rarely microcystic with hemorrhage ("telangiectatic" oncocytoma)	Often unencapsulated or poorly encapsulated; can involve veins or fat, which has not been reported to alter its benign behavior
Angiomyolipoma	Tan-white/fibrous (if myoid predominant), resembling a smooth muscle neoplasm	Resembles normal fat or lipomatous tumor (if fat predominant)	Surgical specimens tend to be myoid predominant, since those containing fat can be recognized by imaging and removed only if there is concern for large size or rupture
Tubulocystic RCC	"Bubble wrap" appearance with uniform cystic cut surface		
Multilocular cystic renal neoplasm of low malignant potential	Entirely cystic architecture with fluid-filled cysts (no grossly visible solid areas)		Formerly known as multilocular cystic RCC; tumors with a visible solid component should be classified as extensively cystic clear cell RCC

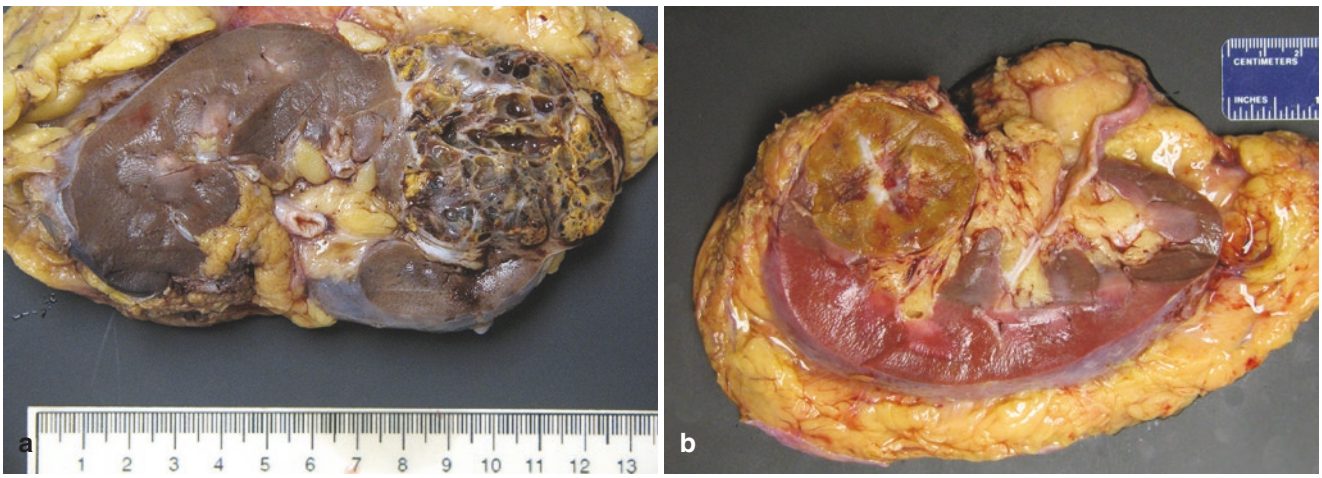

Fig. 1.3 (**a**) This clear cell renal cell carcinoma is solid and cystic with a heterogeneous red-brown to golden-yellow cut surface. (**b**) This oncocytoma is a uniform tan-brown color with a central scar, which is classic but not specific for oncocytoma

What Are the Key Histologic Features for Common Renal Epithelial Tumors?

Most renal tumors can either be diagnosed based on histologic features alone, or a narrow differential diagnosis can be readily discerned based on the tumor histology.

Table 1.5 shows key histologic features of common renal epithelial tumors (see also Fig. 1.4).

References: [17, 21].

What Are the Key Features of Cystic Renal Tumors?

Most renal tumors have the potential to be at least partly cystic; however, tumors that are most commonly cystic include clear cell RCC, multilocular cystic renal neoplasm of low malignant potential (formerly multilocular cystic RCC), clear cell papillary RCC, and tubulocystic RCC. In general, a cystic component is thought to be favorable for

Table 1.5 Key histologic features of common renal epithelial tumors

	Histology	Pitfalls	Notes
Clear cell RCC	Cells with clear cytoplasm arranged in nests, tubules, or alveolar structures	Eosinophilic cytoplasm (Fig. 1.4a) and/or marked pleomorphism are not unusual in high-grade tumors	Thorough sampling for straightforward low-grade component is helpful for high-grade or eosinophilic cases
Papillary RCC, type 1	Basophilic cuboidal cells lining papillary, tubular, or solid structures	Cytoplasmic clearing is not uncommon (at least focally; Fig. 1.4b), but is usually highly vacuolated rather than entirely clear	Foamy macrophages, psammoma bodies are helpful ancillary clues in cases with less evident papillary architecture
Papillary RCC, type 2	Eosinophilic cells with elongated, pseudostratified nuclei (Fig. 1.4c)	Eosinophilic cells alone are not sufficient for classification as type 2	In modern practice, it has become a relative diagnosis of exclusion after FH-deficient RCC/HLRCC syndrome and other RCC types are excluded
Chromophobe RCC	Cells with pale cytoplasm, prominent cell borders, variable nuclear size, wrinkled nuclear contours; some cells appear to have no nuclei (due to sectioning artifact; Fig. 1.4d)	Eosinophilic variant can closely resemble oncocytoma (Fig. 1.4e); clues include perinuclear clearing, trabecular architecture	Immunohistochemistry may be needed to distinguish difficult cases of eosinophilic variant
Oncocytoma	Granular eosinophilic cytoplasm, round/uniform nuclei, occasional nuclei with smudged degenerative chromatin, nested/solid/tubular architecture (Fig. 1.4f), central scar	Succinate dehydrogenase (SDH)-deficient RCC can have monotonous eosinophilic cell morphology that mimics oncocytoma	
Clear cell papillary RCC	Tubular, cystic, papillary architecture with branched glandular structures, small papillae into cystic spaces, alignment of nuclei at the same height within the cytoplasm (Fig. 1.4g)	Some areas closely resemble clear cell RCC (immunohistochemistry often required); papillary component is not always prominent	Immunohistochemistry often needed for confirmation

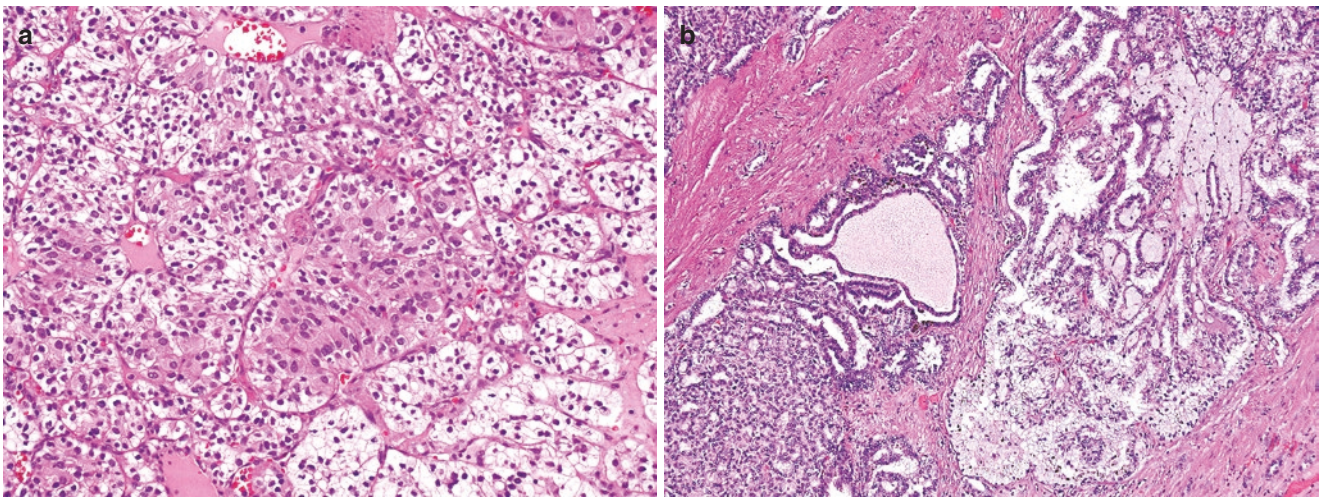

Fig. 1.4 (**a**) Clear cell renal cell carcinoma can have substantial areas with eosinophilic cells, shown in this case with abrupt transition from clear cells to eosinophilic cells. (**b**) Papillary renal cell carcinoma, type 1, is characteristically composed of papillary structures lined by basophilic cells (left) but can also have substantial clear cell changes, often caused by vacuolated cytoplasm (right). (**c**) Papillary renal cell carcinoma, type 2, exhibits elongated nuclei with pseudostratification and eosinophilic cytoplasm. (**d**) Classic chromophobe renal cell carcinoma exhibits prominent cell borders and low nuclear-cytoplasmic ratio with some cells appearing to have no nucleus (due to sectioning artifact). (**e**) Eosinophilic chromophobe renal cell carcinoma remains difficult to distinguish from oncocytoma. However, clues can include prominent trabecular architecture and perinuclear clearing. This case also contains cystic spaces with pigment. (**f**) Oncocytoma is characteristically composed of uniform eosinophilic cells with round, regular nuclei. Although large areas may appear solid, often discrete round nests are present in areas of edematous stroma. (**g**) Clear cell papillary renal cell carcinoma exhibits branched glandular structures with variable amounts of clear cytoplasm. Often, the nuclei appear to be aligned at the same height within the cytoplasm

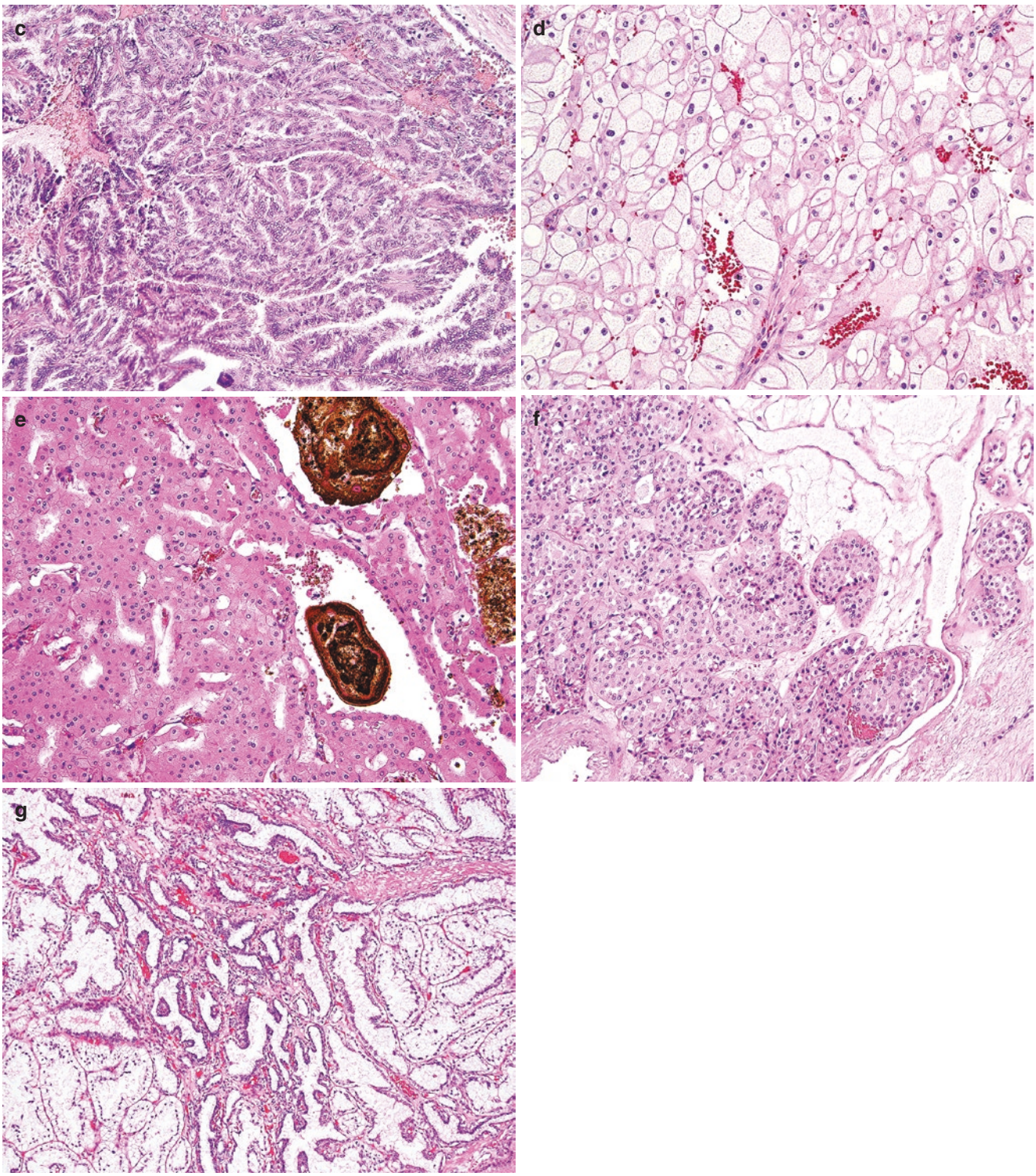

Fig. 1.4 (continued)

clear cell RCC, even if the tumor does not meet the strict definition for a multilocular cystic tumor. Most tumors have a mixture of cystic and tubular architecture throughout the neoplasm; however, rarer variations that have been described include predominant central cystic necrosis or degeneration, leaving only a rim of viable neoplasm around a central cavity, and a single solid tumor growing in the wall of a cyst.

Table 1.6 shows key features of cystic renal tumors (see also Fig. 1.5).

References: [4, 25–31].

Table 1.6 Key features of cystic renal tumors

	Histology	Components	Immunohistochemistry	Genetics
Clear cell RCC	Cells with clear cytoplasm	Solid, tubular, cystic (no true papillary structures except non-cohesive areas)	Carbonic anhydrase IX positive, cytokeratin 7 focal/limited	*VHL* mutation, 3p25 deletion
Multilocular cystic renal neoplasm	Cells with clear cytoplasm, small clusters of cells within septa	Exclusively cystic (no solid component; Fig. 1.5a); papillary structures favor clear cell papillary RCC	Carbonic anhydrase IX positive, cytokeratin 7 often substantial, CD10 positive	*VHL* mutation, 3p25 deletion, possibly lower rates than conventional clear cell
Clear cell papillary RCC	Cells with clear cytoplasm, nuclei aligned above the basement membrane, branched glandular structures, small or complex papillae in cystic spaces	Tubular/glandular, cystic, solid, papillary (Fig. 1.5b)	Carbonic anhydrase IX positive (cup shaped), cytokeratin 7 diffuse, CD10 negative (except cysts), high molecular weight cytokeratin often positive, GATA3 often positive, AMACR negative/minimal	Negative for *VHL* mutation or 3p25 loss, no consistent copy number abnormalities
Mixed epithelial and stromal tumor	Variable epithelium, most commonly cuboidal cells, spindle cell stroma	Cystic and solid (variable percentages)	Common estrogen and progesterone receptor positivity, positivity for CD34, WT1, smooth muscle actin, or desmin; minimal or negative carbonic anhydrase IX	
Tubulocystic RCC	Eosinophilic cells with prominent nucleoli lining tubular and cystic spaces with fibrous stroma (Fig. 1.5c)	Tubular and cystic	AMACR positive, cytokeratin 7 negative or focal, carbonic anhydrase IX negative or focal	Usually lacking trisomy 7/17 (contrast to papillary RCC), if pure

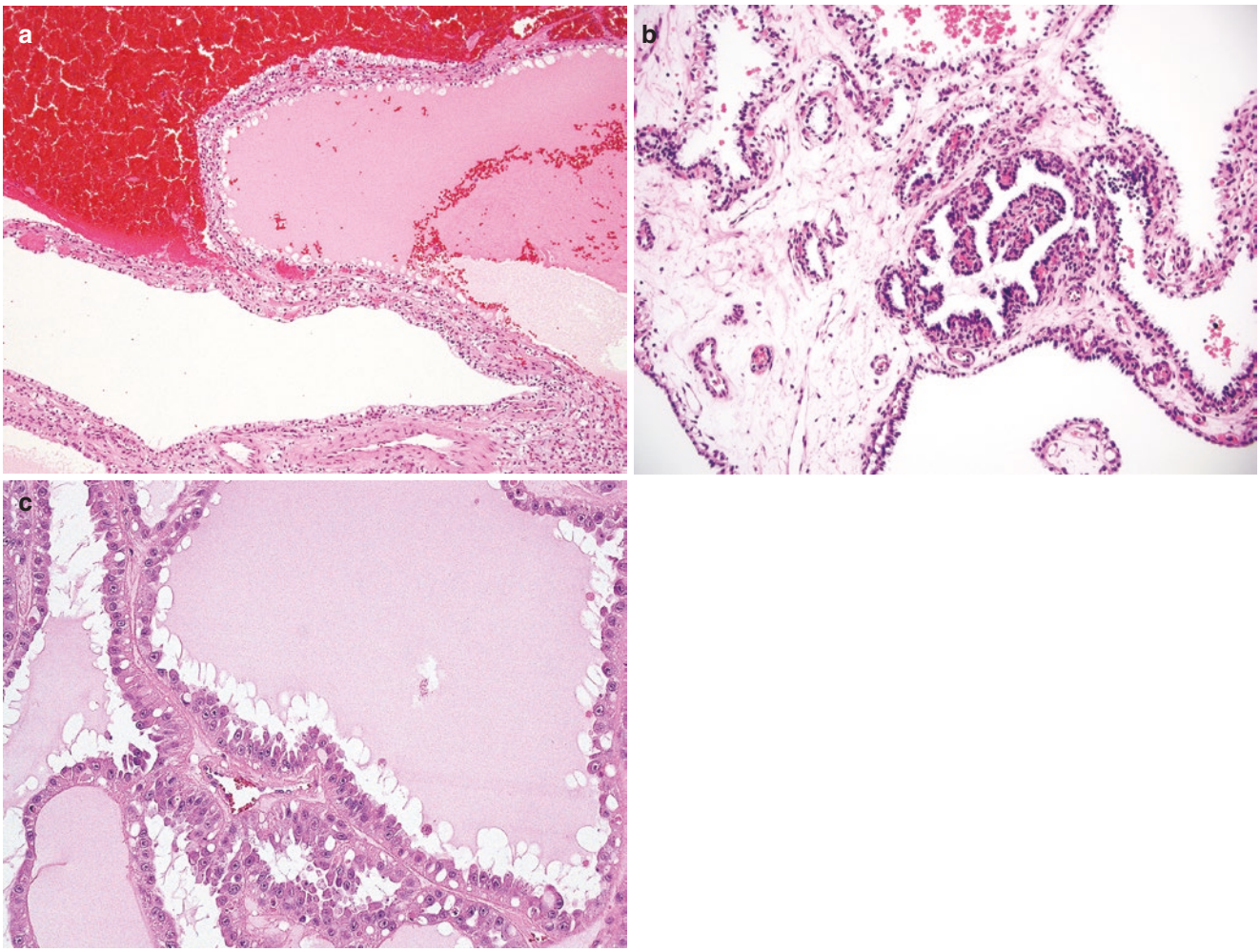

Fig. 1.5 (**a**) Multilocular cystic renal neoplasm of low malignant potential is composed entirely of cysts lined by cells with clear cytoplasm. The septa can contain small clusters of tumor cells, but there should be no mass-forming solid component. (**b**) Clear cell papillary renal cell carcinoma can have an extensive cystic component, resembling multilocular cystic neoplasms; however, the presence of papillary structures or branched glands within the stroma favors clear cell papillary renal cell carcinoma. (**c**) Tubulocystic renal cell carcinoma is composed of eosinophilic, hobnail-shaped cells with prominent nucleoli lining cystic and tubular spaces. The nuclear grade is usually equivalent to ISUP/WHO grade 3

What Are the Commonly Used Immunohistochemical Markers in Differentiating Renal Tumors?

Immunohistochemistry can be helpful in resolving differential diagnoses of renal tumors; however, it is important to take immunohistochemical (IHC) markers in the context of the histologic appearance and to know their limitations, as very few are highly specific in isolation. Predominant results are described in Table 1.7, with some notable exceptions or caveats as follows:

- Carbonic anhydrase IX is a robust marker of clear cell RCC, showing diffuse membranous staining in most cases (Fig. 1.6a). However, since carbonic anhydrase IX is part of the hypoxia pathway, many tumors and tissues can have some positivity in areas of ischemia or necrosis. In large tissue sections with abundant viable tumor cells, this typically does not account for more than focal positivity (Fig. 1.6b), but interpretation should be approached with caution for small biopsies with limited viable cells.
- Specificity of carbonic anhydrase IX is also lower in the context of unknown primary cancer, as many non-renal cancers can have positivity.
- Diffuse strong intensity for AMACR is characteristic of papillary RCC (Fig. 1.6c); however, many other tumors can have some degree of positivity. A very strong positive reaction (similar to normal proximal renal tubules) is supportive of papillary RCC but should be taken in the context of the other findings.
- In chromophobe RCC vs. oncocytoma, the classic expectation is that chromophobe will exhibit diffuse membranous cytokeratin 7 reactivity. However, this is most reliable only in tumors with classic (pale cell) features.
- In oncocytoma, a pattern of only scattered rare cells positive for cytokeratin 7 is expected (Fig. 1.6d).
- A cutoff for an amount of cytokeratin 7 positivity that warrants a diagnosis of eosinophilic chromophobe is not well agreed upon, but the amount of positivity can be much more limited than that of classic chromophobe.
- Positivity for cytokeratin 7 is most consistent in type 1 papillary RCC. In type 2 papillary RCC or tumors with eosinophilic features, reactivity for cytokeratin 7 is often focal or absent.
- TFE3 and TFEB protein immunohistochemistry may be helpful for raising suspicion for translocation-associated RCC (if strong); however, weak reactivity is less specific for gene rearrangement and often is better confirmed with molecular studies.

References: [4, 21, 29, 32–36].

What Are the Useful Molecular Tests in Diagnosis of Renal Epithelial Tumors?

Classification of renal cell neoplasms has evolved over the years based on integration of tumor histology with immunohistochemistry and genetics; however, fortunately in current practice, classification can still be achieved without using routine genetic assays, rather by relying on immunohistochemical and histologic surrogates of existing genetic knowledge. Still, several molecular techniques can be helpful in select instances, ranging from mutation analysis to copy number studies to fluorescence in situ hybridization (FISH).

Table 1.8 shows helpful molecular markers for renal tumor diagnosis (see also Fig. 1.7).

References: [17, 21, 37–49].

Table 1.7 Most widely used immunohistochemical markers for differential diagnosis of renal tumors

	Carbonic anhydrase IX	AMACR	Cytokeratin 7	KIT (CD117)	High molecular weight cytokeratin	GATA3	Vimentin	Melanocytic	Cathepsin-K
Clear cell RCC	+++	+/−	−/+	−	−/+	−	+/−	−	−
Papillary RCC, type 1	−/+	+++	+++	−	+/−		+/−	−	−
Papillary RCC, eosinophilic or type 2	−/+	+++	−/+	−			+/−	−	−
Chromophobe RCC, classic	−/+	+/−	+++	+		+/−	−	−	−
Chromophobe RCC, eosinophilic	−/+	+/−	+/−	+			−	−	−
Oncocytoma	−/+	+/−	−/+*	+		−/+	−	−	−
Clear cell papillary RCC	+++	−	+++		+	+/−	+	−	−
Translocation RCC (*TFE3* or *TFEB*)	−/+	+/−	−/+	−		−	−/+	+/−	+/−

Note: +++ = consistent diffuse strong positive, + = positive, +/− = may be positive but not consistent, −/+ = usually negative but can be rarely or focally positive, − = negative, * = only rare scattered cells positive

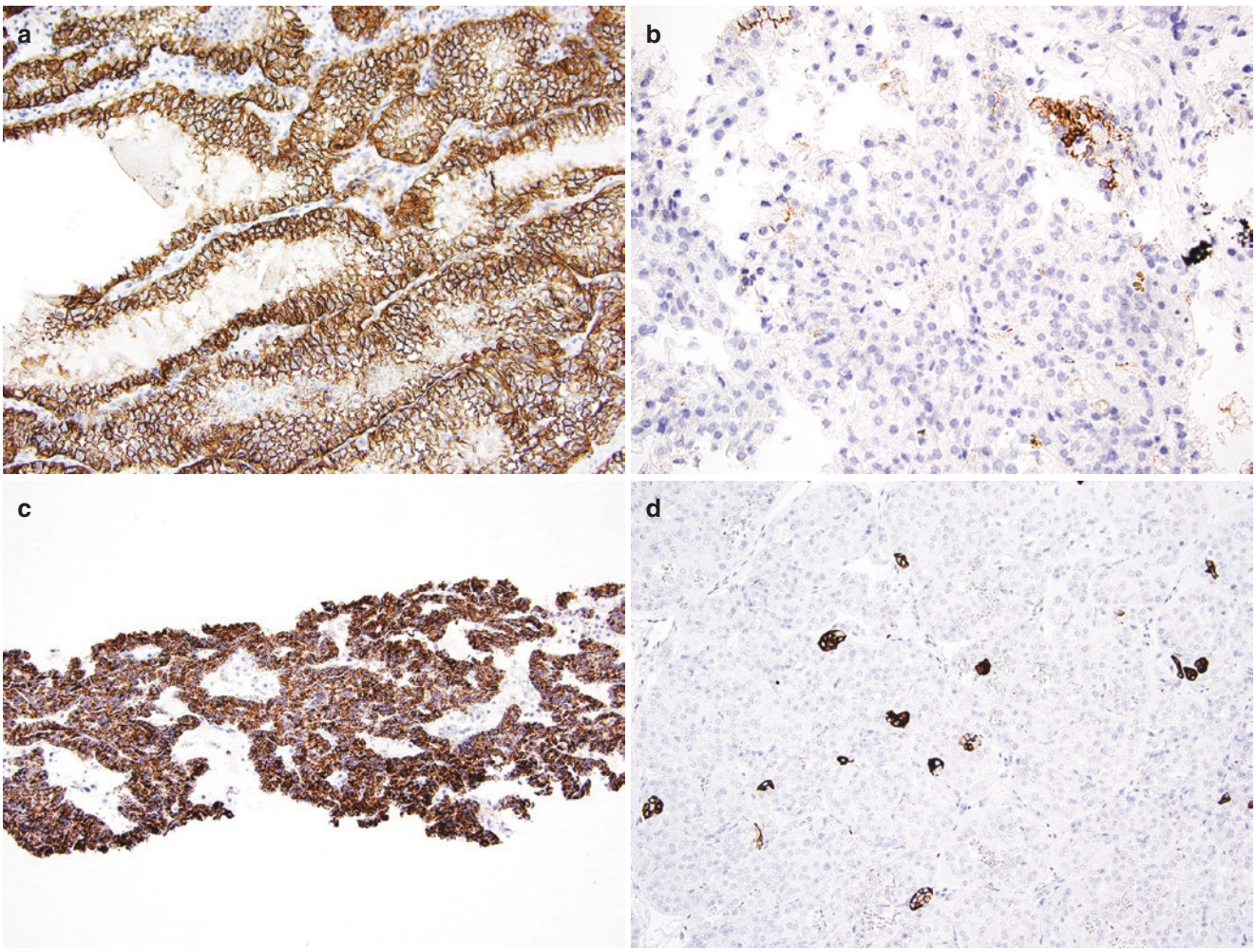

Fig. 1.6 (**a**) Clear cell renal cell carcinoma characteristically exhibits diffuse membrane positivity for carbonic anhydrase IX. (**b**) In contrast to clear cell cancer, other subtypes of renal cell carcinoma may exhibit focal nonspecific staining for carbonic anhydrase IX, which should not be interpreted as favoring clear cell subtype. (**c**) Diffuse strong staining for alpha-methylacyl-CoA racemase (AMACR) similar to that of the proximal renal tubules is supportive of papillary renal cell carcinoma in the appropriate context, although other renal cell neoplasms may exhibit some degree of positivity. (**d**) Oncocytoma characteristically exhibits a pattern of scattered cells positive for cytokeratin 7, usually not accounting for more than a few percent of tumor cells

Table 1.8 Helpful molecular markers for renal tumor diagnosis

	Tumor type	Comments
VHL mutation	Clear cell RCC	Over 50% of clear cell RCCs have mutation; however, other mechanisms of inactivation occur, including promoter hypermethylation and chromosome arm loss. Therefore, absence of mutation does not exclude a clear cell RCC
3p25 FISH	Clear cell RCC	Many clear cell RCCs have a copy loss of the chromosome 3p arm, which contains *VHL* and several other genes now known to be frequently altered in clear cell RCC (*PBRM1, SETD2, BAP1*). The specificity is less clear, however, as other reports have occasionally described 3p loss in non-clear-cell tumors. When combined with other mechanisms of *VHL* inactivation, over 90% of tumors have an alteration of *VHL*/3p25
Trisomy 7/17; loss of Y	Papillary RCC	Trisomy of chromosomes 7 and/or 17 is common in type 1 papillary RCC; however, the specificity of these alterations is less clear, as they have been reported in other neoplasms
TFE3/*TFEB* studies	Translocation RCC	Molecular studies to evaluate the *TFE3* and/or *TFEB* genes are helpful in confirming a diagnosis of translocation-associated RCC. The most common assay is break-apart FISH, which often can detect rearrangement (Fig. 1.7). However, a few recent fusions have been noted to result in a chromosomal inversion with a subtle, potentially false-negative FISH result (notably *NONO-TFE*3 and *RBM10-TFE3* fusions). Next-generation sequencing studies or real-time polymerase chain reaction (RT-PCR) may be alternate methods to detect these gene fusions; however, these are less widely available. Recently, a subset of aggressive RCCs has been found to have amplification of 6p21 including *TFEB*, which can be detected by FISH or other copy number analyses

Table 1.8 (continued)

	Tumor type	Comments
FH studies	FH-deficient RCC/HLRCC syndrome	The simplest way to detect alterations of *FH* is immunohistochemistry for the FH protein. An abnormal result is loss (negative staining of the tumor cells with positive internal control of normal tissues). However, a subset of neoplasms exhibits a normal staining pattern even in the presence of confirmed mutation. Therefore, routine histopathology with immunohistochemistry and recommendation for genetic counseling may be necessary to capture all patients with the HLRCC syndrome. FH-deficient is used for tumors that are abnormal for FH in the absence of known germline mutation
Copy number analysis	Other RCC types	Other RCC types sometimes have recurrent copy number changes that can be detected by copy number analyses, such as FISH, comparative genomic hybridization (CGH), or single nucleotide polymorphism (SNP) array. For example, mucinous tubular and spindle cell carcinoma has some overlapping features with papillary RCC; however, it has been shown to have multiple chromosomal losses involving chromosomes 1, 4, 6, 8, 9, 13, 14, 15, and 22 rather than 7/17 gain. For oncocytoma vs. chromophobe RCC, the latter tends to have multiple losses involving chromosomes 1, 2, 6, 10, 13, 17, and 21, in contrast to loss of chromosome 1 only or 11q rearrangement in oncocytoma
CCND1 rearrangement	Oncocytoma	Recent data have shown that a subset of oncocytomas has rearrangement of *CCND1* (cyclin D1). The precise role for using this knowledge for diagnosis remains incompletely understood; however, it appears that tumors with immunohistochemical positivity tend to be those with rearrangement (although incompletely specific), whereas those with negative immunohistochemistry are usually not rearranged

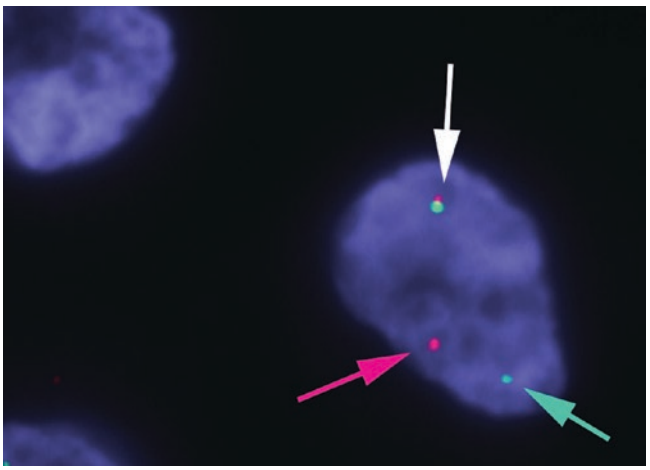

Fig. 1.7 Break-apart fluorescence in situ hybridization (FISH) for the *TFEB* gene in this case of *TFEB* rearranged renal cell carcinoma shows one normal signal result (white arrow). The other copy of the 6p21 region shows a split signal pattern (red and green signals and arrows)

Accurate Grading of Renal Cell Carcinoma in Small Tissue Biopsy and Nephrectomy Specimens

- The original Fuhrman grading system for renal cell carcinoma relied on several parameters to assign grade, including nuclear size, nuclear irregularity, and nucleolar prominence.
- Based on the difficulty of assessing multiple nuclear parameters at once, combined with data supporting nucleolar prominence as the key parameter, the 2013 ISUP Vancouver Consensus and 2016 WHO Classification recommend a modified grading system that relies primarily on the nucleolar prominence (Table 1.9, Fig. 1.8).

Table 1.9 ISUP/WHO grading of RCC

ISUP/WHO RCC grading	Features
1	Nucleoli inconspicuous or absent at 400x magnification (40x objective)
2	Nucleoli conspicuous/eosinophilic at 400x magnification (40x objective) but not at 100x magnification (10x objective)
3	Nucleoli conspicuous/eosinophilic at 100x magnification (10x objective; Fig. 1.8)
4	Extreme nuclear pleomorphism, tumor giant cells, or sarcomatoid/rhabdoid features

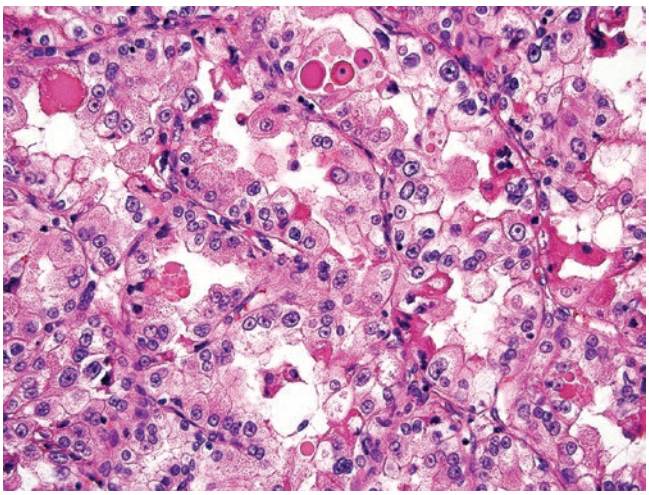

Fig. 1.8 The main defining criterion for nuclear grade in the modified grading system is prominent nucleoli recognizable at 100x magnification (10x objective), which warrants grade 3. Prominent nucleoli recognizable only at higher magnification warrant grade 2, whereas inconspicuous nucleoli even at high magnification warrant grade 1

- The minimum number of cells showing a higher grade required to assign the higher grade overall is debatable; however, the most established method is to identify at least an entire high-power field composed of the higher grade.
- An alternate system incorporating tumor necrosis has also been proposed; however, in most practices, the nucleolar method endorsed by ISUP/WHO is now used, with presence or absence of necrosis also noted in synoptic reports.
- The nucleolar grading system is recommended for use in clear cell and papillary RCC. For other RCC subtypes, it can be used descriptively, but has not been validated as a prognostic factor.
- Chromophobe RCC has a favorable prognosis, yet often has inherent nuclear atypia. It is recommended that grading not be applied to chromophobe RCC, as it has not been shown to have definite prognostic value.
- An alternate grading system has been proposed for chromophobe RCC based predominantly on nuclear crowding (chromophobe tumor grade), although reporting this is currently not required (Table 1.10).
- Grading is approached in a similar way for core biopsy samples. Recent attention has been drawn to risk stratifying tumors in the biopsy setting based on histologic subtype of tumor and grade, such that grade 1–2 tumors of specific histologies may be more amenable to surveillance or less aggressive therapy.

References: [1, 50–55].

What Are the Histologic Growth Patterns and Variants for Clear Cell RCC?

- Clear cell RCC can have a variety of patterns, especially when tumors are high-grade.
- A common pattern is that of eosinophilic cells (which likely often fell into the now defunct former category of "granular cell" RCC) (Fig. 1.9a).

Table 1.10 Proposed "chromophobe tumor grade" as an alternate grading scheme for chromophobe RCC

Chromophobe tumor grade (Paner et al. [53])	Features
1	Lack of nuclear crowding or anaplasia, as defined for grades 2 and 3
2	Nuclear crowding detectable at 100× magnification (10× objective), some nuclei in direct contact with each other at 400× magnification (40× objective), and threefold nuclear size variation (non-degenerative)
3	Frank anaplasia, including multilobated nuclei, tumor giant cells, or sarcomatoid change

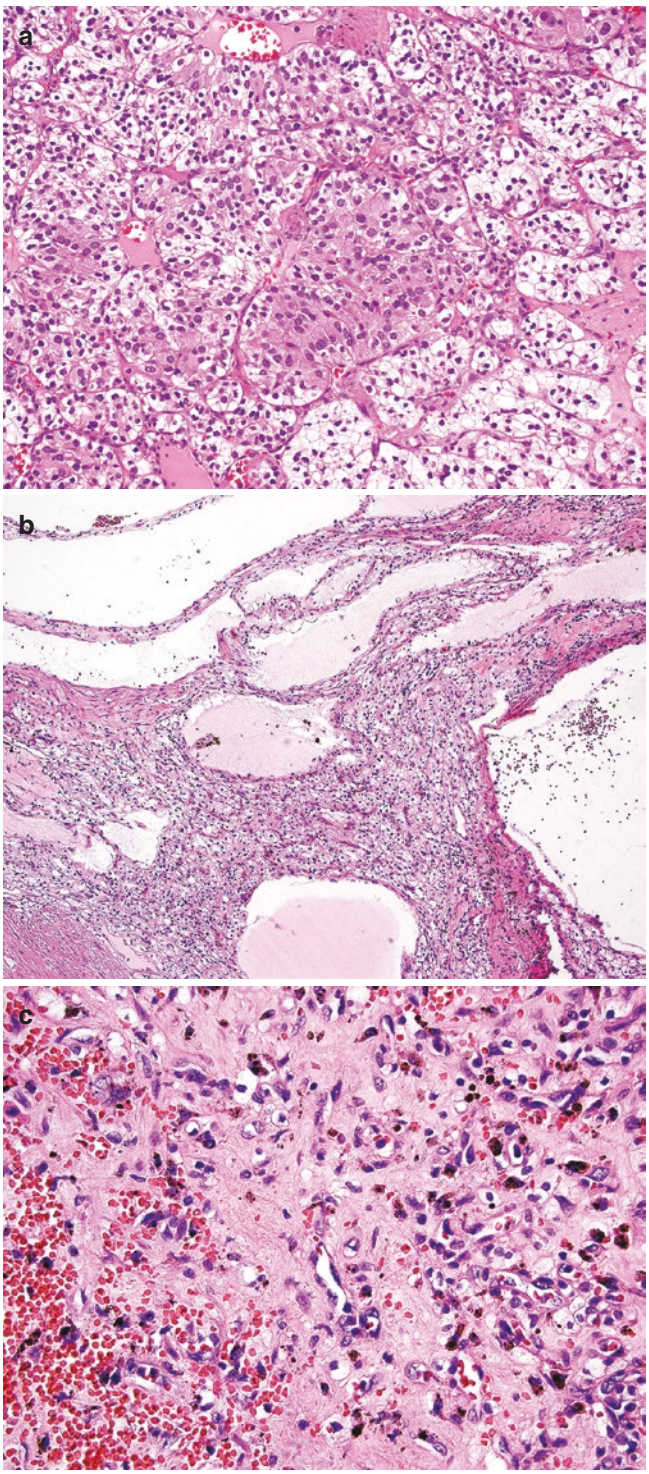

Fig. 1.9 (**a**) Clear cell renal cell carcinoma can have a transition to granular eosinophilic cytoplasm (formerly known as granular cell renal cell carcinoma); however, identification of a classic low-grade clear cell component supports interpretation as clear cell renal cell carcinoma. (**b**) Some clear cell renal cell carcinomas are extensively cystic such that they mimic multilocular cystic low malignant potential tumors; however, a solid mass-forming component, as shown here, precludes a diagnosis of multilocular cystic neoplasm. Still, the behavior may be favorable, and a comment regarding extensive cystic change can be included. (**c**) In some cases, the epithelial component of a clear cell renal cell carcinoma is subtle or obliterated by scarring, which can mimic a hemangioma. Identification of classic clear cell areas or confirmation of epithelial tumors cells with immunohistochemistry can resolve this distinction

- Clear cell RCC can often have cystic change (often accompanied by fibrosis and hemorrhage), with some areas mimicking multilocular cystic neoplasm of low malignant potential. Any solid component (defined as an expansile nodule that would be grossly visible, Fig. 1.9b) precludes a diagnosis of multilocular cystic neoplasm and favors clear cell RCC.
- Some clear cell RCCs have extensive degeneration and sclerosis, so that the vascular component predominates, mimicking hemangioma (Fig. 1.9c).
- Keys to recognizing an unusual RCC as clear cell RCC include: identification of classic golden-yellow/orange areas grossly (even if focal), identification of classic low-grade clear cell areas histologically (may require additional sampling), and diffuse membrane positivity for carbonic anhydrase IX.
- A list of select variants is discussed in Table 1.11.

References: [8, 56–62].

What Are the Differential Diagnoses for Renal Epithelial Tumors with both Clear Cell and Papillary Features?

- Renal epithelial tumors with both clear cell and papillary features can include several different diagnostic entities, ranging from clear cell RCC to translocation RCC to the entity clear cell papillary (tubulopapillary) RCC.
- Key features helpful in distinguishing these entities are shown in Table 1.12 (see also Fig. 1.10).

References: [4, 9, 17, 47–49, 60–63].

Clear Cell RCC vs. Chromophobe RCC

Usually, distinction of clear cell RCC and chromophobe RCC is straightforward, based on their characteristic histologic features; however, some tumors may exhibit overlapping features that necessitate immunohistochemistry or other studies to resolve the differential diagnosis (Fig. 1.11). The behavior of chromophobe RCC is considered favorable, with few demonstrating progression or metastasis, compared to clear cell RCC, which can be less predictable, especially with larger tumor sizes.

Table 1.13 shows how to distinguish clear cell from chromophobe RCC.

References: [17, 32, 57, 64].

Table 1.11 Deceptive variants of clear cell RCC

Variant pattern	Notes
Cystic clear cell RCC	Solid nodule (grossly appreciable) precludes diagnosis of multilocular cystic neoplasm of low malignant potential. immunohistochemistry may help identify tumor cells in areas of bland cyst lining or lymphocyte-like tumor cells within the stroma (PAX8, carbonic anhydrase IX)
Clear cell RCC with eosinophilic cells	Additional sampling may help in identifying classic low-grade areas (may focus on areas of golden-yellow/orange grossly). Diffuse positivity for carbonic anhydrase IX (not limited to necrosis or ischemic areas) supports clear cell subtype
Clear cell RCC with syncytial-type giant cells	Bizarre giant tumor cells with numerous nuclei and marked pleomorphism, often associated with necrosis and sometimes containing emperipolesis. Frequently has an abrupt transition to clear cell RCC with classic features. Even areas of severe atypia usually have similar immunohistochemical features to low-grade clear cell RCC (carbonic anhydrase IX and epithelial markers)
Hemangioma-like clear cell RCC	Epithelial component is subtle/inconspicuous, with associated capillary vascular network mimicking hemangioma. Additional sampling or careful search for epithelial areas may be helpful. immunohistochemistry for epithelial markers (keratin, epithelial membrane antigen [EMA], PAX8) or carbonic anhydrase IX can highlight a subtle epithelial component that resembles capillaries or inflammatory cells
Sarcomatoid clear cell RCC	The most helpful clue to recognizing a sarcomatoid neoplasm as clear cell RCC is additional sampling in search of conventional clear cell areas. Positivity for PAX8 would support a sarcomatoid carcinoma over sarcoma and generally favors RCC over urothelial carcinoma; however, some overlap in the patterns of GATA3 and PAX8 in upper urinary tract sarcomatoid neoplasms has been reported. almost any type of RCC can undergo sarcomatoid dedifferentiation; however, clear cell RCC accounts for the most cases due to its higher incidence. Some studies have suggested that chromophobe RCC has a paradoxically high incidence of sarcomatoid change
Clear cell papillary RCC-like pattern	Although clear cell papillary (or tubulopapillary) RCC is now recognized as a distinct entity with favorable prognosis, there occur cases of clear cell RCC with overlapping morphology. If the immunohistochemical features are not perfect for the entity clear cell papillary RCC (such as incomplete cytokeratin 7 positivity or positivity for CD10 and/or AMACR), it appears that these are better classified as clear cell RCC. These sometimes have higher-stage parameters, larger tumor size, necrosis, etc., which are unexpected in the indolent clear cell papillary RCC. The same also holds true of patients with von Hippel-Lindau (VHL) disease (tumors that resemble clear cell papillary RCC occur, but their immunohistochemical profile is usually not a perfect fit)

Table 1.12 Differential diagnosis of renal epithelial tumors with clear cell and papillary features

	Features	Immunohistochemistry	Genetics
Clear cell RCC with pseudopapillary structures (Fig. 1.10a)	Usually some areas with conventional clear cell features, usually high-grade (ISUP/WHO grade 3). Debatable whether clear cell can have true papillae or this represents loss of cohesion and exclusively pseudopapillary structures	Carbonic anhydrase IX diffuse membrane positive, cytokeratin 7 and high molecular weight cytokeratin negative or partial, AMACR variable, CD10 often positive, melanocytic markers negative	*VHL* mutation and/or 3p25 loss
Papillary RCC with clear cytoplasm (Fig. 1.10b)	Cytoplasm usually vacuolated, with or without hemosiderin, rather than totally clear. Foamy macrophages with similar cytoplasm or psammoma bodies often present	AMACR diffuse strong positive, carbonic anhydrase IX focal or negative, cytokeratin 7 usually diffuse (for type 1 tumors)	Trisomy 7 or 17, loss of Y
Clear cell papillary (tubulopapillary) RCC (Fig. 1.10c)	Branched glandular structures with nuclei aligned above the basement membrane, stubby to complex papillae into cystic spaces, usually small tumors (pT1a)	Carbonic anhydrase IX diffuse positive with "cup-shape" (spares cell apex), cytokeratin 7 diffuse positive, high molecular weight cytokeratin frequently positive, GATA3 frequently positive, AMACR extremely weak or negative, CD10 positive in cysts only or negative	Few/no recurrent genetic alterations
Translocation RCC (Fig. 1.10d)	Variable nested, papillary, clear cell, and eosinophilic cell features. May have voluminous cytoplasm, hyalinized stroma, pigment, or psammoma bodies	Carbonic anhydrase IX minimal or negative, sometimes negative for keratins or vimentin, often melanocytic markers or cathepsin-K positive, AMACR variable, TFE3 or TFEB immunohistochemistry positive	*TFE3* or *TFEB* gene fusion (or rarely *MITF*); occasional false-negative FISH (*RBM10-TFE3* and *NONO-TFE3*)
Clear cell RCC with overlap resembling clear cell papillary RCC (Fig. 1.10e, f)	Branched glands or nuclear alignment mimicking clear cell papillary RCC	Cytokeratin 7 ranges from focal to diffuse, but other markers not supportive of clear cell papillary (CD10 and/or AMACR positive), high molecular weight cytokeratin minimal or negative	At least two-thirds with 3p25 deletion like clear cell RCC

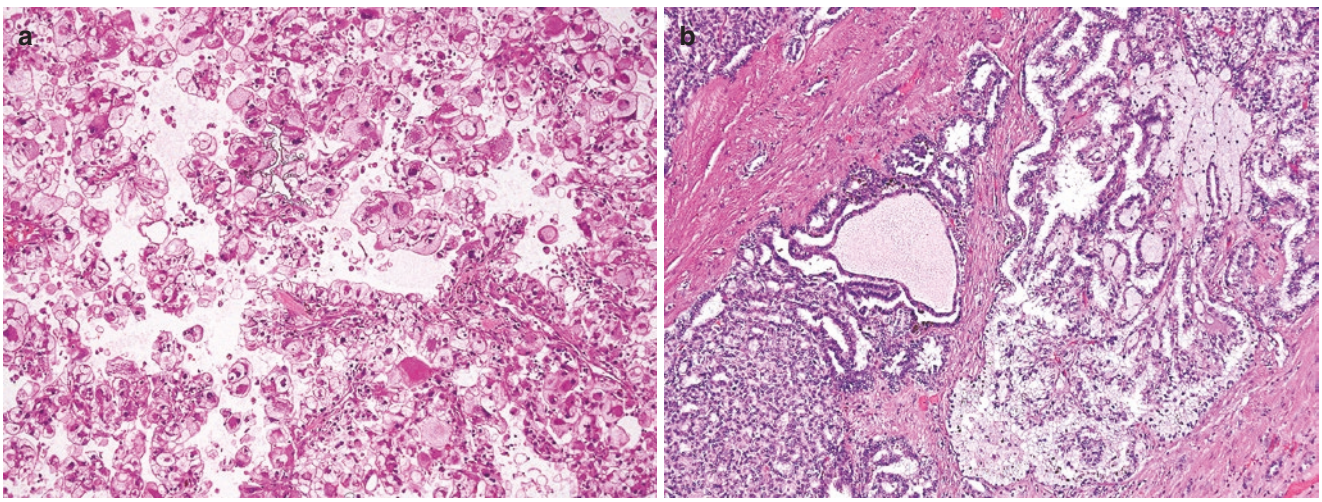

Fig. 1.10 (**a**) Rarely clear cell renal cell carcinoma can exhibit papillary structures, often likely resulting from lack of cohesion in higher-grade tumors. (**b**) Clear cytoplasmic change can be observed in a subset of papillary renal cell carcinomas, often manifesting as numerous cytoplasmic vacuoles. (**c**) The entity clear cell papillary (tubulopapillary) renal cell carcinoma is composed of branched glandular structures with alignment of the nuclei at a similar height within the cytoplasm. (**d**) Translocation renal cell carcinomas often have mixed clear cell and eosinophilic patterns, as well as mixed nested and papillary patterns. The presence of psammoma bodies, as in this case, favors a translocation renal cell carcinoma over clear cell renal cell carcinoma. (**e**) Some clear cell renal cell carcinomas can have overlapping features of clear cell papillary (tubulopapillary) renal cell carcinoma. However, if the immunohistochemical phenotype is not perfect, a diagnosis of clear cell renal cell carcinoma should be used. (**f**) The same case as shown in 10E demonstrates areas more suggestive of typical clear cell renal cell carcinoma

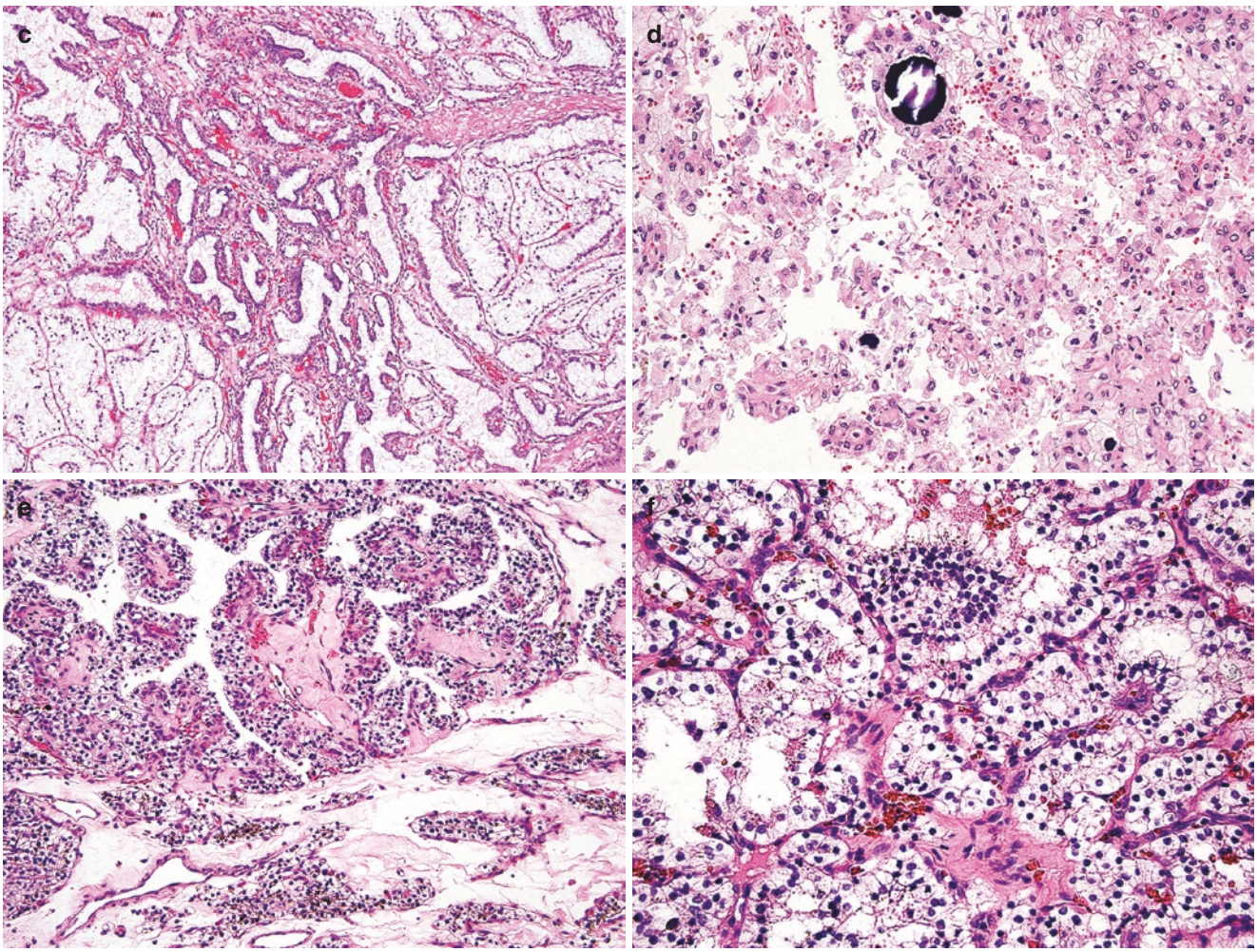

Fig. 1.10 (continued)

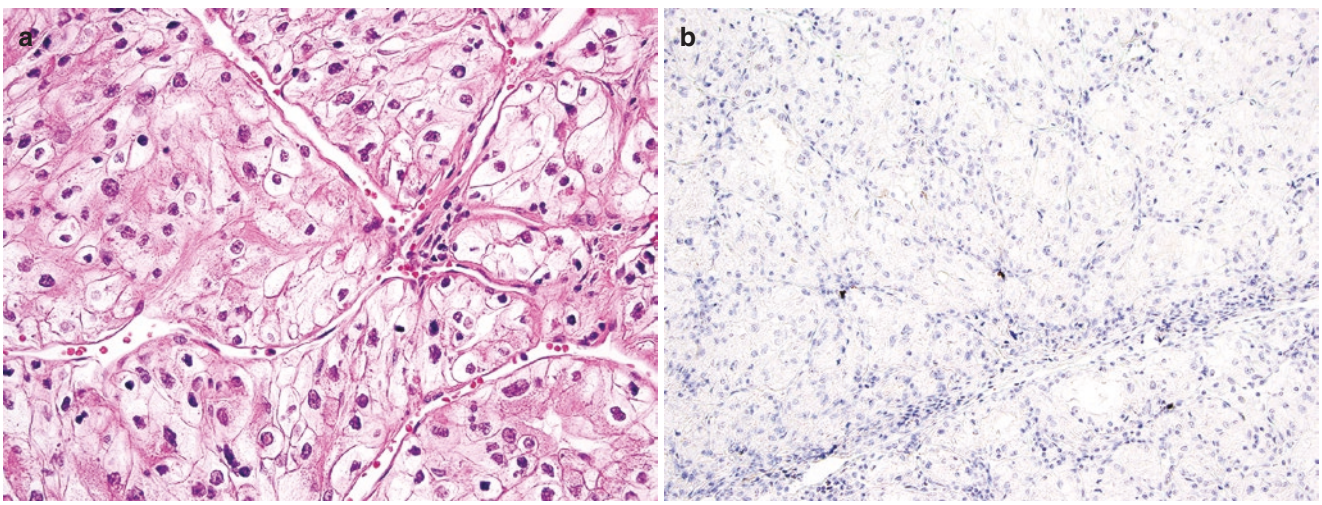

Fig. 1.11 (**a**) This clear cell renal cell carcinoma demonstrates some nuclear wrinkling and prominent cell borders, raising consideration of chromophobe renal cell carcinoma. (**b**) The same case shows negative immunohistochemistry for KIT (CD117), arguing against chromophobe renal cell carcinoma. Other results included positive carbonic anhydrase IX and negative cytokeratin 7, further supporting this classification (not pictured)

Table 1.13 Distinguishing clear cell from chromophobe RCC

	Clear cell RCC	Chromophobe RCC
Gross	Golden-yellow, orange	Pale, tan
Histology	Nests of cells with complex vascular network, clear cytoplasm	Solid or trabecular architecture with voluminous cytoplasm, prominent cell borders, wrinkled nuclei
Immunohistochemistry and other staining	Carbonic anhydrase IX diffuse positive, KIT (CD117) negative, vimentin frequently positive (especially with higher grade), cytokeratin 7 negative or focal. colloidal iron may have reticular positive pattern	KIT (CD117) positive, cytokeratin 7 usually diffuse positive (for classic chromophobe, less for eosinophilic type), vimentin negative (consistently). Diffuse colloidal iron positive
Genetics	*VHL* mutation, loss of 3p25	Loss of chromosomes 1, 2, 6, 10, 13, 17, and 21

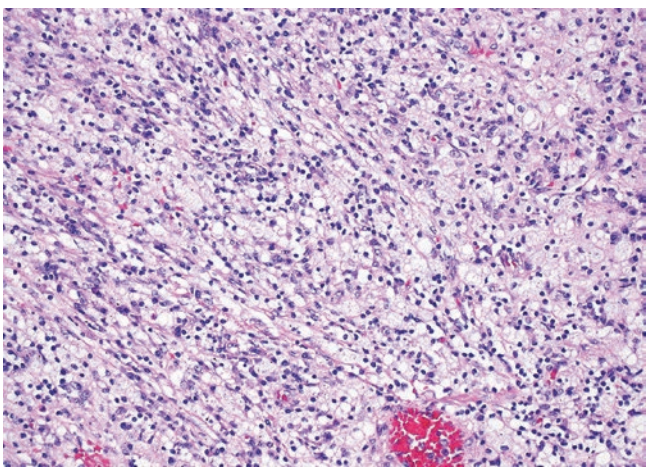

Fig. 1.12 The foamy histiocytes of xanthogranulomatous pyelonephritis can mimic a renal cell carcinoma microscopically

RCC vs. Xanthogranulomatous Pyelonephritis

Xanthogranulomatous pyelonephritis is an unusual granulomatous process that may involve the kidney entirely or partially. This can variably mimic a renal neoplasm clinically, grossly, or microscopically (Fig. 1.12).

- Xanthogranulomatous pyelonephritis is associated with urinary tract infection, particularly with organisms like *Escherichia coli* or *Proteus mirabilis*, and obstruction.
- "Staghorn" calculus of the renal pelvis is also common.
- Extension of xanthogranulomatous pyelonephritis locally can mimic high-stage renal cancer, such as with involvement of the psoas muscle.
- Gross appearance of xanthogranulomatous pyelonephritis includes yellow nodules reminiscent of clear cell RCC, although often arrangement around the calyces is a clue to the infectious/inflammatory nature of this entity.
- Histologic differential diagnosis of xanthogranulomatous pyelonephritis could include sarcomatoid or poorly differentiated RCC, due to sheets of lipid-laden histiocytic cells (mimicking clear cell RCC cells), with lack of distinct glandular architecture.
- Cells of interest in xanthogranulomatous pyelonephritis are predominantly histiocytic and positive for histiocytic markers, such as CD68 or CD163.
- Cells of interest in RCC should have at least some evidence of epithelial differentiation, which with immunohistochemistry can include PAX8, keratin, or epithelial membrane antigen (EMA) positivity.
- Vimentin, although frequently positive in clear cell RCC, is also positive in xanthogranulomatous pyelonephritis and does not distinguish these entities.
- Other differential diagnostic considerations for xanthogranulomatous pyelonephritis include malakoplakia (in which Michaelis-Gutmann bodies can be found) or other nonspecific infectious/inflammatory processes.

Ref: [65].

Papillary RCC vs. Papillary Adenoma

- Papillary RCC and papillary adenoma are analogous lesions, with distinction based predominantly on a few key parameters.
- In the prior WHO Classification (2004), the definition of papillary adenoma required size 5 mm or less to distinguish papillary adenoma from RCC.
- The current WHO Classification (2016) has increased the size threshold for papillary adenoma to 15 mm.
- Other requirements include lack of a fibrous pseudocapsule and low nucleolar grade (ISUP/WHO grades 1 and 2) (Fig. 1.13a, b).
- This change is based on data showing a lack of aggressive behavior from RCC tumors in general under 2.0 cm.
- Otherwise, the features of papillary adenoma are essentially identical to those of type 1 papillary RCC, including basophilic cuboidal cells, papillary or tubular architecture, and psammoma bodies or foamy macrophages.
- In view of this size threshold, it is now conceivable that papillary adenomas could be intentionally subjected to renal mass biopsy, in which case a diagnosis for a tumor up to 1.5 cm could be "papillary renal cell neoplasm"

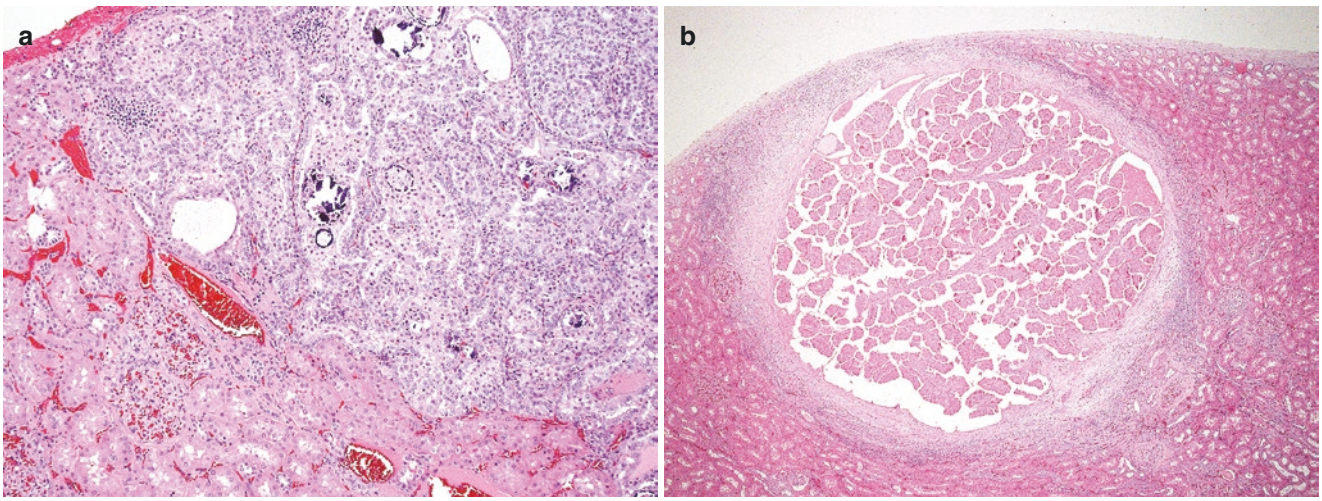

Fig. 1.13 (**a**) Papillary adenomas generally resemble a grade 1–2 papillary renal cell carcinoma, but they are less than 15 mm (in the 2016 World Health Organization Classification) and lack a fibrous pseudocapsule. (**b**) This papillary lesion meets the size criteria for adenoma, but would in the current classification warrant designation as a small renal cell carcinoma due to fibrous pseudocapsule

with a comment that distinction between adenoma and RCC is based on size, encapsulation, and grade, which cannot be entirely assessed in a biopsy.

References: [66, 67].

Papillary Adenoma and RCC vs. Metanephric Adenoma and Wilms Tumor

- Differential diagnostic considerations for unusual patterns of papillary renal cell neoplasms include metanephric adenoma and Wilms tumor (nephroblastoma).
- In contrast to papillary neoplasms, metanephric adenomas typically have highly monotonous cells with very small, bland nuclei (Fig. 1.14).
- Conversely, Wilms tumor (nephroblastoma) exhibits prominent atypia and mitotic activity, especially in the blastemal component, and often will have more than one of the characteristic patterns of blastema, tubules, and stroma.
- Studies for chromosomes 7, 17, and Y can be used, as trisomy 7/17 and loss of Y appear largely specific to papillary RCC in this context and typically lacking in metanephric adenoma and Wilms tumor.
- Metanephric adenomas are often *BRAF* mutant and many label for mutant BRAF protein with immunohistochemistry.

Table 1.14 shows features distinguishing papillary renal cell neoplasms from metanephric adenoma and nephroblastoma.

References: [68–70].

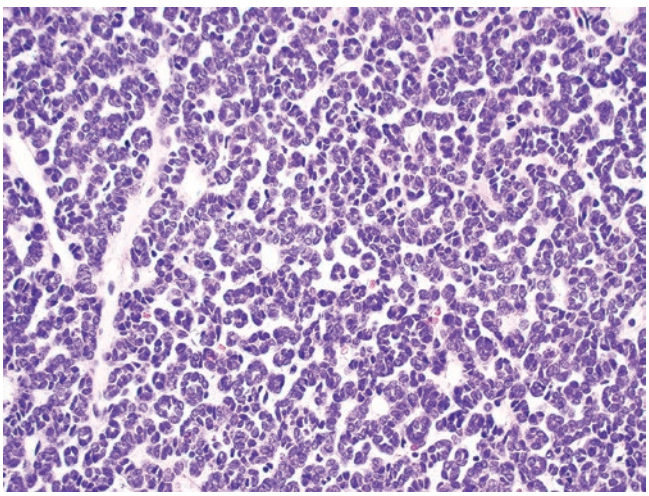

Fig. 1.14 Metanephric adenomas may closely resemble papillary renal cell carcinomas in several ways; however, they are notable for their highly monotonous small, bland nuclei forming tight tubular structures or papillae (not pictured)

Type 1 Papillary RCC vs. Type 2 Papillary RCC

Type 1 and type 2 papillary RCC have been distinguished for many years, based on more aggressive behavior in the latter; however, some recent increased understanding of these two morphological types has challenged the thinking about some cases, particularly the subset of type 2 tumors that are now considered a distinct entity, fumarate hydratase (FH)-deficient RCC/HLRCC syndrome.

Table 1.15 shows a comparison of type 1 vs. type 2 papillary RCC and HLRCC syndrome/FH-deficient RCC (see also Fig. 1.15).

References: [6, 17, 71–73].

Table 1.14 Features distinguishing papillary renal cell neoplasms from metanephric adenoma and nephroblastoma

	Morphology	Immunohistochemistry
Papillary RCC/ adenoma	Nuclei variable, ranging from ISUP grades 1 to 3, sometimes prominent nucleoli. Papillary structures, foamy macrophages, psammoma bodies	AMACR diffuse strong positive, cytokeratin 7 typically positive (type 1 tumors), WT1, CD57 negative
Metanephric adenoma	Highly monotonous small bland nuclei. Can have papillary structures and psammoma bodies, mimicking papillary RCC	AMACR and cytokeratin 7 negative (or focal), WT1 and CD57 positive, epithelial membrane antigen usually negative
Wilms tumor/ nephroblastoma	Often more than one pattern of: Blastema, tubules, stroma. Atypical with brisk mitotic activity	WT1 positive, lesser CD57 than metanephric adenoma, AMACR and cytokeratin 7 typically negative

Table 1.15 Comparison of type 1 vs. type 2 papillary RCC and HLRCC syndrome/FH-deficient RCC

	Type 1 papillary	Type 2 papillary	HLRCC/FH-deficient
Morphology	Basophilic, cuboidal cells (Fig. 1.15a)	Elongated eosinophilic cells with pseudostratified nuclei (Fig. 1.15b)	Cells with very prominent nucleoli (Fig. 1.15c) and perinucleolar clearing; heterogeneous architectural patterns including tubulocystic, papillary, sarcomatoid, or collecting duct carcinoma-like
Immunohistochemistry	Cytokeratin 7 typically positive, AMACR positive	Cytokeratin 7 typically negative or minimal, AMACR positive	Largely nonspecific, but with abnormal negative staining for FH protein and positive 2-succino-cysteine (2SC). Note: Normal FH staining in the presence of mutation is still possible and requires genetic testing
Genetics	Trisomy 7/17, *MET* alterations (especially in the hereditary papillary RCC syndrome)	*CDKN2A* silencing, *SETD2* mutations. Note: Must exclude FH-deficient RCC/HLRCC syndrome	Alterations of *FH* gene, predominantly germline, but likely rare sporadic
Behavior	Nonaggressive	More aggressive	Highly aggressive
Notes	Most common	Diagnosis of exclusion if FH-deficient/HLRCC excluded	Now a distinct entity from papillary RCC

Papillary RCC vs. Mucinous Tubular and Spindle Cell Carcinoma

Mucinous tubular and spindle cell carcinoma is an unusual renal cell neoplasm composed of tubular structures resembling those of papillary RCC, mixed with areas of spindle-shaped cells (likely representing unusual compressed epithelial structures), and extracellular mucinous material. Papillary RCC and mucinous tubular and spindle cell carcinoma share several overlapping features, such that it has been speculated whether the latter is a variant of the same entity. Nonetheless, enough differences, including a distinct copy number profile, have been recognized such that mucinous tubular and spindle cell carcinoma is recognized as a distinct entity in the WHO Classification. Distinct features are summarized in Table 1.16 (see also Fig. 1.16).

References: [74–80].

Papillary RCC vs. Papillary Urothelial Carcinoma

Papillary RCC and urothelial carcinoma are usually readily distinguished, due to their different clinical presentations (involvement of the renal pelvis with or without extension into the kidney vs. renal parenchymal spherical tumor with rare extension into renal pelvis) and different histologic features. However, rare cases can be challenging, such as for papillary RCCs that extend into the calyceal system (Fig. 1.17) or high-grade sarcomatoid tumors that overgrow the kidney. Features that may be helpful in such cases are summarized in Table 1.17.

References: [8, 34, 81].

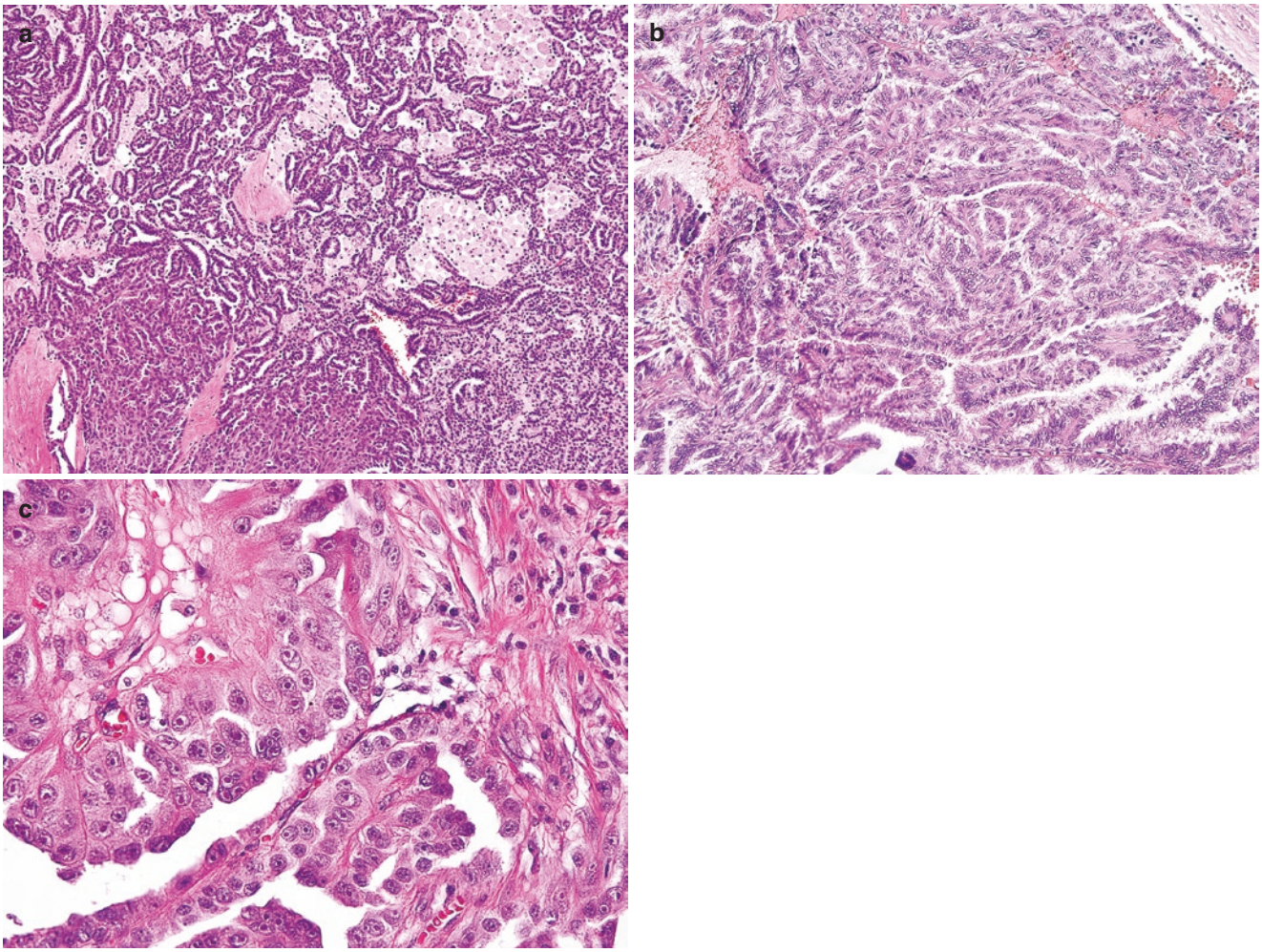

Fig. 1.15 (**a**) Type 1 papillary renal cell carcinomas are characteristically composed of cuboidal basophilic cells, often associated with foamy macrophages or psammoma bodies. (**b**) Type 2 papillary renal cell carcinomas contain eosinophilic cells with elongated pseudostratified nuclei. (**c**) A renal cell neoplasm with mixed histologic patterns (papillary, tubulocystic, collecting duct-like) and prominent nucleoli should raise concern for the possibility of hereditary leiomyomatosis and renal cell carcinoma syndrome/FH-deficient renal cell carcinoma

Table 1.16 Comparison of papillary RCC and mucinous tubular and spindle cell carcinoma

	Papillary RCC	Mucinous tubular spindle cell carcinoma
Morphology	Papillary structures, tubules, solid, psammoma bodies, foamy macrophages	Tubular structures (similar to those of papillary RCC; Fig. 1.16a), elongated spindle-shaped cells (likely compressed glandular structures; Fig. 1.16b), mucinous stromal material
Immunohistochemistry	Strongly positive AMACR, cytokeratin 7 (type 1 tumors)	Similar positivity for AMACR and cytokeratin 7, mixed results for markers of distal nephron. Overall, limited significant differences. Recent study found VSTM2A overexpression by in situ hybridization, different from papillary RCC
Genetics	Trisomy 7/17, loss of Y	Loss of chromosomes 1, 4, 6, 8, 9, 13, 14, 15, and 22 in typical cases. Those with overlapping features of papillary RCC have been reported to have 7/17 gains. Recent discovery of alterations in hippo pathway, including *NF2* and *PTPN14* genes
Behavior	Generally nonaggressive with small, organ-confined tumors	Generally nonaggressive but local recurrence, metastasis, and sarcomatoid cases have been described

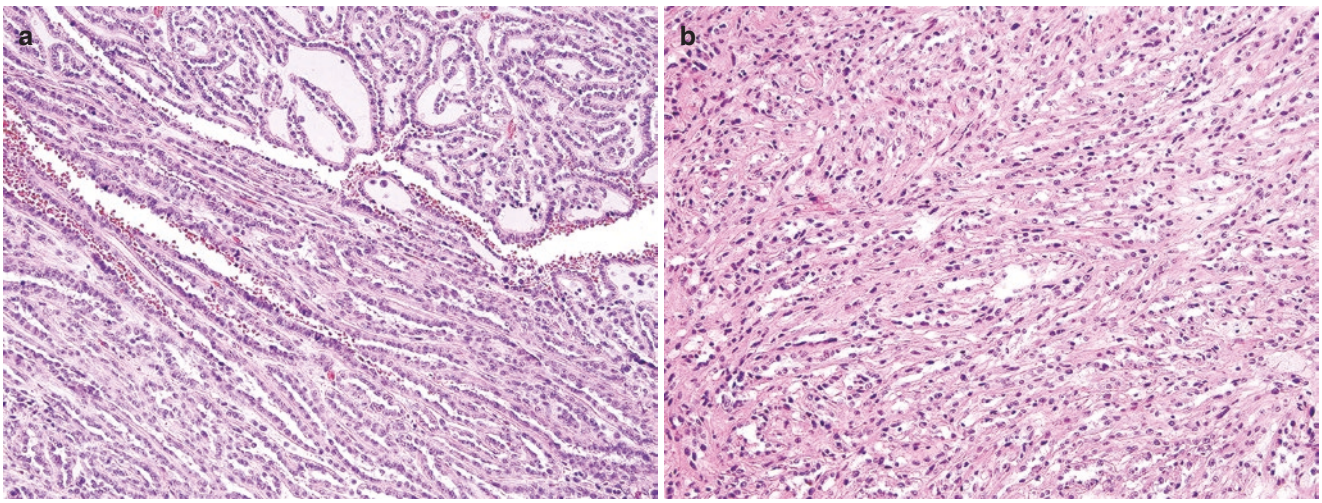

Fig. 1.16 (**a**) Mucinous tubular and spindle cell carcinoma is composed of cuboidal glandular cells, similar to those of papillary renal cell carcinoma, with associated basophilic mucinous material. (**b**) Mucinous tubular and spindle cell carcinoma also contains areas of compact spindle-shaped cells, which despite their mesenchymal appearance are likely of epithelial origin (same case)

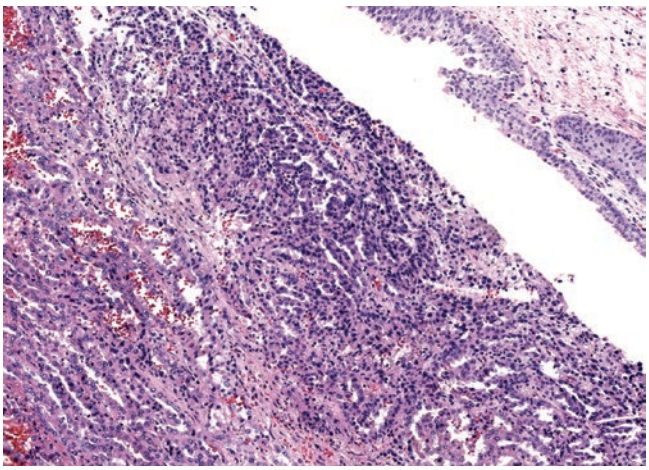

Fig. 1.17 This papillary renal cell carcinoma extended into the renal pelvis and was originally diagnosed by a ureteroscopic biopsy, clinically mimicking urothelial carcinoma. Renal pelvis mucosa is evident at far right

Table 1.17 Features distinguishing papillary RCC from urothelial carcinoma

	Papillary RCC	Urothelial carcinoma
Gross growth pattern	Spherical/ovoid tumor, well circumscribed, with infrequent extension into renal pelvis	Renal pelvis or ureter-based but may infiltrate the kidney; usually poorly circumscribed if mimicking a renal mass
Histologic features	Cuboidal or columnar cells lining papillae, usually monolayered; psammoma bodies or foamy macrophages often present	Often multilayered cells lining papillae, but may be monolayered in areas of partial mucosal denudation; pleomorphism usually greater
Immunohistochemistry	PAX8 positive, AMACR strongly positive, cytokeratin 7 usually positive (type 1/non-eosinophilic tumors), p63 and GATA3 typically negative, cytokeratin 20 typically negative	GATA3 and p63 typically positive, AMACR variable, cytokeratin 20 often positive Note: PAX8 would be ideally negative but has been reported in some urothelial carcinomas, including sarcomatoid urothelial carcinoma of the upper tract
In situ lesion of renal pelvis or ureter	None, except with rare coexistence of concurrent unrelated tumors	If present, favors urothelial carcinoma, but cannot always be found

Chromophobe RCC vs. Oncocytoma

Despite being recognized as distinct tumors for decades, chromophobe RCC vs. oncocytoma continues to be a challenge for urologic pathologists, even today, owing to a lack of robust discriminatory markers. It remains incompletely understood whether these are two entirely unrelated entities that sometimes mimic each other, or if they exist as parts of a spectrum. Numerous histochemical and immunohistochemical markers have been explored over the years; however, only a few are widely used, with the most prevalent being cytokeratin 7. Helpful features are summarized in Table 1.18 (see also Fig. 1.18). Classic chromophobe RCC

Table 1.18 Features distinguishing oncocytoma from chromophobe RCC with eosinophilic features

	Oncocytoma	Chromophobe RCC (eosinophilic)
Gross appearance	Red-brown ("mahogany"), similar in color to normal kidney, sometimes central scar	Pale tan but can closely mimic oncocytoma, sometimes central scar
Histology	Discrete round nests or tubules composed of oncocytic cells with round regular nuclei	Solid growth or trabecular structures (Fig. 1.18c), perinuclear clearing
Atypical cells	Can have smudged cells with degenerative chromatin (Fig. 1.18a)	Nuclear wrinkling and irregularity (raisin-like), low nuclear-cytoplasmic ratio
Colloidal iron histochemistry	Negative or minimal apical positivity	Uniform cytoplasmic positivity
Cytokeratin 7	Rare scattered individual cells (Fig. 1.18b), can be increased in central scar areas	Ranges from oncocytoma-like pattern to small contiguous patches of positive cells (Fig. 1.18d) to diffuse
Vimentin	Negative, except in central scar	Negative
KIT (CD117)	Often positive, may be weak	Often positive
Chromosomal	No chromosomal alterations, or loss of 1, loss of Y, translocation of 11q (*CCND1* gene)	Multiple losses of 1, 2, 6, 10, 13, 17, and 21, possibly chromosomal gains, may have less abnormalities in more eosinophilic cases
Deceptive features	Can extend into fat or vein branches, which does not appear to alter the benign behavior; clear cytoplasmic change or basophilic features can occur in central scar areas	Very oncocytic cases may have minimal differences from oncocytoma, making distinction challenging

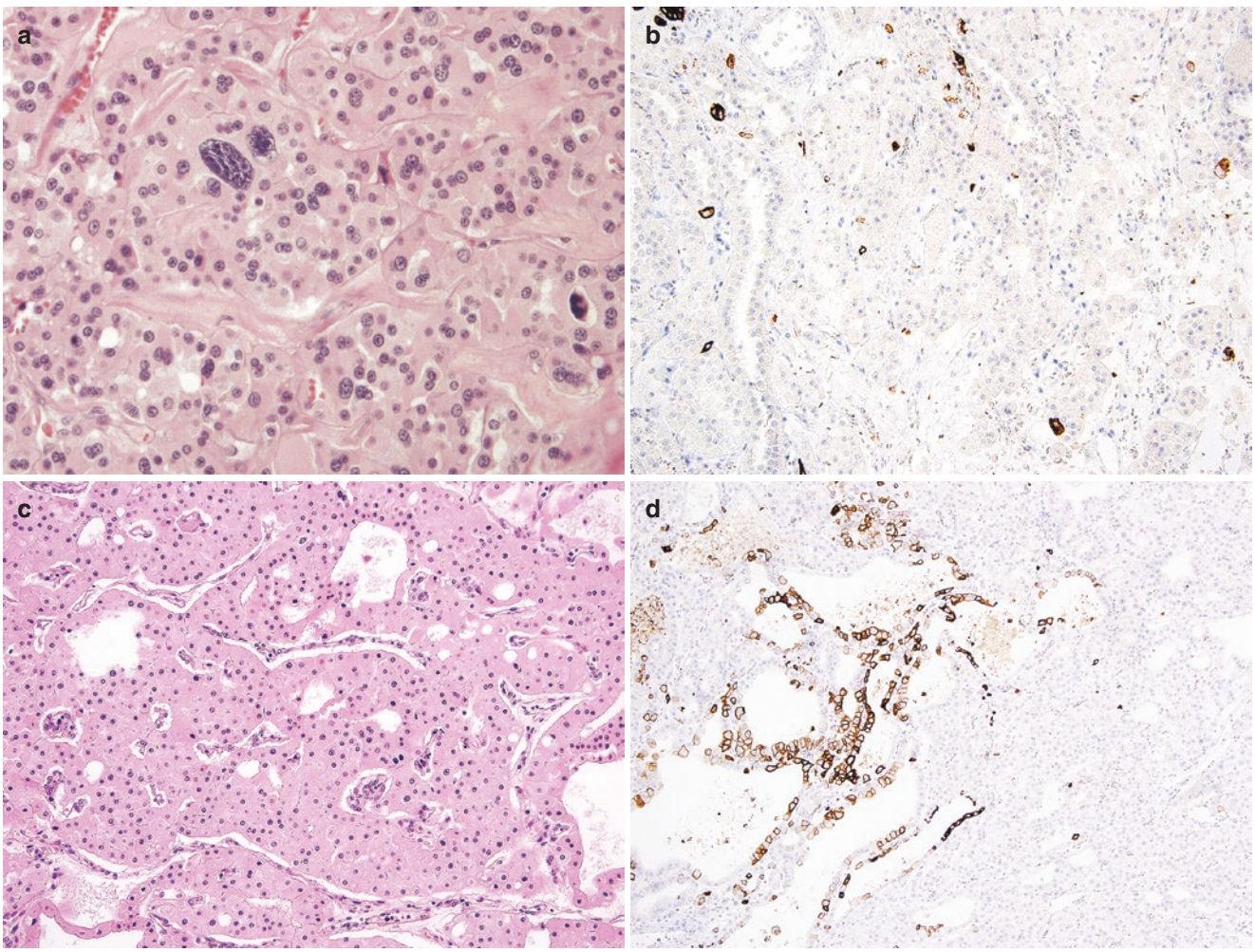

Fig. 1.18 (**a**) Oncocytoma can contain occasional atypical cells, generally considered to represent degenerative atypia. (**b**) The expected staining pattern of cytokeratin 7 in oncocytoma is labeling of scattered individual cells. (**c**) Eosinophilic chromophobe can mimic the cytology of oncocytoma, but extensive trabecular growth is a clue to the diagnosis. (**d**) Eosinophilic chromophobe may not necessarily exhibit diffuse cytokeratin 7, as expected of classic cases. However, patch-like contiguous areas of staining, as shown here, would be an argument against oncocytoma

with pale cells rarely presents a diagnostic challenge with oncocytoma, and so this discussion focuses on eosinophilic chromophobe.

References: [20, 21, 23, 32, 36, 57, 64, 82–85].

Collecting Duct Carcinoma vs. Mimics

With increased understanding of the pathology and genetics of renal cancer, collecting duct carcinoma has become essentially a diagnosis of exclusion, after several other entities are excluded. These tumors are highly aggressive renal malignancies, often necessitating aggressive therapy more akin to that of urothelial carcinoma than renal cell carcinoma. Features distinguishing this group of closely related entities are summarized in Table 1.19.

- All of the mimics of collecting duct carcinoma can have similar histologic features, including: infiltrating glands or cords/sheets/nests, papillary or tubular-papillary structures, or cribriform structures.
- Recently, disruption of INI-1 (*SMARCB1* product) has been recognized in renal medullary carcinoma (Fig. 1.19a). Although medullary carcinoma occurs essentially by definition in the setting of sickle cell trait, an emerging subgroup of tumors with INI-1 loss in the absence of sickle

Table 1.19 Collecting duct carcinoma vs. mimics

	Collecting duct carcinoma	Medullary carcinoma	Fumarate hydratase-deficient RCC	Urothelial carcinoma	Secondary metastatic carcinoma
Gross features	May be partly centered on medulla	May be partly centered on medulla	Less medullary centered	Renal pelvis or ureter involvement with careful search, may overrun the kidney	Often single mass (not necessarily multiple)
Clinical scenario	None of the others apply and metastasis from another organ argued against	Sickle cell trait (if not, then "RCC unclassified with medullary phenotype")	HLRCC syndrome (uterine and cutaneous leiomyomas); if no germline alteration, "FH-deficient RCC"	Association with in situ lesion(s) of renal pelvis or ureter	History of cancer of another organ, may be long duration (10–20 years)
Helpful immunohistochemistry	PAX8 positive, other phenotypes excluded	INI-1 (*SMARCB1* product) abnormal negative	Abnormal negative FH, positive 2-succino-cysteine	GATA3 or p63 positive	Positive markers of another primary cancer (e.g., TTF1 for lung cancer)
Genetics	Alterations of *NF2, SETD2, CDKN2A*; alteration of *SMARCB1* has been reported, but may represent "medullary phenotype"	*SMARCB1* (INI1) alterations/ translocations	*FH* mutations (usually germline, possible rare sporadic cases)	*TP53* alterations, *TERT* promoter mutations	As applicable to patient's primary cancer

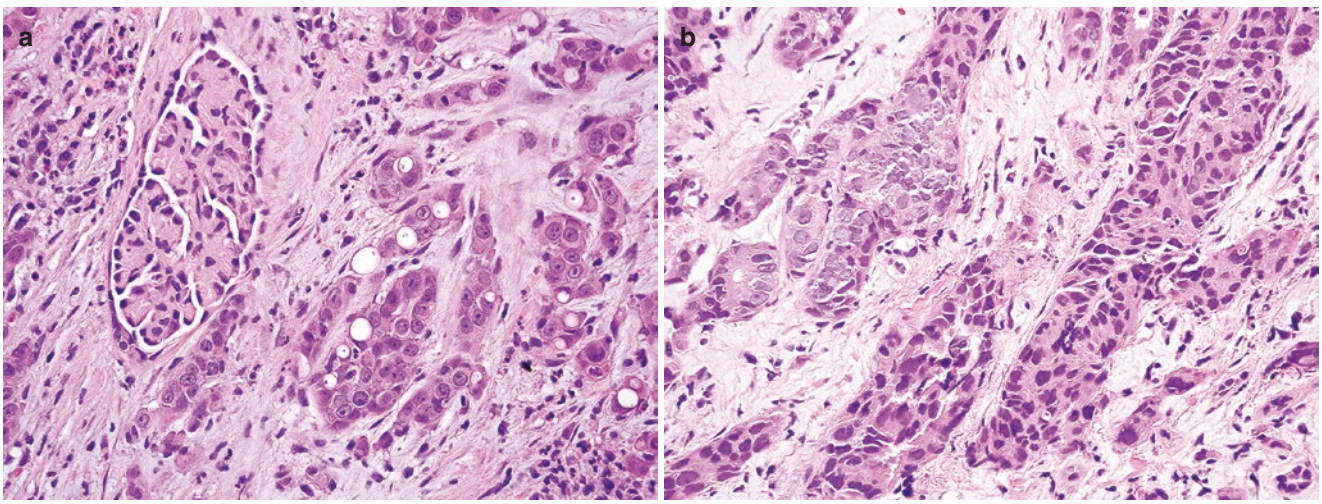

Fig. 1.19 (**a**) Histologic features of renal medullary carcinoma (pictured), collecting duct carcinoma, fumarate hydratase-deficient carcinoma, and urothelial carcinoma can overlap significantly, such that the clinical scenario and special studies are routinely needed. This example is a medullary carcinoma in a 16-year-old boy with sickle trait. (**b**) Metastases to the kidney can mimic primary neoplasms. This is a metastatic adenocarcinoma of lung origin involving the kidney in a renal mass biopsy

trait has been described, under the proposed name "RCC unclassified with medullary phenotype."
- Metastases to the kidney can mimic primary tumors, including solitary masses mimicking a primary tumor many years after original diagnosis.
- Most common metastases to the kidney include those of: lung (Fig. 1.19b), breast, gynecologic, colorectal, and head and neck primary origins.

References: [6, 7, 72, 73, 86–92].

Diagnostic Criteria for Sarcomatoid RCC and Clinical Significance

- The presence of sarcomatoid (sarcoma-like) histology is associated with a poor prognosis in cancers arising from various organs, and renal cell carcinoma with sarcomatoid differentiation represents the most aggressive, treatment-resistant group of renal tumors.
- RCC with sarcomatoid features is not currently recognized as a specific type of RCC mainly because sarcomatoid areas can be observed in all histologic subtypes of RCC. If no underlying RCC subtype is detected, then a tumor with pure sarcomatoid differentiation falls into the category of unclassified RCC and should be distinguished from sarcoma.
- The presence of sarcomatoid features is an independent predictor of poor survival and by many studies considered the most influential prognostic variable for patient outcome.
- Several studies have looked at the effect of the percentage of sarcomatoid differentiation on prognosis and demonstrated that greater amounts were associated with a worse outcome, however there is no agreed upon cut-point for risk stratification at this time. Therefore, any amount of sarcomatoid morphology and underlying RCC subtype should be reported.
- Recognition and reporting of sarcomatoid change in RCC is also required due to potential treatment implication (i.e., using more aggressive systemic therapy, targeted therapy after molecular profiling, including or excluding patients from experimental clinical trials).
- Sarcomatoid RCC is often considered and managed as a single clinical entity, regardless of the underlying parent RCC subtype with which it is associated. However, recent molecular studies have shown that sarcomatoid RCC is a heterogeneous disease requiring precise molecular classification to improve diagnosis, prognosis, and therapeutic management.
- Detailed characteristics of RCC with sarcomatoid features are listed in Table 1.20 (see also Fig. 1.20).

References: [50, 93–96].

Table 1.20 Detailed diagnostic criteria of sarcomatoid RCC

Criteria	Sarcomatoid RCC
Incidence	1–8% of RCCs, ~1/6 of advanced kidney cancers
Epidemiology	Mean age 60 years
Pathogenesis	Dedifferentiation of a lower-grade RCC (multiple mutational steps)
Presentation	90% patients are symptomatic with pain, hematuria, weight loss, fatigue, and other signs of primary mass or metastases
Associated tumors	Reported in all main RCC subtypes; >80% cases with clear cell RCC
Gross	Large (>10 cm) heterogeneous tumor with multiple solid white or gray areas with fleshy or firm cut surface, infiltrative margins (Fig. 1.20)
Histology: Biphasic—Sarcoma-like plus underlying RCC	Atypical spindle cells arranged into sheets and fascicles with storiform pattern (fibrosarcoma-like) or pleomorphic undifferentiated sarcoma pattern; occasional areas of heterologous elements (osteosarcoma, chondrosarcoma, or rhabdomyosarcoma)
Lower-grade RCC component	Present in the majority of cases with careful sampling (mean ~ 40%, median ~ 50% tumor volume); pure sarcomatoid extremely rare (4%)
Grade	ISUP/WHO grade 4 by definition
Stage	45–85% present at advanced tumor stage 3 or 4
Metastases	~40% patients with distant metastases to lung, bone, nodes, liver, and brain
Molecular findings	Complex set of chromosomal gains and losses, common –13q (75%) and –4q (50%) plus mutations of PTEN, TP53, and RELN
Median survival	4–9 months after diagnosis; 5-year cancer-specific survival 15–22%

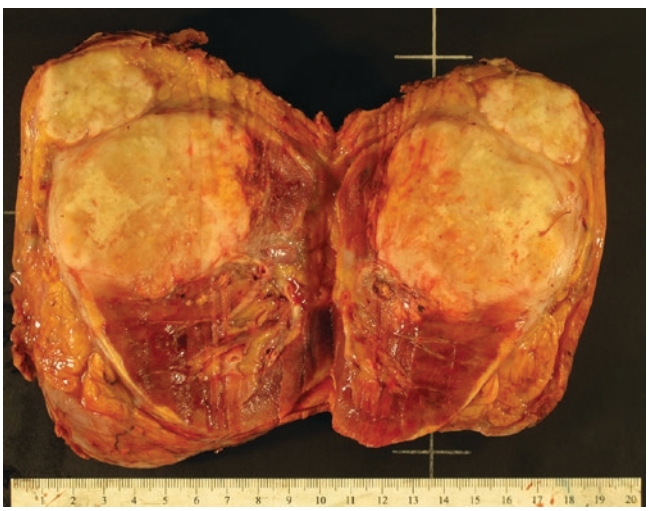

Fig. 1.20 Gross image of clear cell renal cell carcinoma with extensive sarcomatoid dedifferentiation showing heterogeneous fleshy grayish cut surface and areas of geographic necrosis

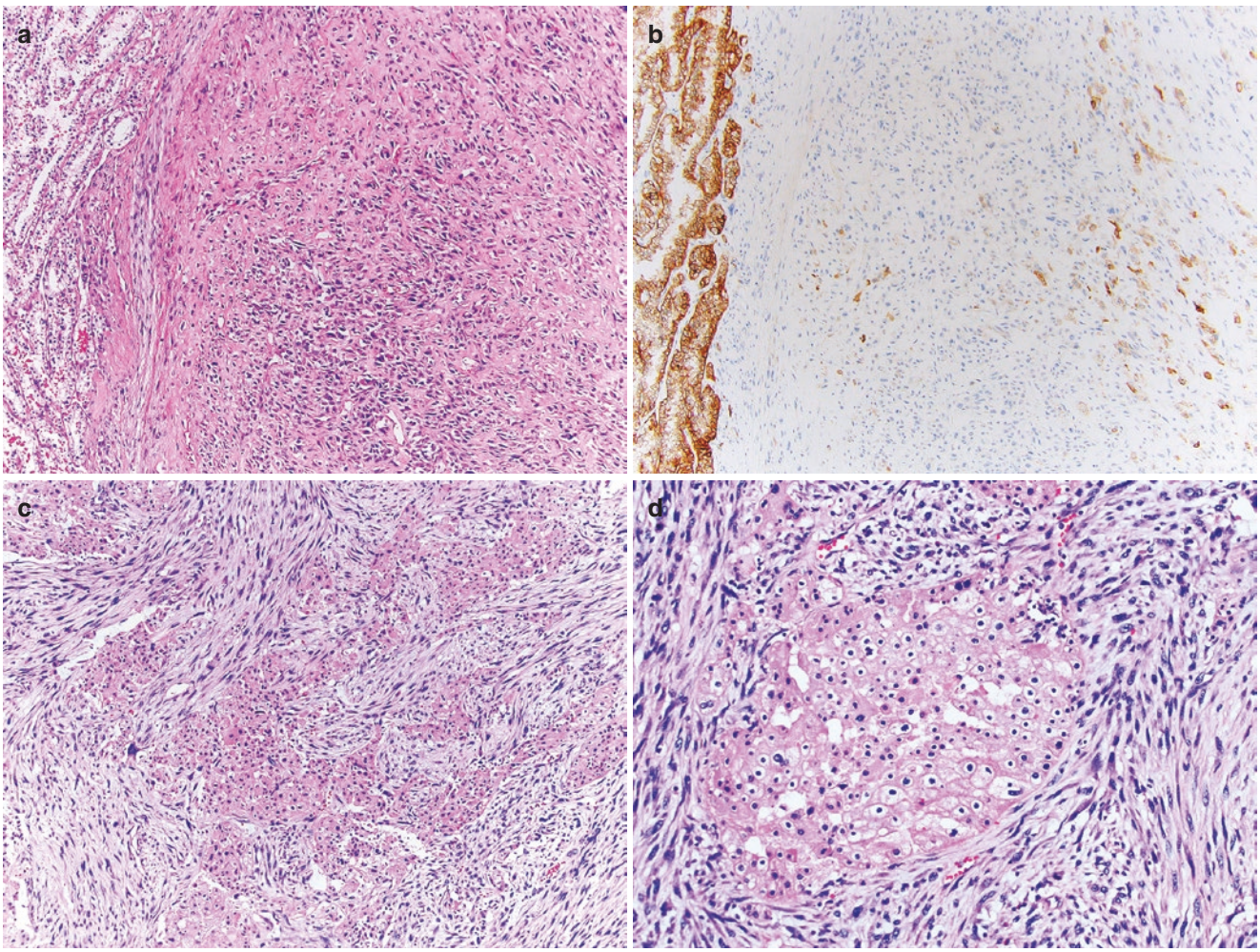

Fig. 1.21 (**a**) Clear cell renal cell carcinoma (left) with abrupt transition to area of sarcomatoid dedifferentiation (right). (**b**) Immunostaining with carbonic anhydrase IX shows strong expression in low-grade clear cell renal cell carcinoma area (left) and only focal scattered positivity within sarcomatoid area (right). (**c**) Microscopic image of sarcomatoid carcinoma arising in a background of chromophobe renal cell carcinoma (100×). (**d**) Higher magnification of sarcomatoid carcinoma surrounding area of low-grade classic chromophobe RCC with plant-like membranous accentuation, raisinoid nuclei, perinuclear halos, and cohesive solid growth pattern (200×)

How to Distinguish Sarcomatoid RCC from a Sarcoma?

Sarcomatoid dedifferentiation can be found in association with any of main subtypes of renal cell carcinoma (RCC). Sarcomatoid dedifferentiation is not very common (<5% of all RCC), but its prevalence is ten times higher than of primary kidney sarcoma.

- Although sarcomatoid RCCs resemble classic sarcomas, it is very important to distinguish them since the prognosis and treatment for both tumors are different.
- Grossly sarcomatoid RCC is centered in the kidney parenchyma, while a sarcoma is often developed from the renal capsule or soft tissue adjacent to the kidney.
- Sarcomatoid RCC can be derived from either low-grade (30%) or high-grade RCC (70%). Therefore, sarcomatoid RCC is typically composed of a low-grade or high-grade RCC component and a high-grade spindle cell sarcomatoid component (Fig. 1.21a–d).
- Sarcomatoid RCC is typically composed of multiple heterogeneous nodules in a large mass greater than 10 cm. Sufficient sampling from different tumor nodules is necessary to identify the lower-grade RCC component.
- Sarcomatoid RCC is usually positive for pan-cytokeratins and PAX8 (at least focally), whereas other markers of RCC subtypes may be negative.
- The comparison between sarcomatoid RCC and sarcoma is listed in Table 1.21.

References: [93–95, 97, 98].

Table 1.21 Sarcomatoid RCC vs. sarcoma

	Sarcomatoid RCC	Sarcoma
Pathogenesis	Dedifferentiation of a lower-grade RCC	Malignant transformation of mesenchymal cells
Tumor epicenter	Renal parenchyma	Renal capsule or perinephric tissue
Gross	Multiple areas of heterogeneous tumor	Large homogenous tumor with fleshy appearance
Presence of lower-grade RCC component	Yes (mean ~40%, median ~50% tumor volume); pure sarcomatoid extremely rare	No
Typical histology	Highly cellular areas of atypical haphazard spindle cells admixed with RCC components	Variable histological patterns: i.e., leiomyosarcoma (most common), liposarcoma, osteosarcoma, angiosarcoma, synovial sarcoma
Immunohistochemical (IHC) with epithelial markers	AE1/AE3, CAM5.2, and EMA are positive at least focally	Negative except for epithelioid angiosarcoma and leiomyosarcoma
Renal marker PAX8	Positive in ~100% lower-grade components and ~70% of sarcomatoid components	Negative
Other IHC markers	Desmin sometimes positive; lower-grade RCC components could be positive for CAIX, AMACR, CK7, CKIT, and TFE3	Expression of histogenesis-specific markers (i.e., SMA, desmin, MDM2, CD31, CD34, ERG, TLE1, and CD99)
Behavior	Always high grade (4); very aggressive malignancy	Low grade can be slow growing, high grade aggressive
Prognosis	Very poor (<30% survival)	Depending on the grade and location, but generally poor
Treatment	Surgery and chemotherapy	Surgery

Table 1.22 Sarcomatoid RCC vs. sarcomatoid urothelial carcinoma (UC)

Parameter	Sarcomatoid RCC	Sarcomatoid UC
Epidemiology	Mean age 60; slight male predominance	Mean age 71; male:Female ratio 3:1
Incidence	1–8% of all RCC	0.3–1.6% of all UC
Pathogenesis	Dedifferentiation of a lower-grade RCC through multistep mutational changes	Dedifferentiation toward mesenchymal lines from pluripotent stem cells of a carcinoma
Associated tumors	Lower-grade RCC (mean ~40%, median ~50% tumor volume)	In situ or invasive urothelial carcinoma
Pure sarcomatoid morphology	Extremely rare (0.2%), called unclassified RCC with sarcomatoid component	Pure sarcomatoid accounts to 0.6% of all urothelial carcinomas
Gross	Large (>10 cm) heterogeneous multinodular tumor with white-gray firm fleshy areas	Large polypoid and infiltrating mass with fleshy cut surface, hemorrhage, necrosis, and cavitation
Typical histology	Highly cellular areas of atypical haphazard spindle cells arranged in fascicles or sheets of pleomorphic cells admixed with RCC components	High-grade spindle and undifferentiated pleomorphic cells admixed with less prominent conventional urothelial, squamous, glandular, or small cells areas (Fig. 1.22a, b)
Heterologous elements	Very rare (case reports), most commonly osteosarcoma	More common (~10%), including osteo-, chondro-, rhabdomyo-, leiomyo-, angio-, and liposarcoma
IHC with epithelial markers	Low molecular weight cytokeratin, AE1/AE3, EMA	High molecular weight cytokeratin, AE1/AE3, EMA
Renal cell markers	PAX8 positive in ~100% lower-grade RCC and ~70% of sarcomatoid components; could also express CK7, AMACR, CD10, and CKIT	Negative, except for 18% cases from upper urinary tract
Urothelial markers	Negative	Positive GATA3 (70%), p63
Prognosis	Median survival 4–9 months	Median survival 14 months

Sarcomatoid RCC vs. Sarcomatoid Urothelial Carcinoma

- Sarcomatoid carcinomas are highly aggressive tumors that demonstrate biphasic epithelial carcinomatous and mesenchymal sarcoma-like differentiation. The mesenchymal or sarcomatoid component of these tumors consists of either undifferentiated spindle cells or elements showing heterologous differentiation.
- Sarcomatoid carcinomas arise from almost any organ system with an epithelial component, including the kidney and urinary tract, and often have overlapping morphology. Distinction between sarcomatoid RCC and sarcomatoid urothelial carcinoma is very important due to different prognosis and patient management (see Table 1.22 and Fig. 1.22).

References: [8, 50, 93, 99–101].

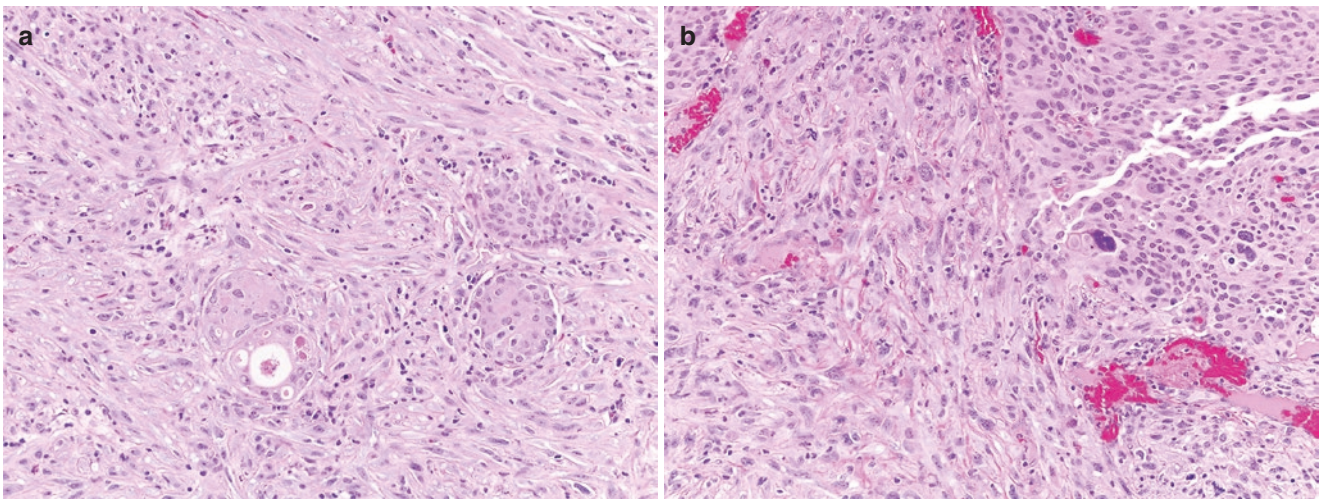

Fig. 1.22 (**a**) Small focus of low-grade urothelial carcinoma embedded into the sarcomatoid carcinoma. (**b**) High-grade urothelial carcinoma transitioning to sarcomatoid area

What Are the Histological Variants of Angiomyolipoma?

- Renal angiomyolipoma (AML) is a mesenchymal tumor composed of three main components in variable proportions: (1) angio—abnormal vasculature, (2) myo—smooth muscle cells, and (3) lipoma—mature adipocytes. Renal AML is believed to originate from pluripotent perivascular epithelioid cells (PEC) and also called PECOMA.
- The vast majority of renal AML are benign indolent tumors, although large tumors have tendency to massive retroperitoneal bleeding, and AML with epithelioid atypical features could show aggressive behavior. Multifocal and bilateral AMLs are often associated with tuberous sclerosis and genetic alterations in tuberous sclerosis genes *TSC1* (hamartin, 9q34) and *TSC2* (tuberin, 16p13.3). All renal AMLs are typically positive for smooth muscle markers actin and caldesmon, as well as melanocytic markers Melan-A (MART-1), HMB-45, MITF, tyrosinase, and cathepsin-K. Renal AMLs are negative for PAX8 and epithelial markers (EMA and cytokeratins) (Fig. 1.23a–f).
- Histological variants of renal AML in decreasing frequency are as follows: typical triphasic AML, predominantly leiomyomatous (fat-poor), lymphangiomyomatous AML, predominantly lipomatous (fat-rich), epithelioid AML, AML with epithelial cysts (AMLEC), oncocytoma-like AML, sclerosing AML, microscopic hamartomatous AML.

Table 1.23 provides description of all histologic variants of AML and differential diagnoses for each of them.

References: [102–106].

Renal Angiomyolipoma vs. Medullary Fibroma

- Both renal angiomyolipoma (AML) and medullary fibroma (also known as renomedullary interstitial cell tumor) represent relatively common mesenchymal neoplasia with overlapping morphology in some cases.
- Monophasic, sclerosing, and microhamartomatous variants of AML are more likely to have similar to medullary fibroma presentation (Fig. 1.24a, b).
- The overwhelming majority of renal AML and medullary fibroma with overlapping morphology are incidental small tumors with benign biological behavior.
- Distinction of renal AML from medullary fibroma is most important in case of multifocal and bilateral tumors due to association with tuberous sclerosis complex.
- The comparison between renal AML and medullary fibroma is listed in Table 1.24.

References: [103, 106–109].

Renal Angiomyolipoma vs. Mixed Epithelial and Stromal Tumor

- Mixed solid mesenchymal and cystic epithelial components could be seen in two unrelated renal tumors: angiomyolipoma with epithelial cysts (AMLEC) and mixed epithelial and stromal tumor (MEST). Despite striking radiologic, morphologic, and even some immunophenotypic overlap between these two neoplasms, their distinction could be made based on our understanding of etiology, pathogenesis, and molecular differences.

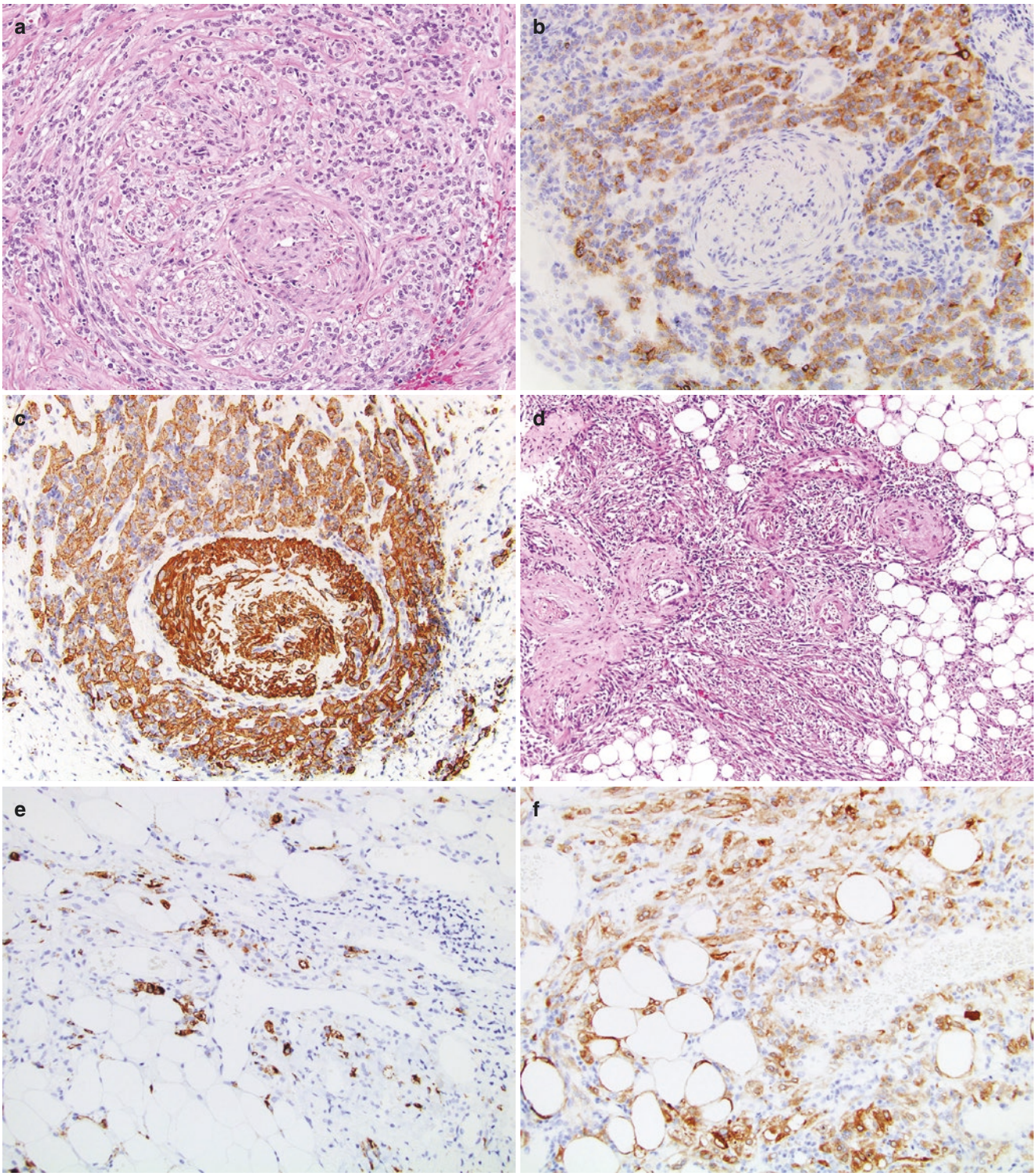

Fig. 1.23 (**a**) Perivascular epithelioid cells (PEC) surrounding abnormal vessel in PECOMA. (**b**) Strong reactivity with Melan-A in perivascular epithelioid cells. (**c**) Smooth muscle actin exhibiting bright labeling of abnormal vessel and spinning out perivascular epithelioid cells of PECOMA. (**d**) Classic morphology of triphasic angiomyolipoma (AML) with clusters of dysmorphic hyalinized vessels, spindled smooth muscle cells, and adipocytes. (**e**) Triphasic AML demonstrating scattered HMB45 positivity. (**f**) Triphasic AML exhibiting strong expression of Melan-A

Table 1.23 Variants of angiomyolipoma (AML)

AML variant	Components	Top differential Dx
Triphasic/classic (most common)	Dysmorphic thick-walled eccentric vessels, mature fat, epithelioid and spindle smooth muscle cells	Clear cell RCC with abundant stroma or sarcomatoid RCC
Predominantly leiomyomatous (fat-poor)	Usually subcapsular; fascicles of spindled or epithelioid smooth muscle cells often radiating of the vessel walls	Leiomyoma and leiomyosarcoma
Lymphangiomyomatous AML	Smooth-muscle proliferation growing in fascicles with clefts and associated thin-walled, branching vessels	Leiomyoma of renal pelvis
Predominantly lipomatous (fat-rich)	Mature adipose tissue with abnormal thick-walled vasculature and scattered small vessels with epithelioid cells	Normal fat, lipoma, and liposarcoma
Epithelioid AML	Sheets and compact nests of large eosinophilic polygonal or plump spindled epithelioid cells comprising >80% of tumor	RCC with oncocytic phenotype, metastatic melanoma
AML with epithelial cysts (AMLEC) or so-called cystic AML	Mixed solid and cystic architecture with epithelial cysts lined by cuboidal to hobnail cells	Mixed epithelial and stromal tumor (MEST) and cystic nephroma
Oncocytoma-like	Homogeneous population of eosinophilic polygonal cells with small nuclei	Oncocytoma
Sclerosing AML	Sheets and cords of spindled cells within abundant sclerotic stroma	Leiomyoma with sclerosis
Microscopic AML (microhamartomatous)	Small nodules of epithelioid perivascular smooth muscle cell proliferations	Medullary fibroma

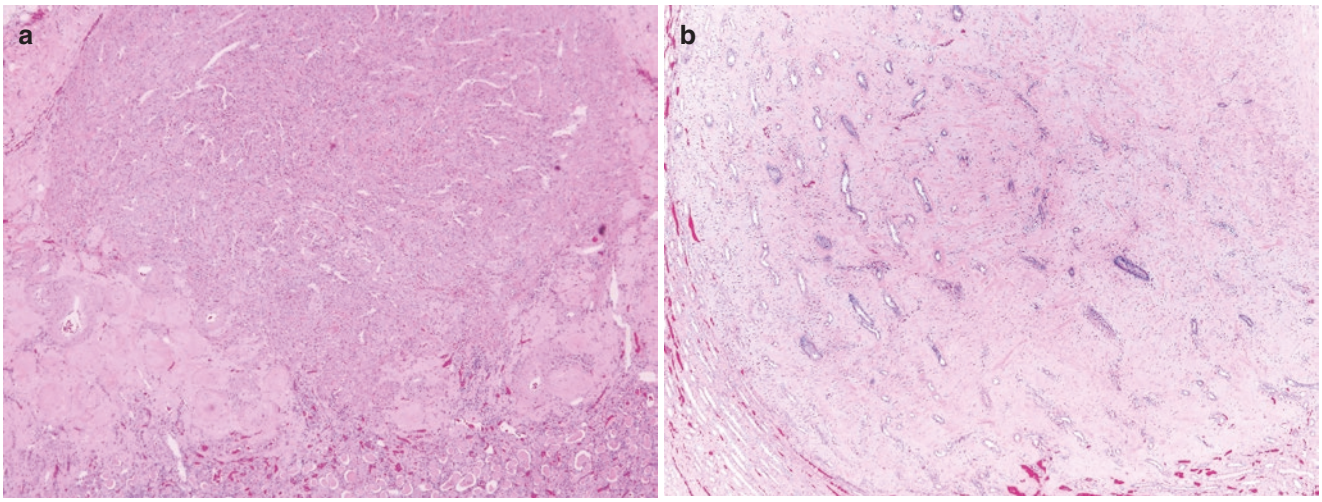

Fig. 1.24 (**a**) Monophasic AML composed of spindled leiomyomatous cells with vascular clefts, abnormal thickened vessels with hyalinization and fibrosis at the periphery. These tumors frequently arise in the kidney capsule (hence the name "capsuloma"). (**b**) Renomedullary fibroma composed of spindled and stellate cells embedded into the myxoid or sclerotic stroma with abundant but normal vessels

- AMLEC represents a very rare variant of fat-poor angiomyolipoma with characteristic combination of dysplastic vessels and plump epithelioid smooth muscle cells, plus cystically dilated epithelial tubules with cuboidal to hobnail lining and underlying compact "cambium-like" Mullerian-like stroma. Like any other angiomyolipoma, AMLEC shows prototypical co-expression of melanocytic and smooth muscle markers within the solid mesenchymal component (Fig. 1.25a, b).
- MEST is another rare biphasic tumor that typically occurs in perimenopausal women and consists of variably sized cysts and glands separated by more or less abundant stroma. Epithelial cells could be cuboidal, hobnailed, columnar, endometrioid, or intestinal type with eosinophilic, amphophilic, or vacuolated cytoplasm. Stroma ranges from scant hypocellular and fibrotic septa (adult cystic nephroma) to markedly cellular, condensed, edematous, and ovarian-like in classic MEST (Fig. 1.25c, d).
- Both AMLEC and MEST stromal component is positive for smooth muscle markers (actin, desmin, caldesmon), estrogen receptor (ER), progesterone receptor (PR), and CD10 highlighting condensed subepithelial Mullerian-like stroma underlying epithelial cysts.
- The detailed comparison focusing on differentiating features between AMLEC and MEST is listed in Table 1.25.

References: [104, 110–114].

Table 1.24 Renal angiomyolipoma (AML) vs. medullary fibroma

	Renal AML	Medullary fibroma
Epidemiology	Adults; peak age fifth decade; female predilection (4:1)	Adults; peak age sixth decade; very common; 10–40% on autopsy
Pathogenesis	Derived from perivascular epithelioid cells (PEC)	Renomedullary interstitial cells producing vasoactive agents
Etiology	Sporadic (>50%) or associated with tuberous sclerosis; mutations in genes *TSC1* or *TSC2*	Sporadic only; >40% multifocal (range 1–23 tumors per patient, mean = 3)
Presentation	Imaging surveillance; pain or hematuria if large	Incidental finding
Localization	Cortical or medullary; often subcapsular or renal pelvis	Renal medulla
Size	Mean size 4–6 cm	Very small; mean size 1.7 mm
Gross	Well circumscribed, unencapsulated with heterogeneous cut surface	Small solid nodules; white or pale-gray
Typical histology	Spindle and epithelioid smooth muscle cells admixed with adipocytes and hyalinized eccentric blood vessels; usually quite cellular although could be sclerotic	Spindle and stellate cells within pale myxoid stroma or densely collagenized low-cellularity tumors with amyloid-like material (typical for older patients)
IHC: Epithelial and renal cell markers	Negative (EMA, pan-cytokeratins, PAX8)	Positive only in occasionally trapped tubules (younger patients)
IHC: Smooth muscle markers	Positive (actin, caldesmon)	Positive (actin)
IHC: Melanocytic markers	Positive (HMB45, Melan-A, MITF, tyrosinase, cathepsin-K)	Negative
IHC: Other markers	ER/PR, CD34, S100 could be positive	ER/PR, CD34, S100 negative; COX2 and PGE2 positive
Behavior	Benign, but risk of retroperitoneal bleeding due to rupture when large and in pregnant patients	Benign, hardly any clinical significance; suspected association with hypertension is not proven
Prognosis	Very good	Excellent
Treatment	Surgery; mTOR inhibitors	None required

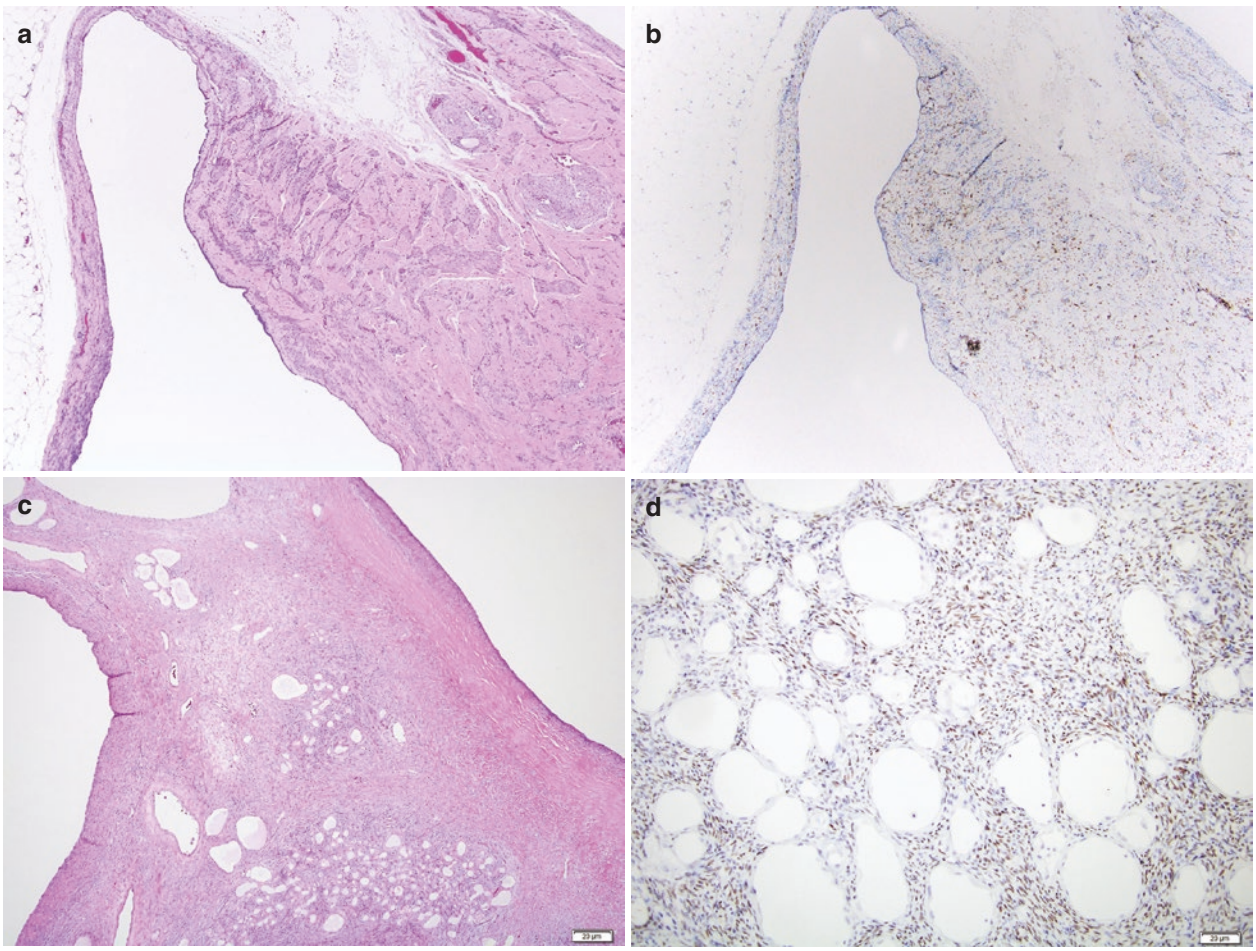

Fig. 1.25 (**a**) Angiomyolipoma with epithelial cysts (AMLEC) consists of solid areas with spindled smooth muscle cells and dysplastic vessels and cystically dilated epithelial cysts (40×). (**b**) Immunohistochemical expression of melanocytic marker HMB45 in AMLEC. (**c**) Mixed epithelial and stromal tumor (MEST) with variably sized cysts and solid component composed of tubules surrounded by spindle cells reminiscent of ovarian-type stroma (40×). (**d**) Mullerian-like stroma of MEST if highlighted by strong diffuse expression of estrogen receptor (ER)

Table 1.25 Renal AMLEC vs. MEST differentiating features

	AMLEC	MEST
Incidence	Very rare, ~20 cases reported; mean age 44; slight female predilection	Rare, mean age 52–53 years; almost exclusively in females
Pathogenesis	Derived from perivascular epithelioid cells (PEC)	Cell of origin is uncertain; hormonally dependent
Etiology	Majority are sporadic; few cases associated with history of tuberous sclerosis or multifocal	Sporadic
Hormonal imbalance	No association	Sex steroid exposure in men; diagnosed during pregnancy or perimenopause due to size increase
Presentation	Majority incidental	Majority symptomatic
Localization	Unilateral, subcapsular	Unilateral, medulla-centered
Size	Mean ~4 cm	Mean ~9 cm
Gross	Well-demarcated partially cystic mass	Multilocular complex cystic mass with firm solid areas
Epithelial component	Cuboidal or hobnailed; reported to express Melan-A and HMB45 in addition to keratins and PAX8	Highly variable: Glands, small and large cysts; cells could be flat, cuboidal, hobnailed, columnar, endometrioid, or urothelial-like
Stromal component	Muscle-predominant cellular stroma with compact subepithelial layer of "cambium-like" Mullerian stroma with chronic inflammation	Variable, ranging from hypocellular fibrotic to markedly cellular; ovarian type; myxoid; edematous or smooth muscle type
Abnormal vasculature	Always contains dysmorphic thick-walled eccentric vessels; muscle cells radiating from vessels	Absent, but have prominent normal vasculature
Stromal luteinization	Not reported	Reported with inhibin and calretinin expression
IHC: Melanocytic markers	Positive (HMB45, Melan-A, MITF, tyrosinase, cathepsin-K)	Negative
Malignant transformation	No reports	In large tumors: Stromal sarcoma, carcinosarcoma, chondrosarcoma, rhabdomyosarcoma, synovial and undifferentiated sarcoma
Behavior	Benign	Benign except for aggressive tumors with secondary malignant transformation
Prognosis	Very good	Good

Epithelioid Angiomyolipoma vs. RCC

- Typically, angiomyolipoma (AML) is composed of three components: abnormal vessels, mature adipocytes, and spindle cells with muscle and melanocytic differentiation. Although it may have focal degenerative atypia within the spindle cell component, it is not a difficult diagnosis. However, epithelioid variant of AML may post diagnostic challenges due to marked pleomorphism, multinucleation, and prominent carcinoma-like appearance reminiscent of various types of high-grade renal cell carcinomas (Fig. 1.26a–d). Moreover, epithelioid AML may develop metastasis or recurrence and is, therefore, considered potentially malignant neoplasm in contrast to other variants of AML.
- According to the current WHO classification, only those AMLs consisting of at least 80% epithelioid components are considered as epithelioid AMLs. The main differential diagnosis is a high-grade RCC with prominent oncocytic change and/or rhabdoid dedifferentiation.

Table 1.26 shows epithelioid angiomyolipoma (eAML) vs. high-grade RCC.

References: [17, 102, 115–118].

What Are Histologic Features Predicting a Malignant Angiomyolipoma?

- Epithelioid variant of angiomyolipoma (AML) constitutes ~5% of all resected AMLs and is characterized by predominantly carcinoma-like epithelioid architecture composing more than 80% of tumor volume.
- Etiology, pathogenesis, and epidemiology of epithelioid AML are similar to other AML variants; however, its morphology and biological behavior are drastically different.
- Five to sixty percent of patients with epithelioid AML develop distant metastases, have recurrence, or suffer death from disease, depending on the study. Although prognostic factors of malignant epithelioid AML are largely undetermined, several histological features have

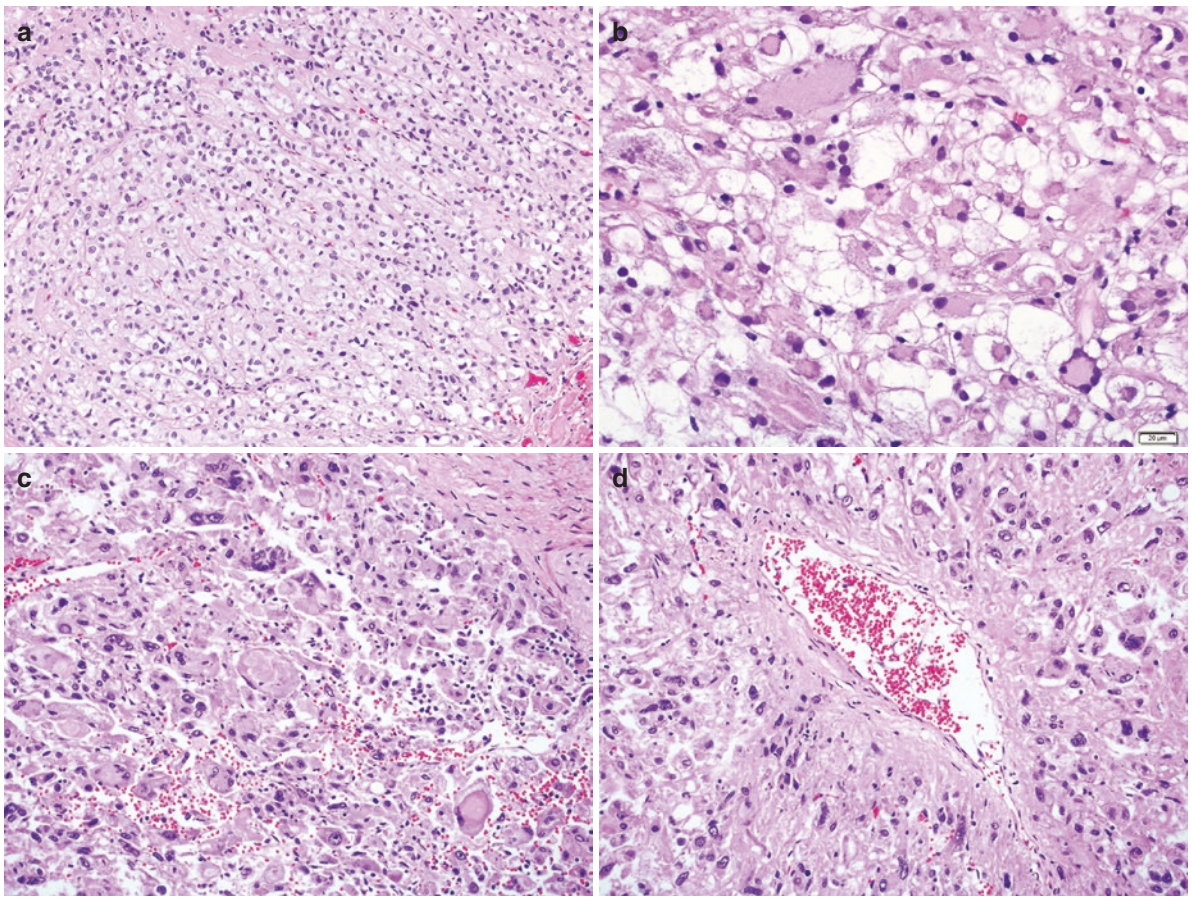

Fig. 1.26 (**a**) Epithelioid AML with "carcinoma-like" growth pattern imitating clear cell RCC. (**b**) Epithelioid AML mimicking clear cell RCC with pleomorphism and multinucleation. (**c**) Epithelioid AML with discohesive high-grade morphology and rhabdoid cells. (**d**) Epithelioid AML featuring perivascular growth pattern characteristic for PECOMAs

Table 1.26 Epithelioid angiomyolipoma (eAML) vs. high-grade RCC

Features	eAML	High-grade RCC
Incidence	Very rare; <5% of all AML	High; 30–50% of all RCC are high-grade tumors
Epidemiology	Peak age fourth decade; women > men	Peak age sixth decade; men > women
Etiology	Alterations in tuberous sclerosis genes *TSC1* (hamartin, 9q34) and *TSC2* (tuberin, 16p13.3)	Alterations of genes *VHL*, *cMET*, or *MiTF/TFE3* family; chromosomal gains and losses depending on RCC type
Pathogenesis	Derived from perivascular epithelioid cells (PEC)	Derived from tubular epithelial cells
Gross characteristics	Solid and circumscribed; gray-tan cut surface; size variable	Solid or cystic, multinodular; bright yellow or patchy cut surface; large size
Necrosis/hemorrhage	Could be present	Frequent
Architecture/morphology	>80% tumor with nests, alveoli, or sheets of plump epithelioid cells with large eosinophilic cytoplasm or smaller uniform cells with clear cytoplasm	Clear cell, papillary, or chromophobe growth patterns with clear and eosinophilic cytoplasm; ISUP/WHO grade 3/4
Atypia	Often markedly pleomorphic cells, multinucleation, giant cells, and ganglion-like cells	Scattered pleomorphic cells with rhabdoid or sarcomatoid features
Typical AML component	Absent or present (0–19%)	Usually absent, although has been reported
Mitoses	Common in pleomorphic tumors; some cases with brisk (>5/10 HPF) and atypical forms	Present, including atypical forms, but usually not brisk
Vasculature	Occasional thick-walled dysmorphic vessels	Usually well-formed, chicken-wire thin vessels
Vascular invasion	May have	Common
Melanocytic markers: HMB45, Melan-A, MITF, cathepsin-K	Positive, usually strong and diffuse, but can be focal	Negative, but TFE3 translocation RCC may be positive
SMA	Positive	Negative
PAX8	Negative	Positive
Pan-cytokeratins, EMA	Negative	Positive
Other markers: CAIX, AMACR, CKIT, TFE3	Negative	Positive depending on subtype
Prognosis	~5% aggressive; risk of malignancy increases if large size (>7 cm), high mitotic rate, atypical mitoses, necrosis, mostly atypical epithelioid morphology (>70%)	Mostly aggressive

been linked to increased risk of aggressive behavior of this tumor and are summarized in Table 1.27.

- The majority of published series agree that presence of three of more of such adverse parameters as large tumor size (>7 cm), necrosis, atypical mitoses, severe atypia, perinephric fat, or renal vein invasion significantly increases the risk of malignant behavior (Fig. 1.27a–c).

References: [115, 117, 119–125].

Renal Angiomyolipoma vs. Sarcoma

- Renal angiomyolipoma (AML) is a mesenchymal tumor that classically exhibits triphasic morphology including abnormal vasculature (angio), smooth muscle cells (myo), and adipose tissue (lipoma). All three components are derived from pluripotent perivascular epithelioid cells (PEC) expressing melanocytic markers, thus renal AML is also known as PECOMA.

Table 1.27 Histologic features of primary epithelioid AML differentiating patients with and without tumor progression

Histologic features	Progressors	Non-progressors
Tumor size	>7 cm or >9 cm	<7 cm
Necrosis and hemorrhage	Often present	Usually absent
Carcinoma-like	Always	Sometimes
Morphological pattern	Large polygonal cells with deeply eosinophilic cytoplasm and high N/C ratios growing in nests, alveoli, or discohesive sheets	Small monomorphic epithelioid cells with uniform nuclei, clear to granular cytoplasm, arranged in densely packed cohesive sheets
Adipocyte differentiation	Absent	Often present
Pleomorphism	Abundant multinucleated, giant, rhabdoid, and ganglion-like cells	Scattered clusters
Atypia/ pleomorphism	>70% (severe)	<25%
Intranuclear inclusions	Common	Rare
Mitotic count	>2/10 high-power fields of view	<2/10 high-power fields of view
Atypical mitoses	Often present	Absent
Renal vein invasion; tumor thrombus	Common	Absent
Perirenal fat invasion	May be present	Absent
P53 overexpression	Present	Absent
Tuberous sclerosis complications	May be present	Not reported

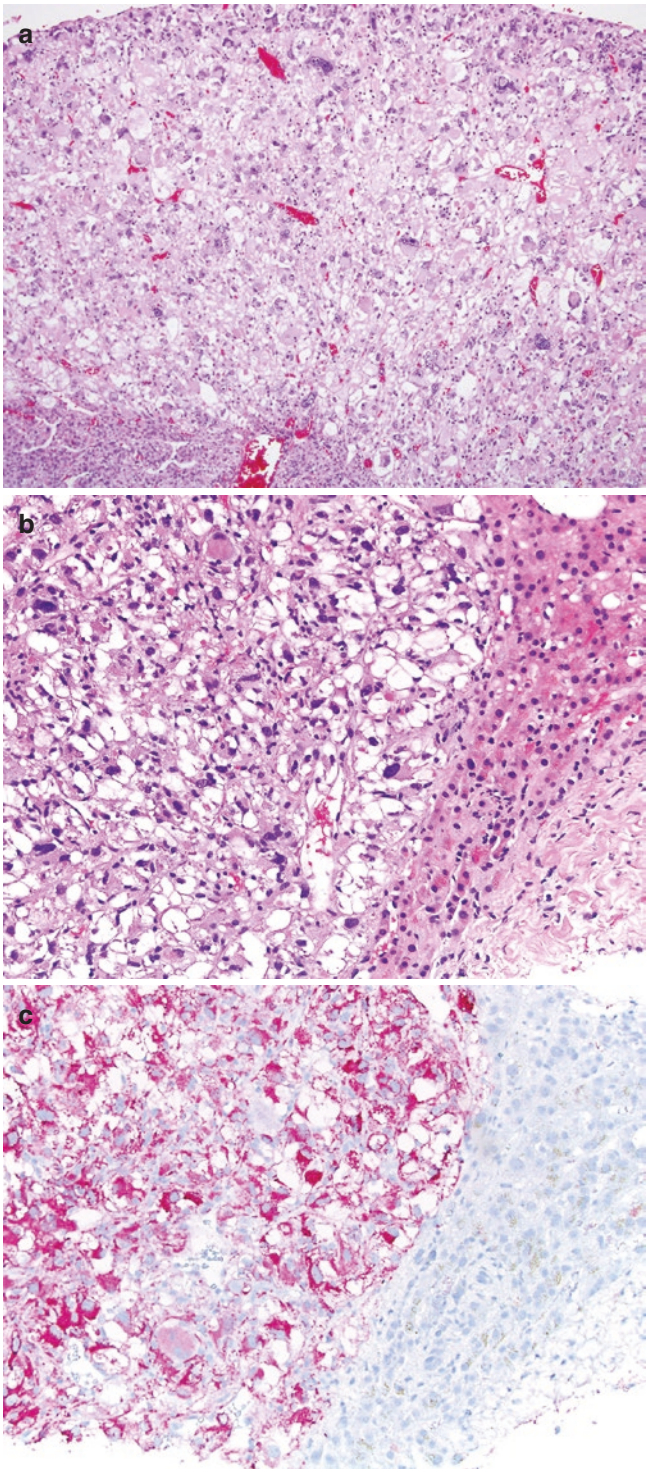

Fig. 1.27 (**a**) Epithelioid AML with severe atypia in >70% cells arising in the background of monophasic leiomyomatous AML. (**b**) Liver metastasis of high-grade neoplasm with marked pleomorphism and atypia mimicking clear cell renal cell carcinoma. (**c**) Diffuse strong expression of Melan-A supports the diagnosis of metastatic epithelioid AML

- Approximately 13% of renal AML have predominantly leiomyomatous (fat-poor) and 5% have predominantly lipomatous (fat-rich) morphology resembling well-differentiated leiomyosarcoma (Fig. 1.28) or liposarcoma, respectively. Their comparisons are presented in Tables 1.28a and 1.28b.

References: [97, 103, 126–128].

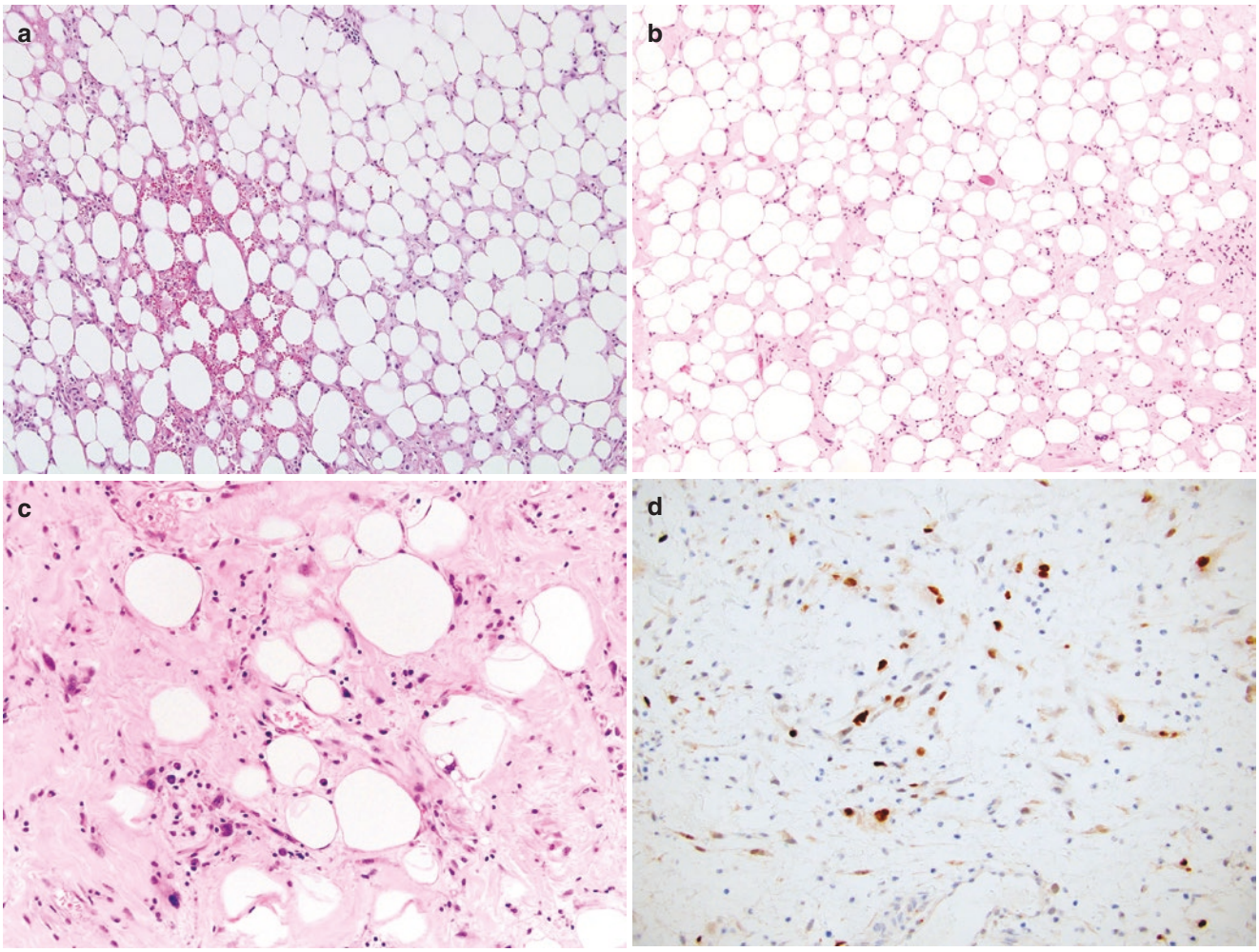

Fig. 1.28 (**a**) Lipomatous AML comprised of large sheets of variably sized fat cells closely resembling atypical lipomatous tumor/well-differentiated liposarcoma. (**b**) Well-differentiated liposarcoma composed of rather mature-looking fat cells with minimal atypia. (**c**) Examination of the same case at higher power allows identification of fibrotic areas with enlarged hyperchromatic cells and lipoblasts. (**d**) Immunohistochemical staining shows strong nuclear reactivity with MDM2 further supported by *MDM2* gene amplification by in situ hybridization in this case of well-differentiated liposarcoma

Table 1.28a Comparison of fat-poor AML and leiomyosarcoma

Feature	Leiomyomatous (fat-poor) AML	Leiomyosarcoma
Epidemiology	5th decade	6th decade
Prevalence	2nd most common AML variant	Most common sarcoma type
Location	Subcapsular cortical or medullary	Commonly involves entire kidney
Gross	Usually small solid rubbery mass; could be multiple and bilateral; extrarenal extension is not a sign of malignancy (common in tuberous sclerosis complex [TSC])	Large (mean 13 cm) encapsulated gray-white solid mass often involving perirenal or hilar fat
Histology	Fascicles of spindled or epithelioid smooth muscle cells often radiating of the vessel walls	Well-formed fascicles with occasional pleomorphic cells with haphazard growth
Mitotic activity	Low	On average 10/HPF
Necrosis	Absent	Common
Other features	Atypical vessels and rare fat cells	Marked atypia, plexiform growth
Melanocytic markers	Positive (HMB45, Melan-A, MiTF, tyrosinase, cathepsin-K)	Negative
Prognosis	Excellent	Poor

Table 1.28b Comparison of fat-rich AML and well-differentiated liposarcoma

Feature	Lipomatous (fat-rich) AML	Liposarcoma
Epidemiology	5th decade	6th decade
Prevalence	3rd most common AML type	2nd most common sarcoma type
Location	Subcapsular or hilar	Perinephric or hilar fat encasing renal parenchyma; true intrarenal tumors are very rare
Gross	Yellow, lobulated; smaller	Large yellow, lobulated
Histology	Mature adipose tissue with abnormal small and medium size thick-walled vessels	Sheets of adipocytes of variable sizes and shapes; enlarged hyperchromatic nuclei
Other features	Scattered epithelioid cells and radial smooth muscle collarets present with careful sampling	Atypical multinucleated stromal cells, lipoblasts, myxoid change; areas of necrosis and sclerosis
Melanocytic and smooth muscle markers	Positive focally	Negative
Prognosis	Excellent	Poor: Locally aggressive tumor

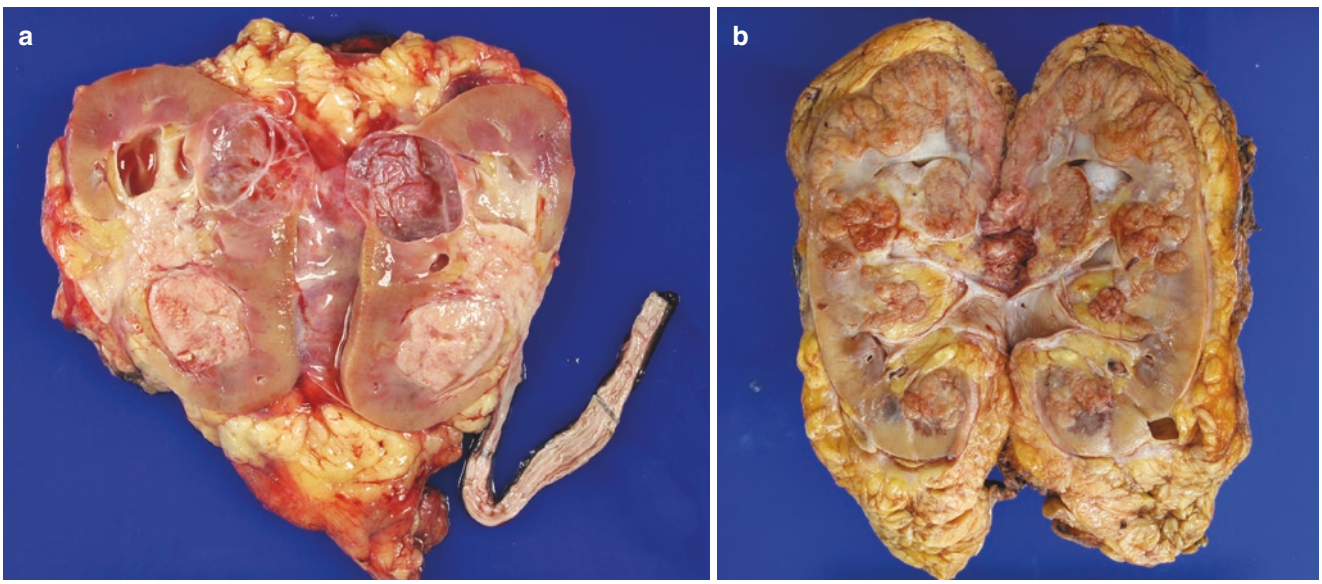

Fig. 1.29 (**a**) Gross photo of radical nephrectomy and ureterectomy performed for resection of urothelial carcinoma of the renal pelvis. (**b**) Gross photo of radical nephrectomy specimen performed for renal cell carcinoma, papillary type

Clinical Significance of Distinguishing Renal Cell Carcinoma from Urothelial Carcinoma of the Renal Pelvis

- Urothelial carcinoma of the renal pelvis (UCRP) develops from the renal pelvic urothelium. In general, UCRP is more aggressive than bladder urothelial carcinoma. In addition, there is a great risk of involving lower urinary tract because of tumor seeding. Therefore, UCRP will be treated more aggressively than either bladder urothelial carcinoma or RCC.
- Invasive and noninvasive UCRP are typically subject to more extensive surgical procedure, which includes radical nephrectomy, ureterectomy, and resection of portion of bladder (bladder cuff) (Fig. 1.29a). Since RCC is not a urothelial disease, it only requires a partial or radical nephrectomy without ureterectomy (Fig. 1.29b).
- If RCC is misdiagnosed as UCRP, the patient would undergo an unnecessary extensive resection including a ureter and portion of bladder. On the other hand, if UCRP is misdiagnosed as RCC, partial or radical nephrectomy alone is not sufficient for its treatment.
- Furthermore, the medical oncologists will use regimens such as gemcitabine or cisplatin-based neoadjuvant chemotherapy for UCRP patients, which are significantly different from treatment for RCC patients such as tyrosine kinase inhibitors (sorafenib, sunitinib), mTOR pathway inhibitors (i.e., everolimus), immune therapy with IL2, specific monoclonal antibodies (bevacizumab against VEGF), or PD1/PD-L1 inhibitors.
- Important clinical features allowing distinction of UCRP from RCC are listed in Table 1.29.

References: [17, 129–133].

Table 1.29 Clinically significant differences between UCRP and RCC

Parameter	UCRP	RCC
Tumor location	Hilar/pelvic region	Renal cortex or medulla
Clinical presentation	Hematuria common and occur at the early tumor stage	Hematuria is a sign of late stage with invasion into renal pelvis
CT/MRI	Pelvic mass if large enough	Renal mass
Ureteroscopy	Mass lesion	Negative
Intravenous pyelogram/ retrograde pyelography (IVP/ RPG)	Positive filling defect	Negative
Urine cytology	Positive	Negative
Preoperative diagnosis	Ureteroscopic biopsy	CT-guided percutaneous needle core biopsy
Cystoscopy	Necessary before and after nephrectomy to rule out lower tract urothelial carcinoma	Unnecessary; no risk of coexisting urothelial carcinoma
Ureter margin	Often need evaluation on frozen section	Not evaluated on frozen section
Surgery	Radical nephrectomy + ureterectomy + bladder cuff	Partial or radical nephrectomy
Chemotherapy	Gemcitabine-, cisplatin-, or carboplatin-based therapy	Required only in advanced disease
Targeted therapy	Not established	Tyrosine kinase inhibitors, mTOR inhibitors, immune therapy

How to Distinguish Urothelial Carcinoma of the Renal Pelvis (UCRP) from RCC by Histopathology and Immunohistochemistry?

- Both UCRP and RCC can have similar clinical presentation mimicking each other. Due to significant differences in surgical and oncologic treatments for these two cancers, it is very important to distinguish UCRP from RCC on pathology diagnosis.
- With limited material from needle core biopsy or fine needle aspirate, it can be difficult to differentiate UCRP from RCC. Moreover, intraoperative frozen section diagnosis to distinguish UCRP from RCC is not accurate and should be avoided if possible. In such a situation, immunohistochemistry can be particularly useful.
- UCRP will be positive for GATA3, S100P, Uroplakin II/ III, high molecular weight cytokeratins (HMWCK), p63, and CK7/CK20. RCC will be positive for PAX8, CD10, RCC, vimentin, and other subtype specific markers (i.e., CAIX for clear cell RCC, AMACR and CK7 for papillary RCC, CD117 and CK7 for chromophobe RCC). However, it should be noted that approximately 18% of UCRP may be positive for PAX8, and a small percentage of RCC could express GATA3. Therefore, utilization of immunohistochemical panels is beneficial in difficult cases. The differential immunohistochemical profiles of these two morphologically overlapping tumors are summarized in Table 1.30 and Fig. 1.30.

Table 1.30 Distinction of UCRP from RCC by pathology and immunohistochemistry

Parameter/marker	UCRP	RCC
Origin	Pelvic urothelium	Renal parenchyma (epithelium of proximal and distal nephron)
Surface histology	Low- or high-grade papillary UC, carcinoma-in-situ	Normal urothelial mucosa
Gross	White friable mass in renal pelvis extending into the renal parenchyma	Bright yellow or tan mass of renal parenchyma rarely extending into the renal pelvis
Tumor border	Poorly defined	Well defined
Histology of invasive component	Small and large irregular nests of cells with mixed low- and high-grade nuclei	Alveoli, solid, or tubulo-papillary architecture with clear to oncocytic cytoplasm; variable nuclear grade
Desmoplastic response	Quite common	Rarely present
Glandular differentiation	Occasional	Always present
Squamous differentiation	Occasional	Extremely rare
GATA3	Positive	Negative
S100P; Uroplakin II/III	Positive	Negative
p63	Positive	Negative
HMWCK	Positive	Negative
CK20	Positive in 50–70% cases	Negative
CK7	Positive	Positive in PRCC, clear cell papillary RCC, and chromophobe
PAX8	Occasionally positive	Uniformly positive
CD10, vimentin, RCC	Negative	Positive
CAIX	Negative	Positive in CCRCC
AMACR	Negative/weakly positive	Strongly positive in PRCC; focally positive in CCRCC

References: [17, 129, 130, 134–136].

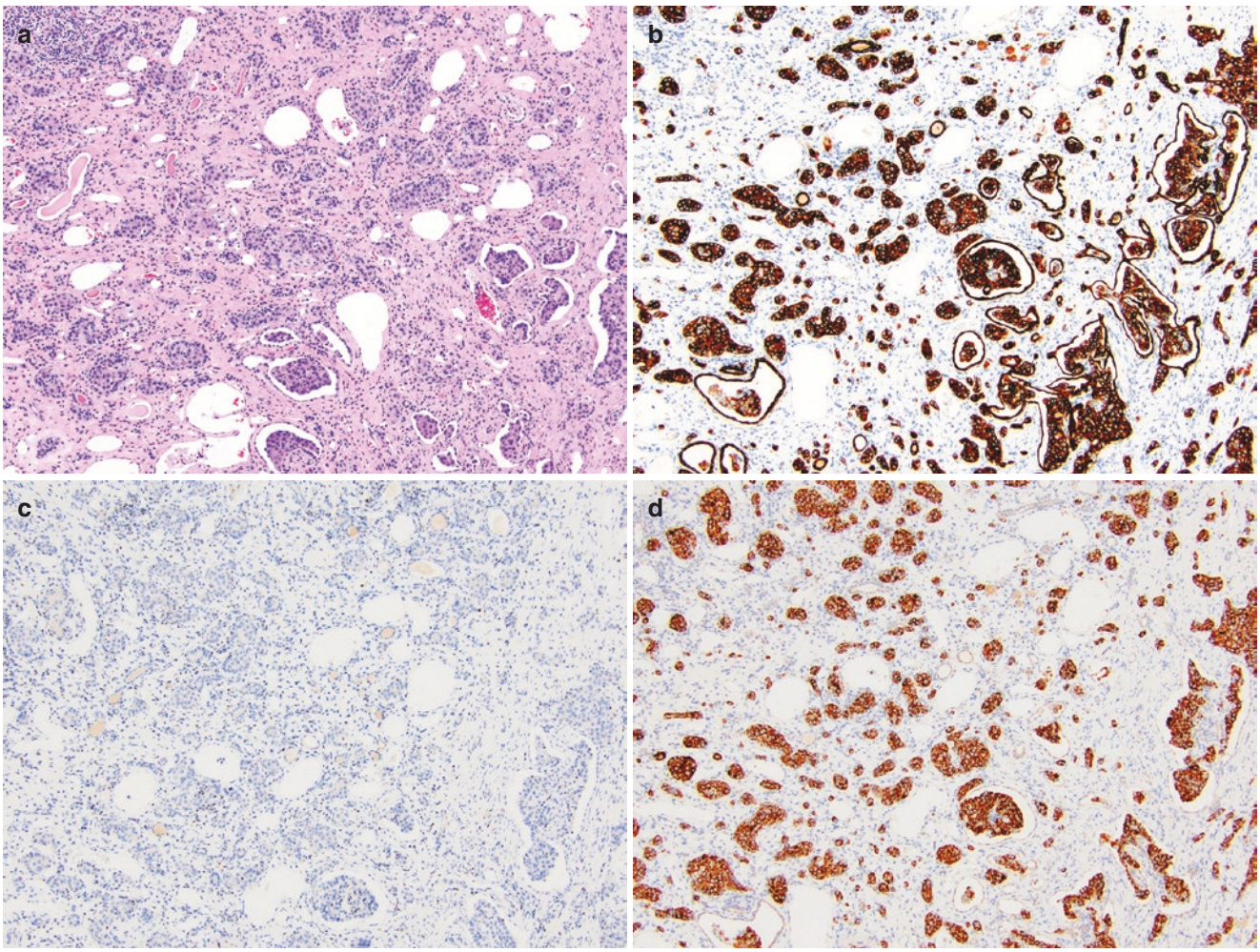

Fig. 1.30 (**a**) This medulla-centered tumor was composed of variably sized tumor nests infiltrating between benign kidney tubules and filling collecting ducts thus closely resembling urothelial carcinoma. (**b**) Strong expression of cytokeratin 7 in this case favors the following differentiation diagnosis: urothelial carcinoma vs. collecting duct carcinoma vs. papillary renal cell carcinoma. (**c**) Negative GATA3 expression in this case in inconsistent with urothelial origin. (**d**) Diffuse and strong expression of AMACR/P504 antibody supports papillary RCC diagnosis

Differential Diagnosis of Small Round Blue Cell Tumors

- "Small round blue cell tumor" (SRBCT) is a descriptive term referring to a large heterogeneous group of highly aggressive neoplasms, composed exclusively/predominantly of undifferentiated, small-sized cells with scant cytoplasm and round hyperchromatic nuclei. Due to their relative rarity in kidneys, similar morphology, and often overlapping immunohistochemical profiles, these tumors may be problematic to diagnose and classify. Moreover, the increasing use of small biopsies in daily practice makes correct diagnosis of these neoplasms even more challenging.
- The main differential diagnoses for SRBCT in pediatric population include Wilms tumor (nephroblastoma), neuroblastoma, clear cell sarcoma of the kidney (CCSK), and desmoplastic small round cell tumor (DSRCT), which are compared in Table 1.31a.
- The main differential diagnoses of SRBCT in adult patients include Ewing sarcoma/primitive neuroectodermal tumor (Ewing/PNET), small cell carcinoma (SmCC), lymphoma, and monophasic synovial sarcoma (SS), which are compared in Table 1.31b and Fig. 1.31a–c.

References: [137–147].

Wilms Tumor vs. Neuroblastoma

- Wilms tumor (nephroblastoma) and neuroblastoma (peripheral neuroblastic tumor) are among the most common childhood malignancies. Both tumors affect the same age group of patients often with similar clinical presentation and mor-

Table 1.31a Differential diagnosis of pediatric SRBCT

Parameter/ marker	Wilms tumor	Neuroblastoma	CCSK	DSRCT
Mean age	2–3 years	1–2 years	3 years	10–20 years
Gross	Circumscribed and encapsulated, nodular, rounded, soft friable tan or gray mass	Solitary mass with necrosis, cysts, and hemorrhage	Large (11 cm), unifocal, soft, mucoid with necrosis	Bulky (>10 cm) firm multinodular mass with necrosis and hemorrhage
Histology	Sheets of undifferentiated, small, closely packed, blastemal cells with nuclear molding	Sheets and rosettes of primitive cells, fibrillary matrix, and rare ganglion cells	Nests, cords, trabeculae of small blue cells with fine chromatin	Solid nests of round-to-oval cells, small blue cells within dense desmoplastic stroma
Survival	>90%	~70%	70%	2 years (median)
WT1	Positive nuclear	Cytoplasmic	Negative	Positive (C-term)
PAX8	Positive	Negative	Some positive	Negative
CD99	Often positive	Some positive	Negative	Some positive
NB84	Negative	Positive	Negative	Negative
Chromogranin	Negative	Positive	Negative	May be focal
Synaptophysin	Negative	Positive	Negative	May be focal
Cytokeratin/ EMA	Some positive	Negative	Negative	Positive
Desmin	Some positive	Negative	Negative	Positive, dot-like
Translocation	None	None	t(10;17) 10%	t(11;22)(p13;q12)
Genetic alterations	*WT1* mutations; *WT2, IGF2, CTNNB1, SIX1/2*; LOH 1p,16q	*N-myc* amplification; LOH 1p and 11q	*YWHAE-NUTM2B*; 85% *BCOR* duplication	*EWS-WT1*

Table 1.31b Differential diagnosis of adult SRBCT

Tumor type	Ewing/PNET	SmCC	Lymphoma	SS
Mean age	27 years	59 years	50–60 years	36 years
Gross	16 cm (mean) yellow lobulated infiltrating mass	Solid, soft, whitish gritty necrotic mass	Diffuse kidney enlargement or solid mass	11 cm (mean), necrotic cystic mass
Histology	Sheets of primitive small round cells and occasional rosettes	Small blue cells with molding, lots of mitoses and no visible nucleoli	Diffusely infiltrating or large sheets of discohesive cells	Monomorphic, highly cellular neoplasm with plump growing in short fascicles
Survival	2 years (median)	1–2 years	2 years	3 years (median)
FLI1	Positive nuclear	Negative	Negative	Negative
CD99	Positive diffusely	Negative	Some positive	Positive
BCL2	Negative	Negative	Positive	Positive
TLE1	Negative	Negative	Negative	Positive
CD45/CD3/ CD20	Negative	Negative	Positive	Negative
Chromogranin	Some positive	Positive	Negative	Negative
Synaptophysin	Some positive	Positive	Negative	Negative
Pan-cytokeratin	Focally positive	Dot-like	Negative	Positive focally
Translocation	t(11;22)(q24;q12)	None	Variable	t(X;18)(p11;q11)
Gene fusion	*EWS-FLI1*	None	Variable	*SYT-SSX*

phological features of undifferentiated small blue cells phenotype making their differential diagnosis challenging, especially on small biopsies. This is particularly true in case of blastemal predominant Wilms tumor and undifferentiated neuroblastoma, which are considered high-risk malignancies and require more aggressive treatment (Fig. 1.32a, b).

- Table 1.32 highlights significant differences in epidemiology, presentation, pathology, molecular findings, and ancillary studies of these tumors.

References: [148–153].

Wilms Tumor vs. Clear Cell Sarcoma

- Both Wilms tumor and clear cell sarcoma of the kidney (CCSK) arise in pediatric patients with peak incidence at 2–3 years, similar presentation, and overlapping morphology.

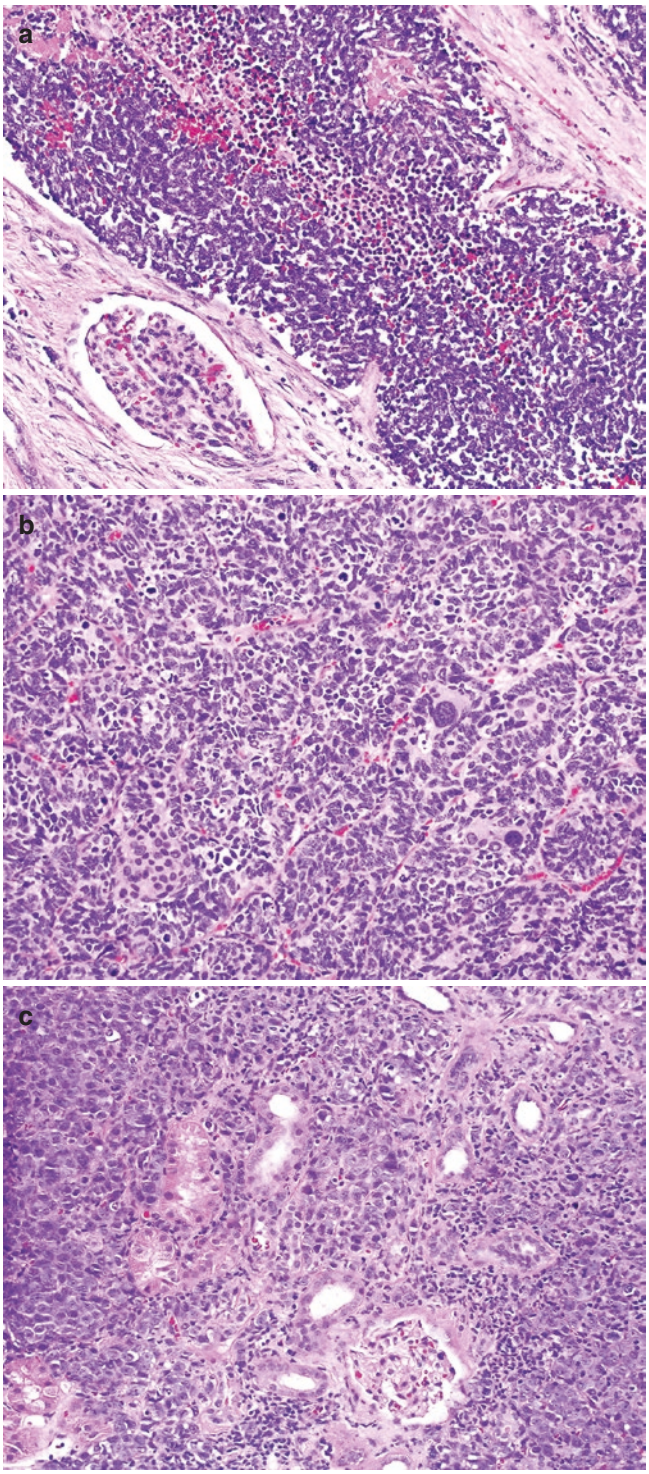

Fig. 1.31 (**a**) Primitive neuroectodermal tumor (PNET) of the kidney. (**b**) Small cell carcinoma with cell molding, lack of nucleoli, and abundant apoptotic debris. (**c**) Diffuse large B-cell lymphoma infiltrating between tubules and glomeruli

- In the National Wilms Tumor Study Group (NWTSG), CCSK is listed as a renal tumor with "unfavorable histology." Historically, CCSK was considered "Bone-metastasizing Wilms tumor," although this term is outdated since CCSK and Wilms tumor are unrelated.
- CCSK classically has three components: (1) small round-to-oval streaming (cord) cells with bland cytology and cytoplasmic clearing, (2) branching chicken-wire vessels forming fibrovascular septa (hallmark feature), and (3) intercellular mucoid matrix. Depending on cellularity and matrix prominence, CCSK could mimic either predominantly blastemal (more cellular) or predominantly stromal (less cellular) monophasic Wilms tumor (Fig. 1.33a, b).
- Table 1.33 highlights distinctive features of these two tumors.

References: [142, 147, 154–156].

Wilms Tumor vs. Rhabdoid Tumor

- Renal malignancies are quite common in children and a leader among them is Wilms tumor (nephroblastoma), representing ~85% of all diagnoses. Fortunately, Wilms tumor also has the best prognosis with overall survival exceeding 90%. Despite advances in treatment achieved with Wilms tumor, other pediatric renal tumors still have overall survival less than 70%. The most aggressive of all pediatric tumors is rhabdoid tumor with overall survival of 15–30%.
- Rhabdoid tumor was initially classified as a possible rhabdomyosarcomatoid variant of Wilms and historically included in the treatment protocols of the National Wilms Tumor Study (NWTS) Group. Absence of muscular differentiation coined the term rhabdoid tumor of the kidney (RTK), which is now recognized as a distinct tumor type of uncertain origin.
- RTK and Wilms tumor could share similar radiologic and morphologic features, especially with blastemal and anaplastic variant. In contrast to Wilms, RTK is characterized by an early onset of local and distant metastases (stage IV), and resistance to chemotherapy.
- Classic RTK exhibit cytological triad of vesicular chromatin, prominent cherry-red nucleoli, and hyaline pink cytoplasmic inclusions. However, many rhabdoid tumors lack characteristic cytologic triad and have the appearance of undifferentiated polyphenotypic tumor (Fig. 1.34a, b).
- A key to the RTK diagnosis is negative immunostaining for SWI/SNF-related, matrix-associated, actin-dependent regulator of chromatin, subfamily B, member 1 INI1.
- In Table 1.34, we outline the most important distinctive features of RTK vs. Wilms tumor, which should raise concern of this aggressive tumor and prompt diagnostic immunostaining.

References: [142, 154, 157–161].

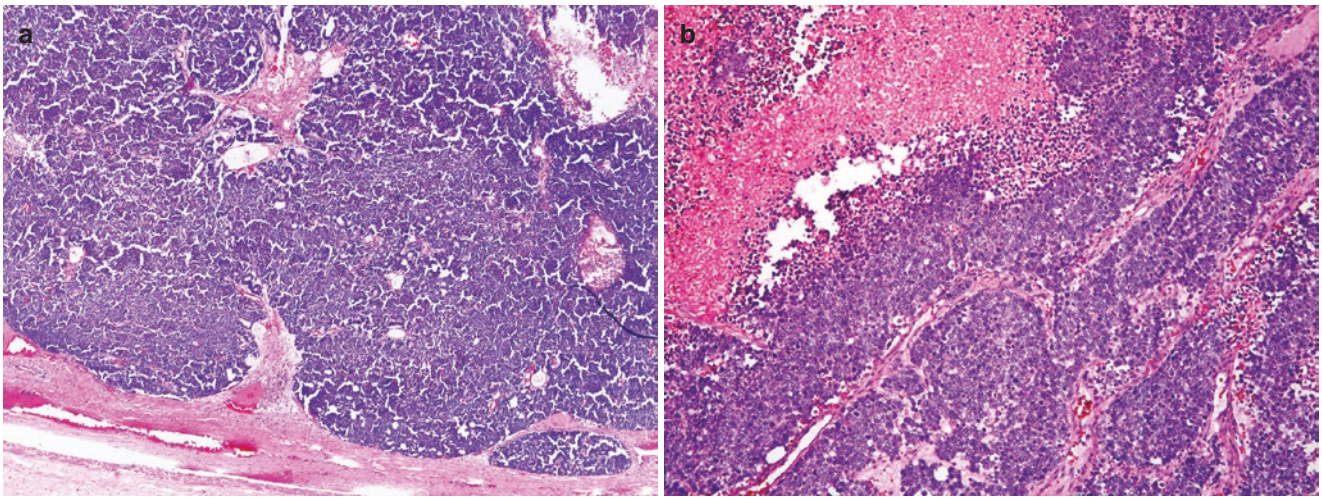

Fig. 1.32 (**a**) Wilms tumor (nephroblastoma) of predominantly blastemal morphology showing sheets of slightly spindled small blue cells. (**b**) Neuroblastoma with geographic necrosis and sheets of undifferentiated small blue cells

Table 1.32 Differential diagnosis of nephroblastoma (Wilms tumor) and neuroblastoma

Parameter/ marker	Wilms, blastemal predominant	Neuroblastoma
Frequency	Most common renal pediatric cancer; 6% of pediatric cancers	Most common extracranial pediatric solid cancer
Peak incidence	Slightly older: 2–4 years	1–2 years; 25% congenital
Syndromic associations	10% syndromic: i.e., trisomies 13 and 18, Beckwith-Wiedemann, WAGR, Denys-Drash, bloom syndromes	Sporadic; 1% autosomal dominant familial cases
Presentation	Hematuria, hypertension, and often painless palpable abdominal mass with mass effect	Nonspecific (fever, weight loss, anemia, HTN) plus painful palpable mass
Prognosis	>90% survival, depends on histologic category (favorable or unfavorable) and stage	>70% survival; depends on age, subclass (level of differentiation), histologic category, *N-myc* status, mitosis-karyorrhexis index, etc.
Cell of origin	Nephrogenic blastema	Neural crest cells, primordial
Location	Kidney-centered; unifocal (88%), bilateral (5%), multifocal (7%)	Abdominal (54%), adrenal-centered (36%), extra-adrenal (18%)
Gross	Circumscribed and encapsulated, nodular, rounded, soft friable tan or gray kidney mass	Solitary mass with necrosis and hemorrhage, 80% with calcifications; adrenal-centered, displacing kidney
Histology	Blastemal predominant composed of sheets of undifferentiated closely packed small cells with nuclear molding; rare rosette-like tubules	Sheets of small round blue cells; Homer Wright rosettes or pseudorosettes; fibrillary neutrophil matrix, rare ganglionic cells
WT1	Positive nuclear	Some cytoplasmic only
PAX8	Positive	Negative
NB84	Negative	Positive
PGP9.5	Negative	Positive
Chromogranin	Negative	Positive
Synaptophysin	Negative	Positive
NSE	Negative	Positive
Cytokeratin/ EMA	Some positive	Negative
Genetic alterations	*WT1* mutations (11p13); *WT2, IGF2, CTNNB1, SIX1/2*; LOH 1p,16q; 1q gain, p53 mutations	*N-myc* amplification (advanced stage); DNA ploidy, LOH 1p and 11q; *ALK* and *PHOX2B* mutations

Cystic Partially Differentiated Nephroblastoma vs. Pediatric Cystic Nephroma

- Unilateral multilocular cystic tumors in pediatric patients are represented by two different entities: cystic partially differentiated nephroblastoma and pediatric cystic nephroma. Both tumors affect young children, and have similar clinical presentation and undistinguishable radiologic and gross features causing significant diagnostic and therapeutic challenge. Definitive discrimination of these two entities should be based on detailed histologic assessment after rigorous tumor sampling.

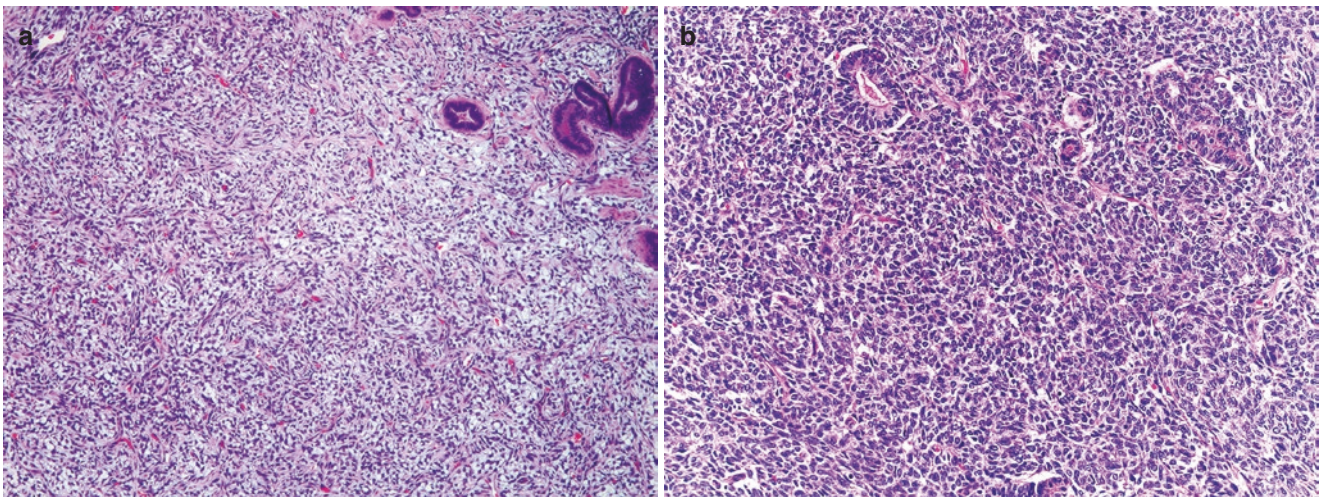

Fig. 1.33 (**a**) Clear cell sarcoma of the kidney composed of spindled clear cells embedded into intercellular mucoid matrix with chicken-wire vascular network and few entrapped tubules. (**b**) Wilms tumor of predominantly blastemal type composed of sheets of spindled hyperchromatic cells with scant cytoplasm and coarse chromatin and few epithelial-like tubules

Table 1.33 Differential diagnosis of Wilms tumor and clear cell sarcoma

Parameter/ marker	Wilms tumor (nephroblastoma)	Clear cell sarcoma of the kidney
Frequency	Common: ~85% of all pediatric renal malignancies	Uncommon: 3–5% of all pediatric renal malignancies
Cell origin	Nephrogenic blastema	Unknown, probably mesenchymal
Syndromic associations	10% syndromic: i.e., trisomies 13 and 18, Beckwith-Wiedemann, WAGR, Denys-Drash, bloom syndromes, etc.	None
Prognosis	>90% survival, depends on histologic category (favorable or unfavorable) and stage	~ 70% survival; more aggressive tumor with pelvic lymph node metastasis in 1/3 patients and propensity to distant metastasis to bone, lung, brain, and liver
Location	Kidney-centered; unifocal (88%), bilateral (5%), multifocal (7%)	Unifocal, initially medulla-centered
Gross	Circumscribed and encapsulated, nodular, rounded, soft friable tan or gray kidney mass	Large (11 cm), unifocal, soft, yellow, mucoid with necrosis; often distorting or replacing kidney
Histology	Blastemal, small, closely packed, hyperchromatic cells with molding, coarse chromatin, scant cytoplasm, or stromal component with nondescript spindled cells	Lobular architecture with thin fibrovascular septa separating nests, cords, and trabeculae of small blue spindled cells with bland cytological features; chicken-wire vessels
Patterns/ variants	Triphasic (>50%); predominantly blastemal, epithelial (tubular, rosette-like, papillary, glomeruloid), and predominantly stromal	Classic (~90%); also myxoid, sclerosing, cellular, epithelioid, palisading, storiform, spindle cell, and sinusoidal patterns
Other	Nephrogenic rests often present	No associated lesions
Anaplasia	~5% tumors	2–3% of primary or recurrent tumors
WT1	Positive nuclear, except stroma	Negative
PAX8	Positive	Some positive
CD99	Often positive	Negative
Cytokeratin/ EMA	Some positive	Negative
Desmin	Blastema often positive	Negative
Genetic alterations	*WT1* mutations (11p13); *WT2*, *IGF2, CTNNB1, SIX1*/2; LOH 1p,16q; 1q gain, p53 mutations (anaplastic cells)	85% *BCOR* duplication; *YWHAE- NUTM2B*; t(10:17) and –14q; p53 mutation in anaplastic variant

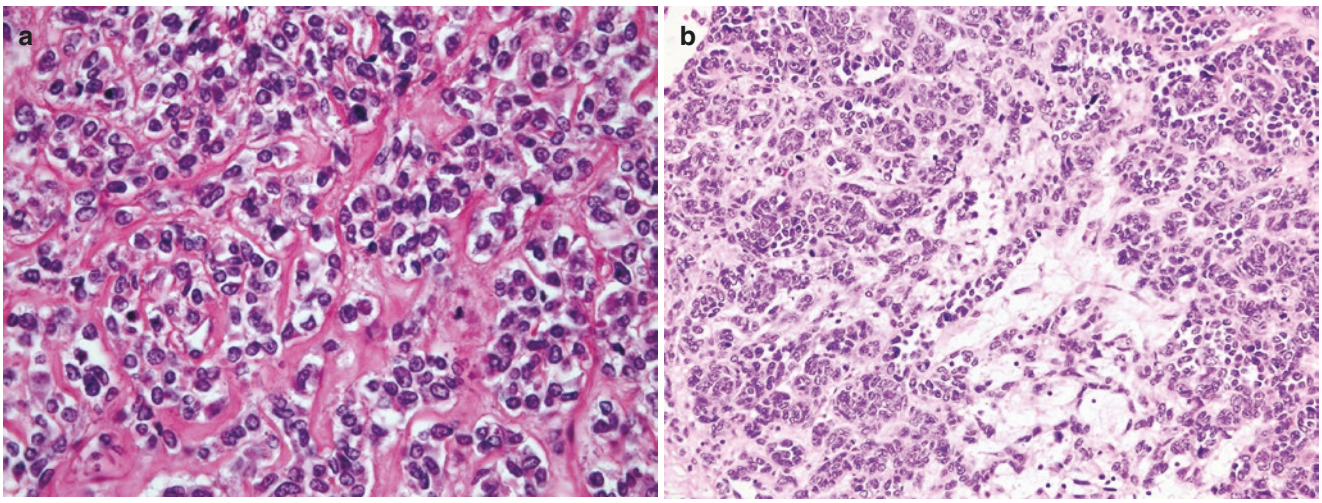

Fig. 1.34 (**a**) Rhabdoid tumor of the kidney composed of nests of undifferentiated cells with irregular nuclei and vesicular chromatin. (**b**) Wilms tumor of blastemal type with anaplastic features composed of pleomorphic cells with coarse chromatin and scant cytoplasm

Table 1.34 Differential diagnosis of nephroblastoma (Wilms tumor) and rhabdoid tumor

Parameter/ marker	Wilms tumor (nephroblastoma)	Rhabdoid tumor
Frequency	~85% of pediatric renal tumors	~2% of pediatric renal tumors
Peak incidence	2–3 years of age	1 year
Cell origin	Nephrogenic blastema	Unknown
Syndromic associations	10% syndromic: i.e., trisomies 13 and 18, Beckwith-Wiedemann, WAGR, Denys-Drash, bloom syndromes, etc.	30% have rhabdoid predisposition syndrome with *hSNF5/INI1* germline mutation
Symptoms	Palpable painless abdominal mass, hematuria, hypertension	Hematuria plus symptoms of widespread metastatic disease
Location	Kidney-centered; unifocal (88%), bilateral (5%), multifocal (7%)	Renal mass plus often concurrent brain/CNS or soft tissue mass
Gross	Circumscribed and encapsulated, nodular, rounded, soft friable tan or gray kidney mass	Large (9.6 cm) irregular infiltrative unencapsulated mass with extensive hemorrhages and necrosis
Histology	Blastemal, small, closely packed, hyperchromatic cells with molding, coarse chromatin, and scant cytoplasm; larger anaplastic cells (3x) with hyperchromasia and multipolar mitoses	Discohesive sheets of polygonal cells with occasional globular or hyaline inclusions and eccentric nuclei ("rhabdoid"); nuclei usually pleomorphic, with vesicular chromatin and large cherry-red nucleoli
Associated lesions	Nephrogenic rests often present	15% patients with synchronous PNET-like brain mass
WT1	Positive nuclear: 75% blastema, 44% stroma	Cytoplasmic, but reported nuclear with C-terminus antibody
INI1/BAF47	Intact nuclear expression	Loss of nuclear expression
Cytokeratin/ EMA	Some positive	Positive, but focal
Desmin	Blastema could be positive	Often positive
Genetic alterations	*WT1* mutations (11p13); *WT2, IGF2, CTNNB1, SIX1/2*; LOH 1p,16q; 1q gain, p53 mutations (anaplastic cells)	Biallelic inactivation of *hSNF5/INI/SMARCB1* tumor suppressor gene (mutation or deletion of 22q11.2)
Prognosis	>90% survival, depends on histologic category (favorable or unfavorable) and stage	Dismal: 15–30% survival; 80% patients die within 2 years from diagnosis (improved with combined surgical/radio−/chemo−/ autologous stem cell transplant treatment)

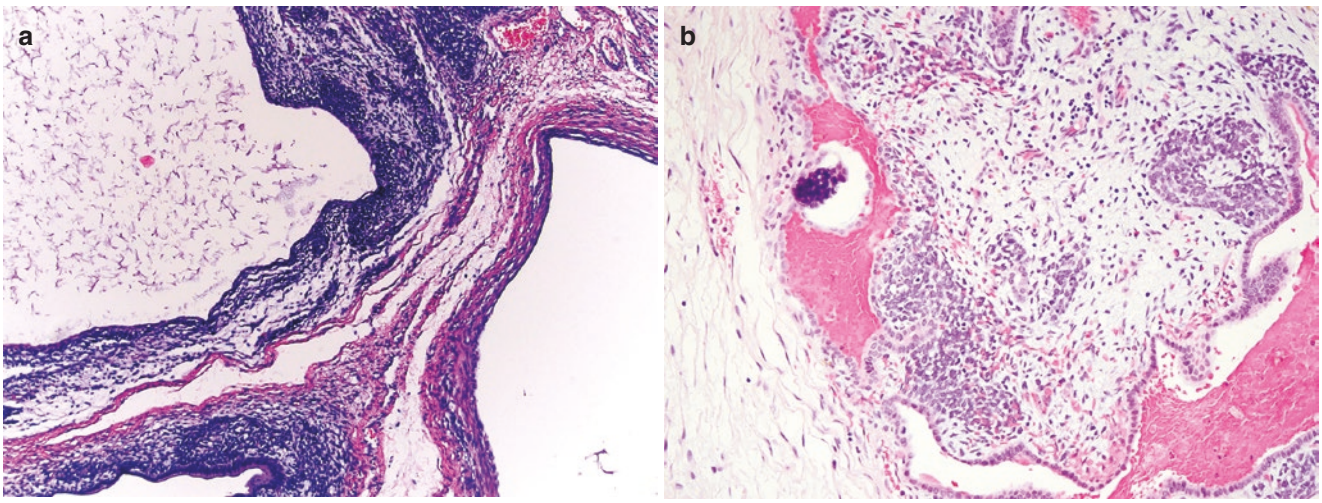

Fig. 1.35 Cystic partially differentiated nephroblastoma (CPDN) is characterized by multilocular architecture lacking expansile solid nodules (**a**) with fibrovascular septa containing immature nephroblastic elements (**b**)

- Cystic partially differentiated nephroblastoma (CPDN) is an indolent variant of Wilms tumor with pure multilocular architecture lacking discernible expansile nodules. Thin fibrovascular septa contain immature blastemal or differentiating epithelial elements that are not distorting septal contours or form expansile nodular areas (Fig. 1.35a, b). Due to low tumor burden, CPDN is characterized by indolent behavior with only two reported recurrences after incomplete resection or tumor spillage.
- Pediatric cystic nephroma (PCN) is a benign pediatric neoplasm composed of multilocular cysts with flattened, cuboidal, or hobnailed epithelium and fibrous septa with entrapped well-differentiated tubules lacking immature nephroblastic elements.
- PCN and CPDN have been regarded as part of the spectrum of Wilms tumor for a long time. However, recent molecular studies showed that *DICER1* mutations are the major genetic event in the development of PCN, which could be rarely detected in conventional Wilms tumors (0.4% cases), but not in CPDN.
- *DICER1* is mapped to chromosome 14q and function as a haplo-insufficient tumor suppressor gene. *DICER1* gene loss of function and hotspot missense mutations were seen respectively in 70% and 90% of PCN cases. Approximately, 30% of PCN cases arise in a syndromic setting with germline-inactivating *DICER1* mutations. These patients also develop more aggressive tumors including malignant pleuropulmonary blastoma (PPB), ovarian Sertoli–Leydig cell tumor, and urogenital embryonal rhabdomyosarcomas. Therefore, accurate diagnosis of PCN is crucial and should prompt further testing for *DICER1* mutations.
- Detailed differential diagnosis between CPDN and PCN is summarized in Table 1.35.

References: [162–170].

Table 1.35 Differential diagnosis of cystic partially differentiated nephroblastoma vs. pediatric cystic nephroma

Parameter/ marker	Cystic partially differentiated nephroblastoma	Pediatric cystic nephroma
Frequency	Rare	Rare
Peak incidence	12 months	18 months
Cell origin	Nephrogenic blastema	Urogenital sinus cells
Syndromic associations	10% syndromic: i.e., trisomies 13 and 18, Beckwith-Wiedemann, WAGR, Denys-Drash, bloom syndromes, etc.	30% with *DICER1* pleuropulmonary blastoma (PPB) familial tumor predisposition syndrome
Presentation	Usually asymptomatic abdominal mass; could be pain, hematuria	Usually asymptomatic abdominal mass; could be pain, hematuria
Gross	Entirely cystic well-circumscribed multiloculated mass; could be large (18 cm); no apparent solid expansile nodules; cysts with clear fluid	Entirely cystic well-circumscribed (9 cm mean size); thin septa (< 5 mm), translucent, uniform; cysts with clear or hemorrhagic fluid
Histology	Thin septations with clusters of immature blastemal cells, epithelial or mesenchymal derivates; no expansile nodules altering shape of septa; luminal papulonodular protrusions acceptable	Flattened, cuboidal, or hobnailed epithelial cyst lining; thin fibrous septa with areas of increased cellularity; entrapped well-differentiated tubules lacking immature nephroblastic elements
WT1	Positive nuclear, except stroma	Negative
ER/PR	Negative	50% cases positive
Cytokeratin/ EMA	Focal positivity only	Uniform strong positivity
Genetic alterations	*WT1* mutations (11p13); *WT2, IGF2, CTNNB1, SIX*1/2; LOH 1p,16q; 1q gain, p53 mutations (anaplastic cells)	*DICER1* gene loss of function (70%) and hotspot missense (90%)
Prognosis	Low-risk tumor, with local recurrence reported in few cases	Benign, but progression to renal sarcoma has been described

Rhabdoid Tumor vs. Rhabdomyosarcoma

- Malignant rhabdoid tumor of the kidney is a highly aggressive neoplasm that occasionally demonstrates phenotypic overlap with other soft tissue malignancies. This tumor was recognized as a distinct type in 1978 and characterized by large polygonal cells with eosinophilic cytoplasmic inclusions and eccentric nuclei suggestive of rhabdomyoblastic differentiation. However, ultrastructural examination revealed the filamentous nature of the cytoplasmic inclusions. Because of its striking microscopic resemblance to rhabdomyosarcoma but lack of acceptable rhabdomyoblastic features, this tumor was termed malignant rhabdoid tumor of the kidney (RTK) in 1981. Follow-up immunohistochemical studies also showed no expression of true myogenic markers in RTK.
- Pediatric rhabdomyosarcomas with exclusive/predominant solid growth pattern may be morphologically confused with RTK (Fig. 1.36). Both tumors are characterized by a frequent metastatic spread and poor prognosis, but their accurate distinction has important prognostic and treatment implications.
- The hallmark molecular feature of RTK is in biallelic inactivation of tumor suppressor gene *hSNF5/INI1/SMARCB1* from SWI/SNF chromatin remodeling complex. Resulting loss of INI1 protein nuclear expression is a key immunohistochemical finding.
- The most important distinctive features of rhabdoid tumor vs. rhabdomyosarcoma are summarized in Table 1.36.

References: [142, 158, 161, 171–174].

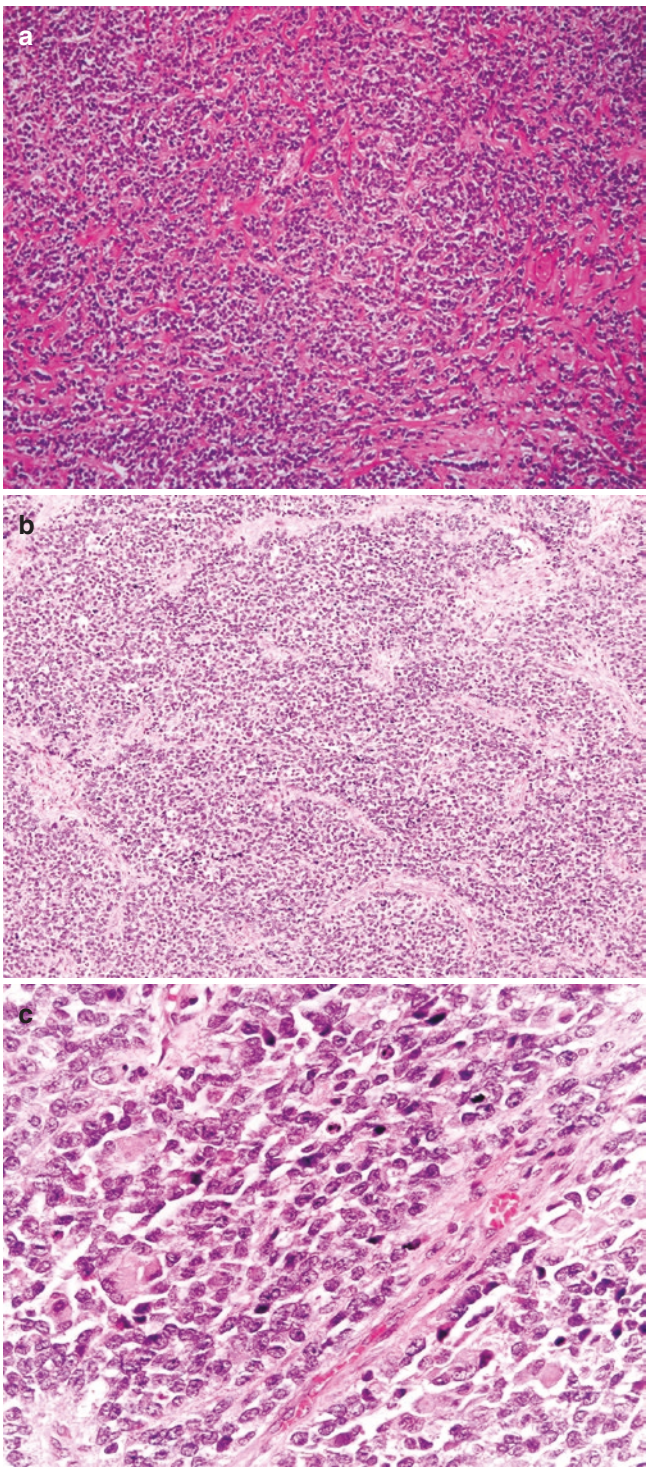

Fig. 1.36 (**a**) Malignant rhabdoid tumor (RTK) of the kidney with sheet-like architecture comprised of loosely cohesive ovoid-to-polygonal cells surrounded by a network of fibrovascular septa. (**b**) Embryonal rhabdomyosarcoma case with very similar to RTK morphology of highly cellular tumor with sheets of monotonous loosely cohesive cells. (**c**) The same tumor at higher magnification composed of spindle, ovoid, and polygonal eosinophilic cells representing rhabdomyoblasts at different stages of differentiation

Mesoblastic Nephroma vs. Wilms Tumor

- Congenital mesoblastic nephroma (CMN) is a mesenchymal renal tumor that was distinguished from Wilms tumor in 1967. CMN is the most frequent renal tumor in the neonates and infants comprising 3–10% of all childhood renal tumors (Fig. 1.37a, b). Three pathological variants of CMN are described: classic CMN (~25%), the more aggressive cellular CMN (~65%), and the mixed variant (~10%). Classic CMN has a good overall prognosis, but cellular CMN is associated with the potential for malignancy, and is capable of recurrence and metastasis. However, surgical resection with nephrectomy is considered an adequate therapy for all subtypes, provided that a complete resection is achieved.
- A differential diagnosis between CMN and Wilms tumor is critical to develop the most effective therapeutic approach. The examination of clinical symptoms, imaging characteristics, and histologic features shows that

Table 1.36 Differential diagnosis of rhabdoid tumor vs. rhabdomyosarcoma

Parameter/ marker	Rhabdoid tumor	Rhabdomyosarcoma
Frequency	~2% of pediatric renal tumors	5–8% of all pediatric tumors
Peak incidence	1 year of age	Bimodal peak: 2–4 and 14 years of age
Cell origin	Unknown	Mesenchymal stem cell
Syndromic associations	30% have rhabdoid predisposition syndrome with *hSNF5/INI1* germline mutation	None
Symptoms	Hematuria plus symptoms of widespread metastatic disease	Suddenly enlarging mass with local symptoms at site of origin
Location	Originally described in kidney, but could be extrarenal in CNS and soft tissue	Deep mass (retroperitoneum, pelvis, genitourinary, etc.); widespread dissemination
Gross	Large (9.6 cm), irregular, infiltrative, unencapsulated mass with extensive hemorrhages and necrosis	Fleshy mass with infiltrative borders, tan cut surface, frequent necrosis and hemorrhage
Histology	Discohesive sheets of polygonal cells with occasional globular or hyaline inclusions and eccentric nuclei ("rhabdoid"); nuclei usually pleomorphic, with vesicular chromatin and large cherry-red nucleoli	Solid variant with sheets of medium-sized cells; vague alveolar architecture and variable degree of rhabdomyoblastic differentiation with cross-striations at higher power; nuclei round-to-oval with hyperchromasia
INI1/BAF47	Loss of nuclear expression	Intact nuclear expression
Myogenin	Negative	Positive
MyoD1	Negative	Positive
Desmin	Often positive (trapped in hyaline globule)	Positive, diffuse and strong
Genetic alterations	Biallelic inactivation of *hSNF5/INI/SMARCB1* tumor suppressor gene (mutation or deletion of 22q11.2)	Balanced translocation: *PAX3/7-FOXO1*: t(2;13), t(1;13); complex karyotypes and frequent LOH
Prognosis	Dismal: 15–30% survival; 80% patients die within 2 years from diagnosis (improved with combined surgical/radio−/chemo−/autologous stem cell transplant treatment)	Variable, depending on disease stage, site, and histologic type (alveolar much worse than embryonal); overall 5-year survival 64.5%

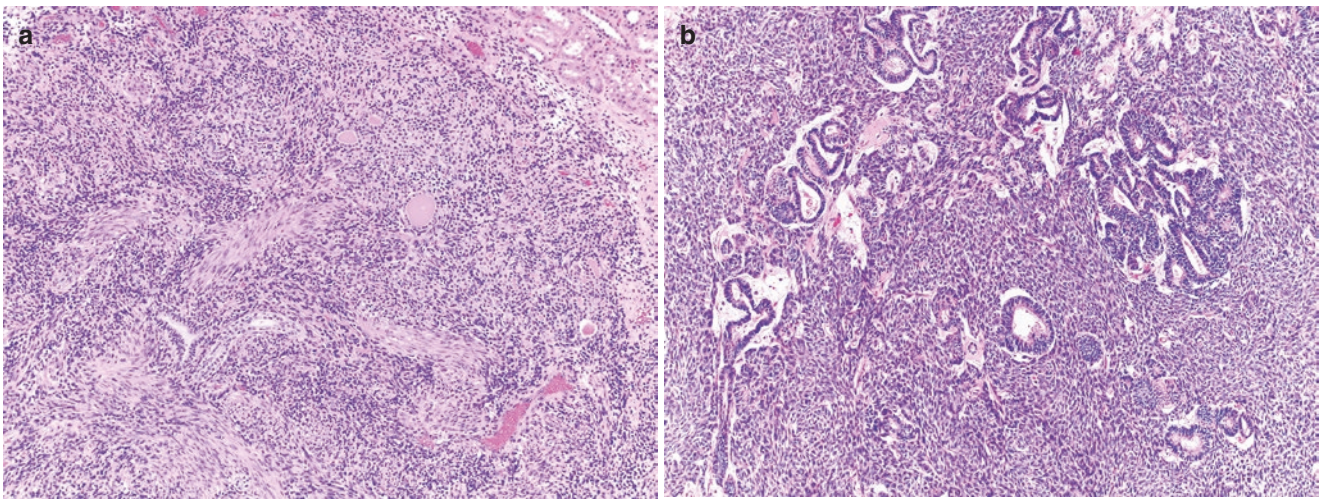

Fig. 1.37 (**a**) Classic variant of congenital mesoblastic nephroma with fascicles and bundles of spindle cells infiltrating between entrapped benign tubules. (**b**) Biphasic nephroblastoma (Wilms tumor) with blastemal and epithelial components

Wilms tumor has a lot of similarities with CMN, particularly the cellular variant. On the other hand, fewer than 2% patients with Wilms tumor (WT) present at under 3 months of age. Tumors with congenital syndromes or anomalies, and the presence of bilateral tumors are more suggestive of Wilms. These and other important characteristics allowing distinction of these two tumors are highlighted in Table 1.37.

References: [153, 159, 175–180].

Metanephric Adenoma vs. Congenital Mesoblastic Nephroma

- Metanephric kidney develops between fifth and ninth weeks of gestation and is derived from two main embryonic structures: nephrogenic blastema and embryonic bud. Nephrogenic blastema is composed of primitive tubules surrounded by cellular condensations developing into the glomeruli. The embryonic bud forms collecting system with cortical and medul-

Table 1.37 Mesoblastic nephroma vs. Wilms tumor

Parameter/ marker	Congenital mesoblastic nephroma	Wilms tumor
Frequency	Most common tumor of infancy	~85% of all pediatric renal tumors
Peak incidence	3 months; >90% occur in first year	2–3 years of age
Cell origin	Embryonic bud stem cells	Nephrogenic blastema
Syndromic associations	Rare association with Beckwith-Wiedemann syndrome	10% syndromic: i.e., trisomies 13 and 18, Beckwith-Wiedemann, WAGR, Denys-Drash, bloom syndromes, etc.
Location	Medulla-centric; infiltrating and extensively involving renal sinus	Kidney-centered; unifocal (88%), bilateral (5%), multifocal (7%)
Symptoms	Abdominal mass, polyhydramnios, premature delivery, hypertension	Abdominal mass, pain, hematuria, hypertension, acute abdominal crisis
Gross	Solitary, unilateral, whorled or trabeculated with gray-white or fleshy surface and indistinct borders; necrosis, cysts, hemorrhage common, but no prognostic significance	Sharply demarcated and often encapsulated, nodular, bulging, soft friable tan or gray kidney mass; could be whorled and firm if contains prominent stromal component
Typical histology	Cellular (2/3): Pushing borders, dense cellularity of spindly small blue myofibroblastic cells growing in fascicles, intersecting bundles, and showing high mitotic activity	Predominantly blastemal: Sheets of small, closely packed, mitotically active cells with scant cytoplasm and overlapping nuclei; admixed epithelial and stroma components
Stroma-rich variants	Classic (1/3): Infiltrating spindle cells resembling fibromatosis with minimal pleomorphism and mitoses; lobular architecture with finger-like extensions and entrapped tubules, glomeruli, islands of cartilage	Predominantly stromal: Nondescript spindled cells with minimal pleomorphism and mitoses within loose, myxoid background; could show rhabdomyoblastic, fibroblastic, or smooth muscle differentiation
WT1	Negative	Positive nuclear expression: 75% blastema, 44% stroma
PAX8	Entrapped tubules only	Positive
Desmin	Negative	Blastema could be positive
Genetic alterations	t(12;15)(p13;q25) *ETV6-NTRK3* (cellular); aneuploidy 11,8,17 (classic)	*WT1* mutations (11p13); *WT2, IGF2, CTNNB1, SIX1/2;* LOH 1p,16q; 1q gain, p53 mutations
Prognosis	Excellent	>90% survival, depends on stage and histology (favorable or unfavorable)

lary ducts, rudimentary calyces and pelvis embedded into supporting mesoblastic stroma. These two components of metanephric kidney are morphologically recapitulated in metanephric tumors including metanephric adenoma (MA), metanephric adenofibroma (MAF), and metanephric stromal tumor (MST), as well as in congenital mesoblastic nephroma (CMN; see Fig. 1.38a, b).

Table 1.38 shows metanephric adenoma vs. congenital mesoblastic nephroma.

References: [68, 177–179, 181, 182].

What Are the Most Common Syndromes Associated with Renal Tumors?

Approximately, 4–5% of all renal tumors are associated with heritable autosomal dominant syndromes. In general, these renal tumors have an earlier age of onset, often multifocal and bilateral. Knowledge of molecular abnormalities, pathogenesis, specifics of renal pathology, and characteristic of extrarenal manifestations is important for early recognition of individuals and families at risk for early screening, active surveillance, and timely management (see Tables 1.39, 1.40, 1.41, 1.42, 1.43, and 1.44).

- Von Hippel-Lindau (VHL) Syndrome.
- Hereditary papillary renal cell carcinoma (PRCC).
- Birt-Hogg-Dube (BDH) syndrome.
- Hereditary leiomyomatosis renal cell carcinoma (HLRCC).
- Tuberous sclerosis complex (TSC).
- Hereditary paraganglioma-pheochromocytoma syndrome or
- Succinate Dehydrogenase (SDH) Complex deficiency syndrome.

References: [183–189].

Case Presentations

Case 1

Learning Objectives

1. To understand differential diagnostic considerations for renal mass biopsy.
2. To become familiar with the immunohistochemical profile of the tumor.
3. To generate a relevant differential diagnosis.

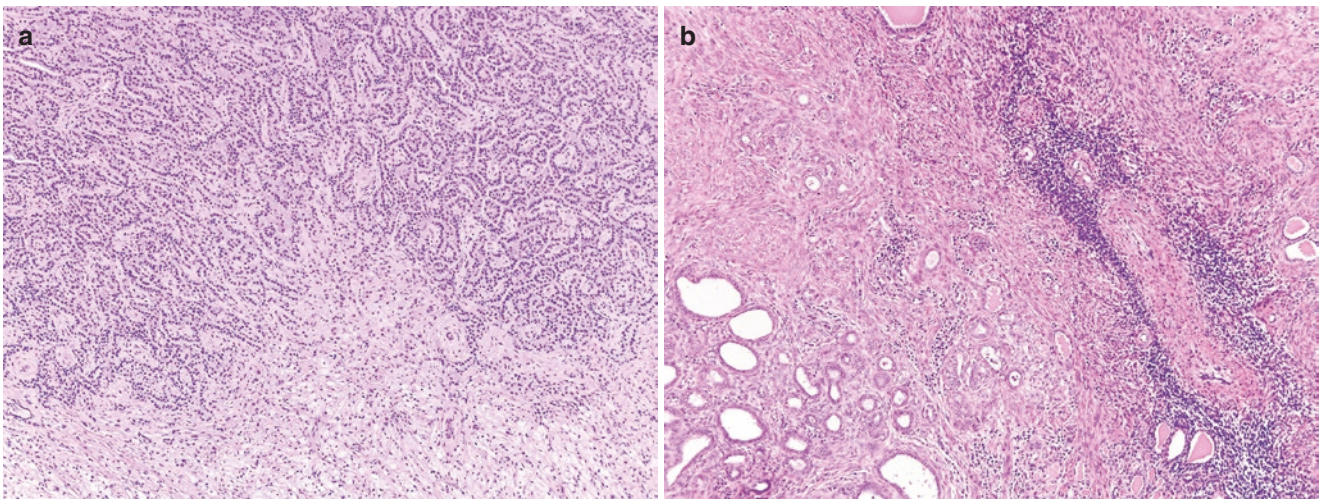

Fig. 1.38 (**a**) Metanephric adenofibroma composed of small blue cells arranged in tubules and papillary structures admixed with sheets of spindled cells within myxoid stroma. (**b**) Classic variant of congenital mesoblastic nephroma composed of tubules embedded into the cellular stroma with intersecting fascicles and bundles of spindle cells with minimal atypia

Table 1.38 Metanephric adenoma vs. congenital mesoblastic nephroma

Parameter/ marker	Metanephric tumors	Congenital mesoblastic nephroma
Frequency	Most common benign tumor in children, but could be seen in any age (range 1–83 years)	Most common tumor of infancy: >90% occur in first year
Location	Renal cortex (MA) or medulla-centric (MAF, MST)	Medulla-centric; infiltrating and extensively involving renal sinus
Symptoms	Usually asymptomatic incidental (>50%); 12% with polycythemia; pain, hematuria, hypertension	Abdominal mass, polyhydramnios, premature delivery, hypertension; Beckwith-Wiedemann syndrome
Cell origin	Persistent blastema cells	Embryonic bud stem cells
Gross	Unilateral, solitary, variable sizes (1–22 cm, mean 3.8–5.5 cm); well-circumscribed, unencapsulated, solid fleshy mass; calcifications in 20%; necrosis, hemorrhage, cysts <15%	Solitary, unilateral, whorled or trabeculated with gray-white or fleshy surface and indistinct borders; necrosis, cysts, hemorrhage common, but no prognostic significance
Typical histology	MA: Tightly packed tubules; papillary and glomeruloid structures; small blue crowded cells with scant cytoplasm; grooved nuclei without discernible nuclei	Cellular (2/3): Pushing borders, dense cellularity of spindly small blue myofibroblastic cells growing in fascicles, intersecting bundles, and showing high mitotic activity
Rare stroma-rich variants	MAF/MST: Spindled stellate cells forming collarets and concentric stromal rings around epithelium and vessels; angiodysplasia, myxoid stroma, hyalinization, calcifications, cysts, or heterologous elements	Classic (1/3): Infiltrating spindle cells resembling fibromatosis with minimal pleomorphism and mitoses; frequently lobular architecture with finger-like extensions and entrapped tubules, glomeruli, islands of cartilage
WT1	Positive in epithelium	Negative
CD57	Positive in epithelium	Negative
BRAF	Positive in epithelium	Negative
AMACR/CK7	Negative	Entrapped tubules
CD34	Positive in stroma	Usually negative
Genetic alterations	*BRAF V600E* mutation in 90% cases; 2p13 alteration in 56% cases	t(12;15)(p13;q25) *ETV6-NTRK3* (cellular); aneuploidy 11,8,17 (classic)
Prognosis	Benign; excellent	Benign; excellent

Case History

A 55-year-old man with history of pancreatic cancer is found to have multiple renal masses. Core biopsy is performed to evaluate for metastasis vs. primary renal neoplasm.

Gross

Core biopsy fragments of 1 mm diameter and 0.5–1.2 cm length are received.

Table 1.39 Von Hippel-Lindau (VHL) Syndrome

Parameter	Description
Gene	*VHL* (tumor suppressor), 3p25–26 3p loss plus *VHL* point mutations/deletions, LOH, hypermethylation
Pathogenesis	Absence of pVHL protein causes accumulation and overexpression of HIF-1α/HIF-2α and increased transcription of hypoxia-inducible genes and proteins: VEGF, PDGF, GLUT1, erythropoietin, CAIX, TGF-α, CXCR4
Renal involvement	Mean age 37 years; high penetrance (70% with RCC by age 70)
Renal tumors	Clear cell RCC (cystic and solid) in a background of numerous renal cysts
Extrarenal lesions	CNS hemangioblastomas, pheochromocytomas, pancreatic tumors and cysts, epididymal cystadenomas, endolymphatic sac tumors of ear
Treatment/ prognosis	Multiple nephron-sparing surgeries to reduce tumor burden and preserve kidney function; rare development of metastatic RCC

Table 1.40 Hereditary papillary renal cell carcinoma (PRCC)

Parameter	Description
Gene	*c-MET* (protooncogene), 7q31
Pathogenesis	Activating mutations/amplification of *c-MET* gene, accumulation of oncoprotein MET with tyrosine kinase function, inducing cell proliferation, stimulating tumor growth and invasion
Renal involvement	Mean age ~55 years; high penetrance (67% develop PRCC by age 60)
Renal tumors	Enumerable bilateral papillary adenomas (<1.5 cm) and PRCCs, type 1
Extrarenal lesions	None
Treatment/ prognosis	*c-MET*-inhibitors; nephron-sparing surgeries to reduce tumor burden and preserve kidney function; rare development of metastatic PRCC

Table 1.41 Birt-Hogg-Dube (BDH) syndrome

Parameter	Description
Gene	*Folliculin (FLCN),* tumor suppressor, 17p12-q11.2
Pathogenesis	Inherited germline mutation of 1 allele followed by frameshift and missense mutations in exons 4–14, hotspot exon 11; activation of mTOR pathway via loss of negative regulation of *FLCN*; cause abnormal differentiation of distal renal tubular cells
Renal involvement	Renal tumors at 50–54 years; low penetrance (~20% of BHD patients)
Renal tumors	Chromophobe RCC, oncocytoma, and hybrid oncocytoma/chromophobe tumors (HOCT) in a background of oncocytosis
Extrarenal lesions	Skin lesions (90%): Fibrofolliculomas, acrochordones, and trichodiscomas; lung cysts (83%) with spontaneous pneumothorax in 23–40%
Treatment/ prognosis	Nephron-sparing surgery; radiologic follow-up; >85% indolent tumors

Table 1.42 Hereditary leiomyomatosis renal cell carcinoma (HLRCC)

Parameter	Description
Gene	*FH* (tumor suppressor gene), 1q42.3–43
Pathogenesis	FH point mutations/deletions or whole gene mutations lead to loss of fumarate hydratase function in Krebs cycle; accumulation of fumarate and 2-succino-cysteine (2SC) with further activation of HIF-1 and its target genes stimulating tumor growth
Renal involvement	Mean age 36–46 years; low penetrance (2–20% of HLRCC patients)
Renal tumors	Unilateral and solitary high-grade and high-stage tumors with heterogeneous solid, papillary, tubular, and cystic architecture; most often morphology similar to papillary RCC, type 2. Hallmark feature: Prominent CMV-like large eosinophilic nucleoli
Extrarenal lesions	Uterine and cutaneous leiomyomas at young age
Treatment/ prognosis	Poor prognosis; most patients develop widely metastatic disease

Table 1.43 Tuberous sclerosis complex (TSC)

Parameter	Description
Gene	*TSC1* (encodes tumor suppressor hamartin), 9q34 *TSC2* (encodes tumor suppressor tuberin), 16p13.3
Pathogenesis	Germline mutations of *TSC1* or *TSC2* lead to activation of mTOR pathway and increased cell proliferation, metabolism, and cytoskeletal abnormalities
Renal involvement	Mean age 30–42 years; variable penetrance (80% for AML and 2.4% for RCC)
Renal tumors	Multiple and bilateral angiomyolipomas with variant histologies (triphasic, fat-rich, fat-poor, sclerosing, AMLEC, epithelioid); polycystic change. Heterogeneous group of RCC: Chromophobe RCC-like, clear cell RCC with smooth muscle stroma, or eosinophilic solid and cystic RCC
Extrarenal lesions	Brain: Cortical tubers, subependymal nodules, and giant cell astrocytoma; Skin: Shagreen patch, hypopigmented macules, facial angiofibroma, forehead plaque, ungula fibromas, retinal hamartomas; Lungs: Lymphangioleiomyomatosis; heart: Rhabdomyomas
Treatment/ prognosis	mTOR inhibitors; death from RCC uncommon

Table 1.44 Hereditary paraganglioma-pheochromocytoma syndrome or succinate dehydrogenase (SDH) complex deficiency syndrome

Parameter	Description
Gene	*SDHA* (5q15), *SDHB* (1p36), *SDHC* (1q21), *SDHD* (11q23)
Pathogenesis	75% mutations affect *SDHB*; germline mutations of SDH-genes plus LOH lead to loss of Krebs cycle related succinate-dehydrogenase enzyme in the inner mitochondrial membrane and loss of efficient electron transport; SDH-complex deficiency causes HIF overexpression and shift of cell metabolism toward anaerobic glycolysis and fatty acid synthesis
Renal involvement	Mean age 37 years; low penetrance (14% RCC by age 70)
Renal tumors	SDH-deficient RCC characterized by solid architecture, eosinophilic cells with pale vacuolated cytoplasm, and flocculent cytoplasmic inclusions
Extrarenal lesions	Pheochromocytomas, paragangliomas, carotid body tumors, GIST
Treatment/ prognosis	Surgical treatment; 2/3 tumors indolent

Histologic Findings

- Sections demonstrate cells with clear cytoplasm forming glands and tubular structures with a somewhat branched configuration in edematous, loose stroma (Fig. 1.39a).
- At higher magnification, there is a suggestion that nuclei are aligned at a similar height within the cytoplasm (Fig. 1.39b).

Differential Diagnosis

- Clear cell RCC.
- Clear cell papillary RCC.
- Papillary RCC with clear cell changes.
- Metastatic pancreatic cancer.

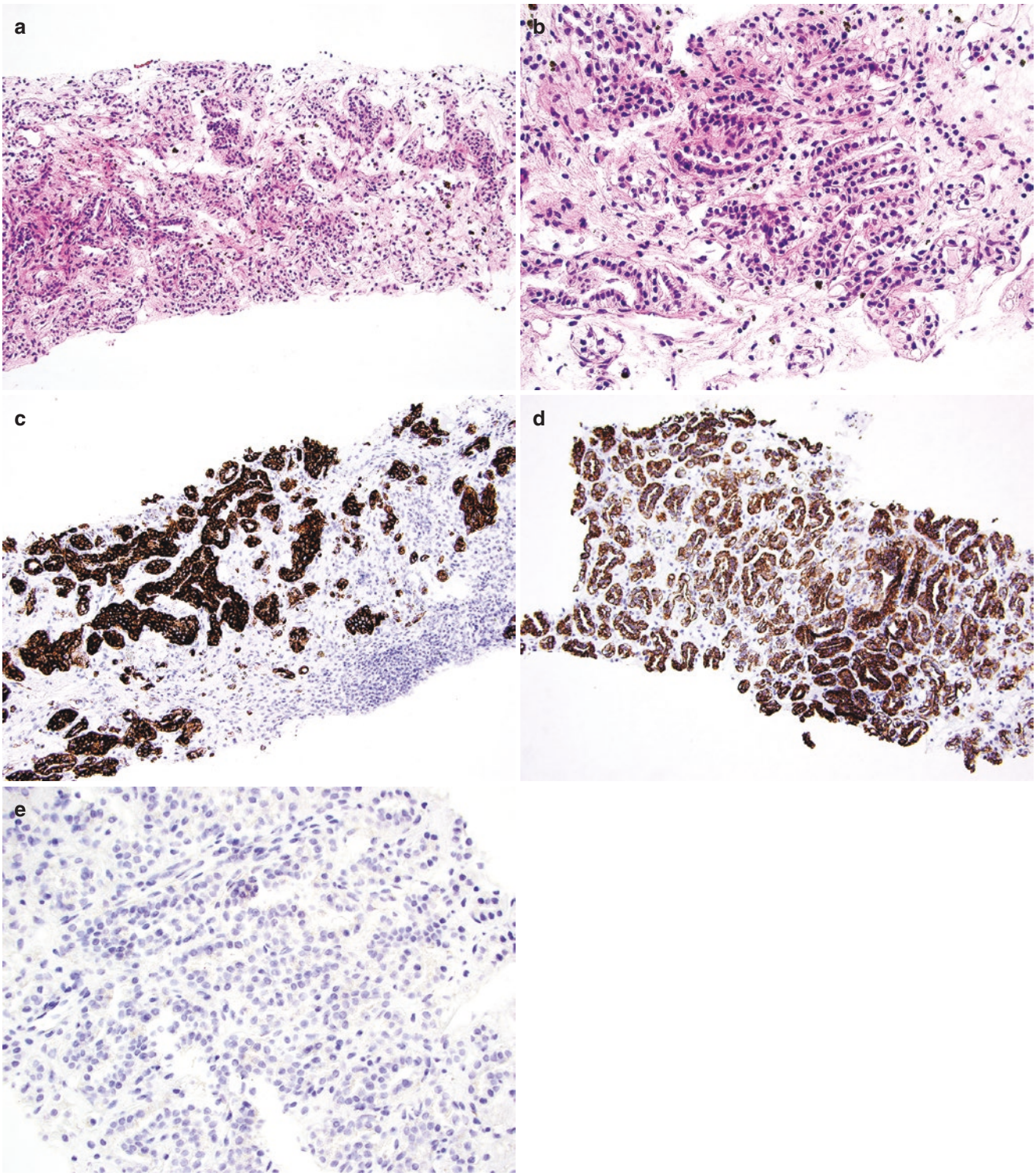

Fig. 1.39 (**a**) Renal mass biopsy shows a neoplasm composed of glandular structures in loose stroma. (**b**) Higher magnification demonstrates some alignment of nuclei at a uniform height in the cytoplasm. (**c**) Immunohistochemistry shows diffuse strong positivity for cytokeratin 7. (**d**) Immunohistochemistry also shows substantial positivity for high molecular weight cytokeratin. (**e**) Immunohistochemistry is negative for alpha-methylacyl-CoA racemase (AMACR)

IHC and Other Ancillary Studies

- Carbonic anhydrase IX diffusely positive with cup-shaped pattern.
- Cytokeratin 7 is diffusely positive (Fig. 1.39c).
- High molecular weight cytokeratin is diffusely positive (Fig. 1.39d).
- AMACR is negative (Fig. 1.39e).
- GATA3 is patchy positive.
- CD10 is negative.

Final Diagnosis

Clear cell papillary (tubulopapillary) RCC.

Take-Home Messages

1. Clear cell papillary RCC is a nonaggressive subtype of RCC that accounts for 3–4% of adult renal neoplasms.
2. Despite similarity to clear cell RCC morphologically, the immunohistochemical profile is distinctive (cytokeratin 7 positive, carbonic anhydrase IX positive, high molecular weight cytokeratin often positive, GATA3 often positive, AMACR negative, CD10 negative).
3. Aggressive behavior from a prototypical case has not been described to date, suggesting this may be reclassified as a low malignant potential or benign neoplasm in the future.
4. Some cases may have multifocal or bilateral tumors, for unknown reasons.
5. This entity is associated with end-stage renal disease; however, most cases likely occur in non-end-stage kidneys.

References: [4, 17, 29].

Case 2

Learning Objectives

1. To understand the differential diagnosis of renal cancers with clear cell and papillary features.
2. To apply relevant immunohistochemical profiles.
3. To understand the role of molecular testing in RCC.

Case History

A 40-year-old man presents for resection of a 5.5 cm renal mass.

Gross

Sectioning reveals a solid, yellow-tan renal mass that bulges from the normal contour of the kidney.

Histologic Findings

- Sections demonstrate a renal cancer composed of cells with clear cytoplasm, arranged in tubulopapillary structures with prominent nuclear alignment (Fig. 1.40a).
- Other areas demonstrate more papillary architecture with psammoma bodies (Fig. 1.40b).

Differential Diagnosis

- Clear cell RCC.
- Papillary RCC.
- Translocation-associated RCC.
- Clear cell papillary RCC.
- Unclassified RCC.

IHC and Other Ancillary Studies

- Cytokeratin 7 negative.
- Carbonic anhydrase IX negative.
- PAX8 positive.
- Melan-A focal positive.
- Break-apart FISH for *TFE3* shows a split signal pattern with small gaps between the signals.

Final Diagnosis

Translocation-associated RCC with *NONO-TFE3* fusion.

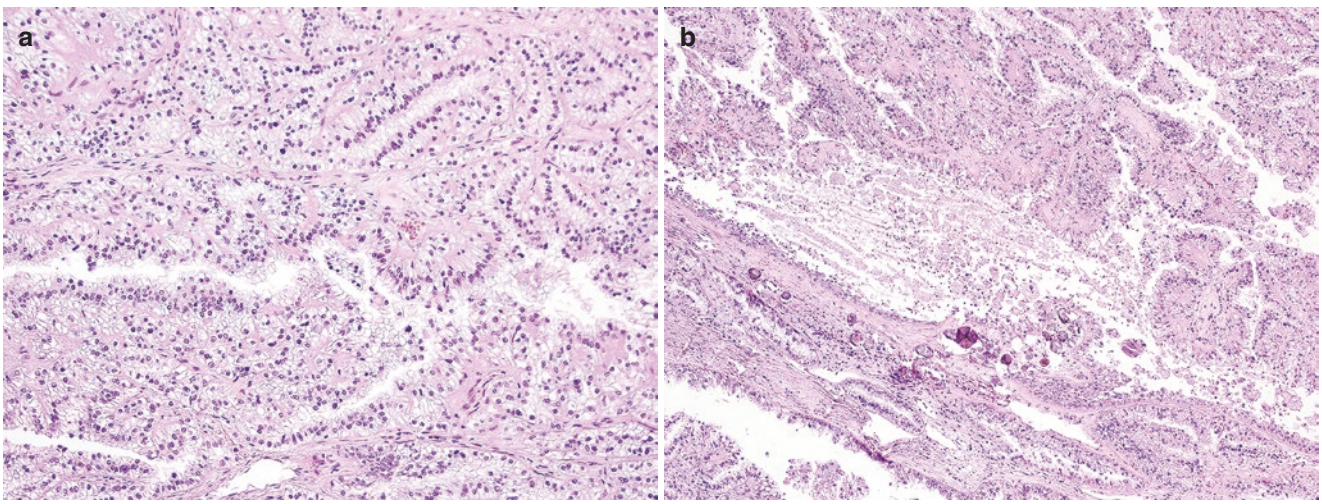

Fig. 1.40 (**a**) Histology demonstrates a renal cell carcinoma with clear to eosinophilic cells and papillary architecture with nuclear alignment. (**b**) More prominent papillary architecture and psammoma bodies are evident in other areas

Take-Home Messages

1. Translocation RCC is a relatively rare subtype of renal cancer.
2. Although children and young adults with RCC are more likely to have translocation tumors, there are likely more cases that occur in older adults in the conventional age range for renal cancer (>55).
3. Translocation tumors are consistently negative for carbonic anhydrase IX, positive for PAX8, and often have positivity for melanocytic markers or cathepsin-K.
4. Translocations *NONO-TFE3* and *RBM10-TFE3* can be difficult to detect with FISH, as both are caused by intrachromosomal fusions on the X chromosome, which may yield a small gap in the split signal, or a false-negative result.
5. *NONO-TFE3* and *SFPQ-TFE3* fusion tumors often have nuclear alignment resembling clear cell papillary RCC; however, psammoma bodies are not typical of the latter.

References: [35, 47, 49, 190].

Case 3

Learning Objectives

1. To recognize morphologic clues for diagnosis of oncocytic renal tumors.
2. To be familiar with immunohistochemistry for diagnosis of oncocytic neoplasms.
3. Integrate genetic findings in the differential diagnosis of oncocytic tumors.

Case History

A 58-year-old woman presented for resection of a 5.5 cm renal mass.

Gross

Sectioning reveals a circumscribed, solid, tan-brown renal mass with a pushing border.

Histologic Findings

- Some areas exhibit nests of oncocytic cells, reminiscent of oncocytoma (Fig. 1.41a).

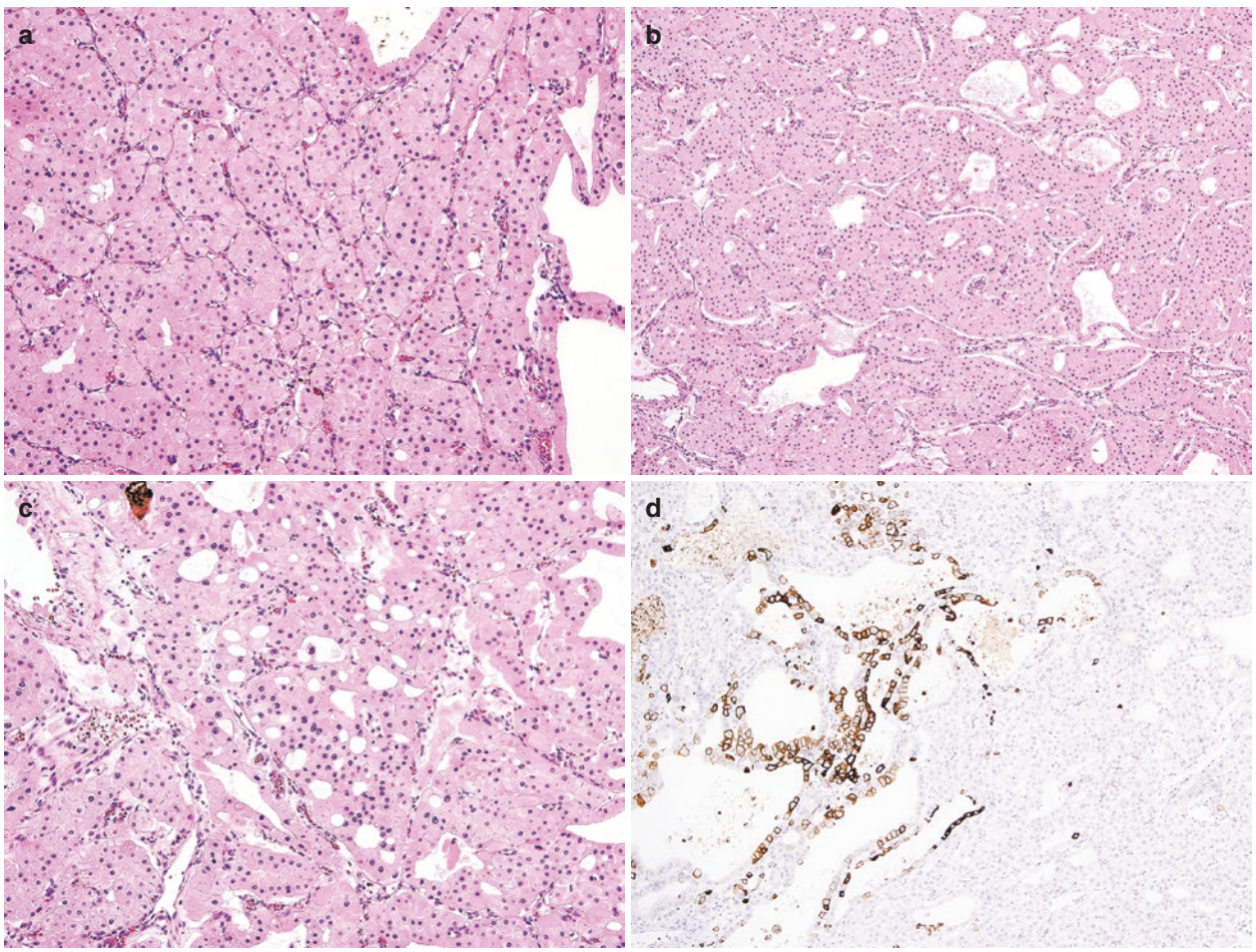

Fig. 1.41 (**a**) Histology demonstrates an oncocytic neoplasm with relatively round, regular nuclei. (**b**) Other areas of the same neoplasm show trabecular architecture. (**c**) Cribriform architecture and some nuclear size variation are also present. (**d**) Immunohistochemistry shows patchy confluent staining for cytokeratin 7

- Other areas contain large trabecular solid and microcystic structures (Fig. 1.41b).
- Higher magnification includes cribriform nests of cells with some nuclear irregularity and nuclear size variation (Fig. 1.41c).

Differential Diagnosis
- Oncocytoma.
- Chromophobe RCC.
- Succinate dehydrogenase-deficient RCC.
- Papillary RCC with oncocytic features.
- Unclassified RCC.

IHC and Other Ancillary Studies
- Cytokeratin 7 shows variable patchy staining with some confluent areas (Fig. 1.41d).
- Vimentin immunohistochemistry is negative.
- KIT (CD117) demonstrates positive membrane staining.
- FISH demonstrates losses of several chromosomes, including 1, 6, and 10.

Final Diagnosis
Eosinophilic variant chromophobe RCC.

Take-Home Messages
1. Distinguishing oncocytoma from chromophobe RCC remains challenging even today, despite numerous immunohistochemical and molecular markers that have been explored.
2. The most commonly used immunohistochemical method for distinguishing oncocytoma from chromophobe RCC is cytokeratin 7 staining, although a precise threshold of positivity that excludes oncocytoma is not well defined.
3. Oncocytoma generally should demonstrate only rare cells and small clusters of cells positive for cytokeratin 7.
4. Oncocytoma and chromophobe RCC are consistently negative for vimentin (except in central scar areas of oncocytoma) and usually positive for KIT.
5. Chromophobe RCC often exhibits losses of multiple chromosomes, particularly Y, 1, 2, 6, 10, 13, 17, and 21.

References: [21, 36, 84, 85].

Case 4

Learning Objectives
1. To understand the differential diagnosis of renal cancers with clear cell and papillary features.
2. To apply relevant immunohistochemical profiles.
3. To be able to counsel clinical colleagues regarding the behavior of RCC variants.

Case History
A 59-year-old man presents for resection of a 5.7 cm renal mass with invasion of the renal sinus.

Gross
Sectioning reveals a circumscribed renal mass with finger-like extensions into the renal sinus. The cut surface is golden-yellow.

Histologic Findings
- The neoplasm is composed of cells with clear cytoplasm lining branched glandular structures (Fig. 1.42a).
- Some areas have small formations of branched papillae (Fig. 1.42b).

Differential Diagnosis
- Clear cell RCC.
- Clear cell papillary RCC.
- Translocation RCC.
- Unclassified RCC.

IHC and Other Ancillary Studies
- Cytokeratin 7 demonstrates patchy (partial) positivity (Fig. 1.42c).
- Carbonic anhydrase IX exhibits diffuse membrane positivity (Fig. 1.42d).
- CD10 demonstrates substantial apical membrane positivity (Fig. 1.42e).
- AMACR demonstrates moderate to strong cytoplasmic positivity (Fig. 1.42f).

Final Diagnosis
Clear cell RCC (with areas mimicking clear cell papillary RCC).

Take-Home Messages
1. Some clear cell RCC tumors can demonstrate morphology overlapping with clear cell papillary RCC.
2. Although these tumors may have partial or substantial positivity for cytokeratin 7, they typically have an otherwise imperfect immunohistochemical profile for clear cell papillary subtype, such as with substantial positivity for AMACR and/or CD10.
3. High molecular weight cytokeratin, which is often positive in clear cell papillary tumors, is usually negative or focal in clear cell RCC, and GATA3 is typically negative.
4. Tumors with these overlapping features have been found to have chromosome 3p abnormalities, necrosis, high-stage parameters, and aggressive behavior, supporting exclusion from the diagnosis of clear cell papillary RCC.

References: [29, 60, 61].

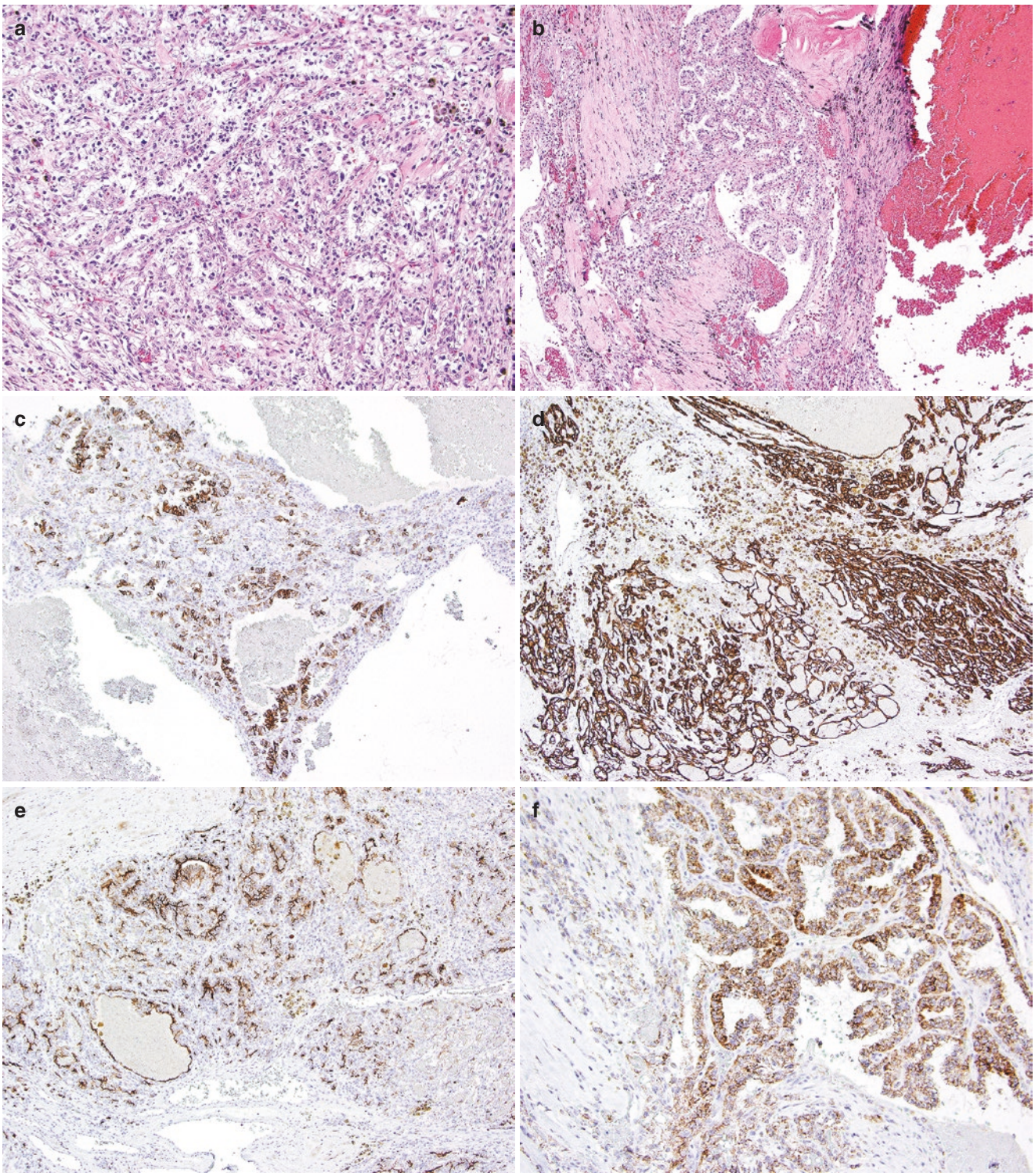

Fig. 1.42 (**a**) Histology demonstrates a neoplasm composed of clear cells arranged in glandular/papillary formations. (**b**) Other areas show small, branched papillary tufts protruding into small cystic spaces. (**c**) Immunohistochemical staining for cytokeratin 7 demonstrates partial but not diffuse positivity. (**d**) Carbonic anhydrase IX demonstrates diffuse positivity. (**e**) Substantial apical membrane positivity for CD10 is also present. (**f**) There is moderate to strong cytoplasmic staining for alpha-methylacyl-CoA racemase (AMACR)

Case 5

Learning Objectives

1. To become familiar with the histologic features of the tumor.
2. To become familiar with the immunohistochemical profile of the tumor.
3. To generate a relevant differential diagnosis.

Case History

A 45-year-old woman presented with polycythemia and a 2.5 cm renal mass. Partial nephrectomy was performed.

Gross

Sectioning reveals a solid, white-tan mass with homogeneous cut surface.

Histologic Findings

- Histology demonstrates a well-circumscribed but unencapsulated neoplasm composed of crowded basophilic cells (Fig. 1.43a).
- Higher magnification demonstrates crowded nests of basophilic cells (Fig. 1.43b).
- Other areas contain edematous stroma with small, tight clusters of basophilic cells with bland nuclei (Fig. 1.43c).

Differential Diagnosis

- Papillary RCC.
- Metanephric adenoma.
- Wilms tumor (nephroblastoma).

IHC and Other Ancillary Studies

- WT1 demonstrates diffuse nuclear positivity (Fig. 1.43d).
- CD57 demonstrates diffuse positivity.
- AMACR, cytokeratin 7, and epithelial membrane antigen are negative.

Final Diagnosis

Metanephric adenoma.

Take-Home Messages

1. Metanephric adenoma is a rare benign renal neoplasm composed of compact clusters of basophilic cells with bland nuclei.
2. Papillary architecture and psammoma bodies can be present.

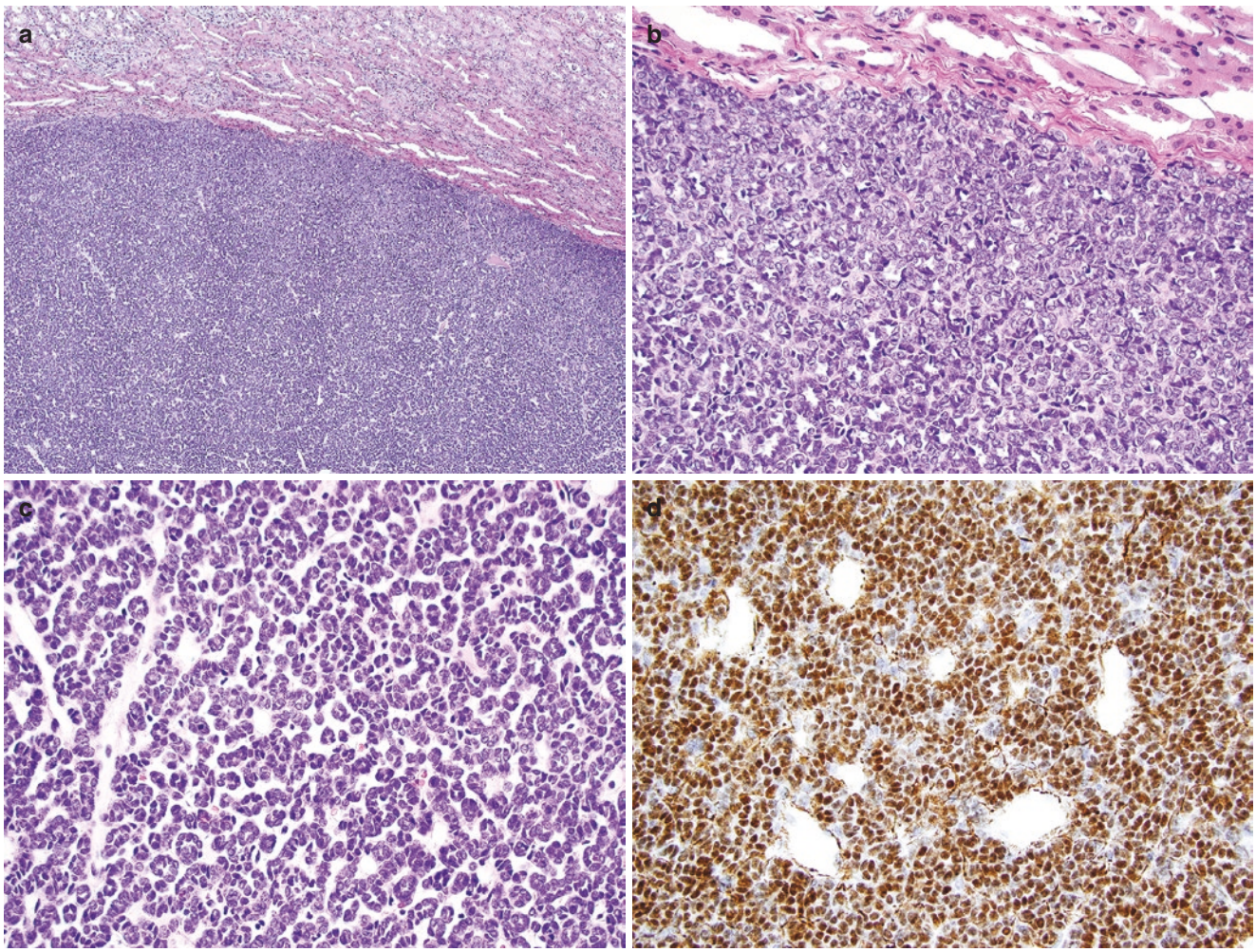

Fig. 1.43 (**a**) Histology demonstrates a circumscribed neoplasm composed of crowded basophilic cells. (**b**) Higher magnification reveals small nests reminiscent of solid papillary renal cell carcinoma. (**c**) Other areas are composed of cells with small, bland nuclei in edematous stroma. (**d**) Diffuse nuclear positivity with WT1 antibody

3. Morphologic features can overlap with papillary RCC and nephroblastoma; however, the immunohistochemical profile is helpful to distinguish these tumors.
4. Metanephric adenoma is typically positive for WT1 and CD57 and negative for AMACR and cytokeratin 7, whereas papillary RCC usually shows the opposite pattern.
5. The majority of metanephric adenomas harbor *BRAF* mutations and immunohistochemistry for the mutant BRAF protein often correlates with mutation.

References: [68–70].

Case 6

Learning Objectives
1. To become familiar with the histologic features of the tumor.
2. To become familiar with the immunohistochemical profile of the tumor.
3. To generate the differential diagnosis.

Case History
A 51-year-old female presented with history of long-standing diabetes and hypertension, with status post renal transplant. She developed hematuria, ureteral stricture, and hydronephrosis in her native kidney. Due to severe stricture and nonfunctioning kidney, the patient elected to have a right nephrectomy.

Gross
A nephrectomy specimen weighing 144 g is bivalved showing dilated renal pelvis and calyces with tan-white smooth and glistening urothelial mucosa. Renal parenchyma is markedly atrophic, pale brown with blurred corticomedullary junction and areas of vague nodularity.

Histologic Findings
- Urothelial lining of renal calyces overlies highly atypical cellular areas of spindled pleomorphic cells with numerous mitoses and discohesive growth (Fig. 1.44a).
- Haphazardly arranged sarcomatoid cells embedded into myxoid stroma and undermine urothelium without any obvious in situ urothelial carcinoma (UC). No low-grade or high-grade renal cell carcinoma (RCC) or invasive UC are identified (Fig. 1.44b).

Differential Diagnosis
- Sarcomatoid UC.
- Sarcomatoid RCC.
- Renal sarcoma.

IHC and Other Ancillary Studies
- CK7 strongly positive (Fig. 1.44c).
- GATA3 variably positive: strong in benign overlying urothelium and variable in sarcomatoid cells (Fig. 1.44d).
- PAX8 negative.

Final Diagnosis
Pure sarcomatoid urothelial carcinoma of the renal pelvis.

Take-Home Messages
1. Carcinomas with pure sarcomatoid morphology of kidney are extremely rare aggressive tumors and pose significant morphologic challenge.
2. Distinction between sarcomatoid RCC and sarcomatoid UC is very important due to different prognosis and patient management. This patient received additional surgical treatment with removal of the entire right ureter with bladder cuff.
3. Immunohistochemistry with pan-cytokeratins, urothelial markers, markers of RCC, or markers of sarcoma histogenesis is important in making this diagnosis.

References: [8, 93].

Case 7

Learning Objectives
1. To become familiar with the histologic and immunohistochemical features of the tumor.
2. To generate the differential diagnosis.

Case History
A 50-year-old male presented with back pain, weight loss, and hematuria.

Gross
Radical nephrectomy specimen with renal mass measuring 20.5 cm × 18 × 8 cm. On cut surface the tumor is partly cystic and partly solid with yellow-maroon variegated cut surface and friable necrotic hemorrhagic areas.

Histologic Findings
The neoplasm consists of sheets and nests of epithelioid cells with clear cytoplasm and well-defined cytoplasmic borders. Focal perinuclear clearing and nuclear wrinkling are seen. Other areas have a more prominent oncocytic appearance, in which the nuclei are round with prominent nucleoli and coarsely granular eosinophilic cytoplasm. There are also multiple entrapped benign renal tubules (Fig. 1.45a).

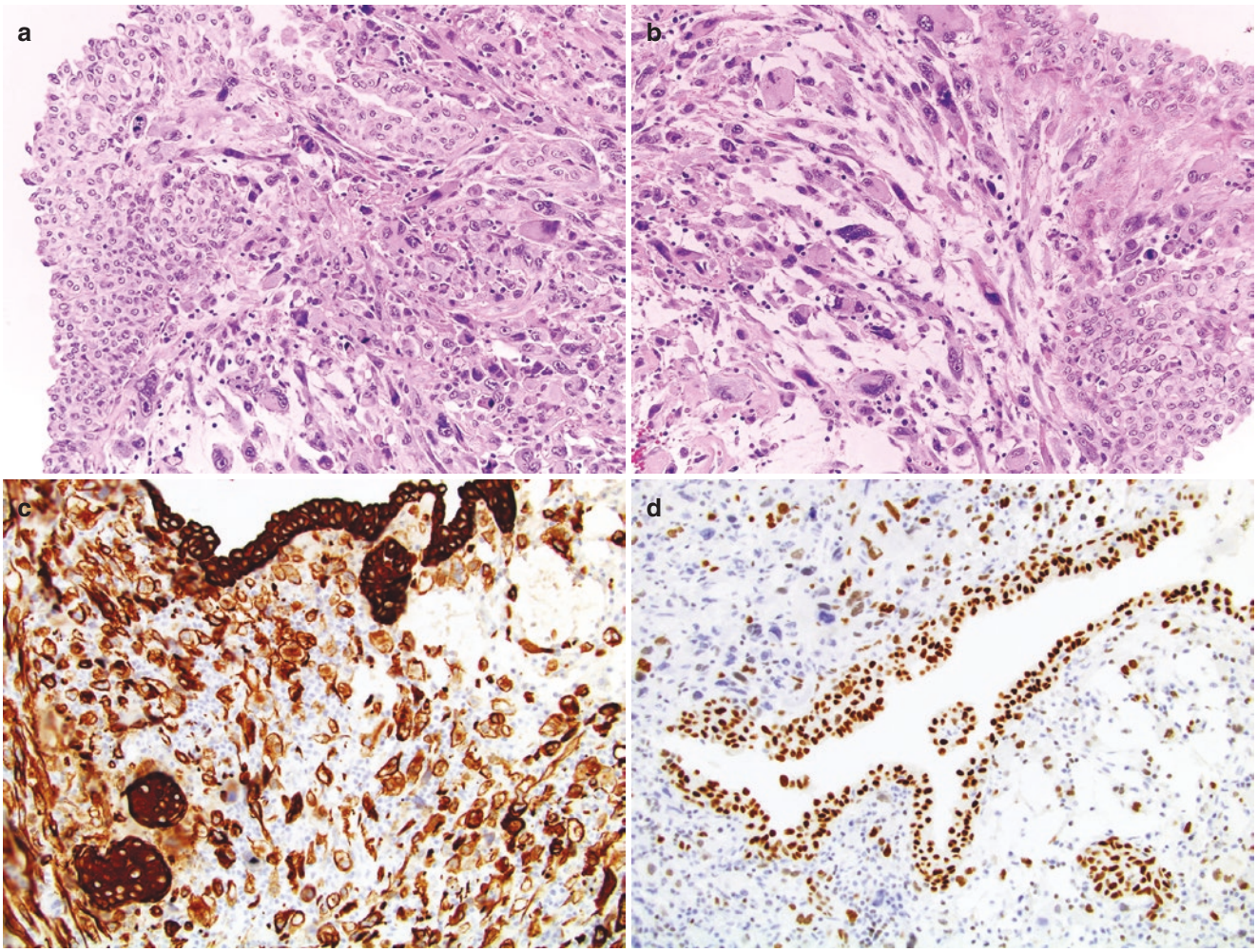

Fig. 1.44 (**a**) Histology shows high-grade pleomorphic cells undermining benign appearing surface urothelium of the renal pelvis. (**b**) Higher magnification reveals spindled malignant cells with multinucleation, hyperchromasia, and bizarre atypical nuclei. (**c**) Strong CK7 immunoreactivity in both infiltrating malignant tumor cells and urothelium. (**d**) GATA3 nuclear positivity is variable in sarcomatoid cells in contrast to strong expression in benign urothelium

Differential Diagnosis

- Clear cell renal cell carcinoma with eosinophilic features.
- Chromophobe renal cell carcinoma, eosinophilic variant.
- Oncocytoma.
- Epithelioid angiomyolipoma.

First Round of IHC Studies

- Positive immunostains: Vimentin, CAIX (focally), Cytokeratin 7 (focally).
- Negative immunostains: CD10, CKIT, TFE3.

Second Round of IHC Studies

- Positive immunostains: HMB45 (Fig. 1.45b), Melan-A (Fig. 1.45c).
- Negative immunostains: Smooth muscle actin (SMA).

Final Diagnosis

Epithelioid angiomyolipoma.

Take-Home Messages

1. Epithelioid angiomyolipomas (AMLs) show substantial morphologic overlap with oncocytoma and various subtypes of renal cell carcinoma posing diagnostic difficulties.
2. AMLs are always negative for PAX8, mostly negative for cytokeratins while positive for vimentin, SMA, and melanocytic markers.
3. Expression of melanocytic markers and SMA in epithelioid AML could be very focal or even negative; therefore, a panel of 3–4 markers may be necessary for definitive diagnosis.

References: [116, 117].

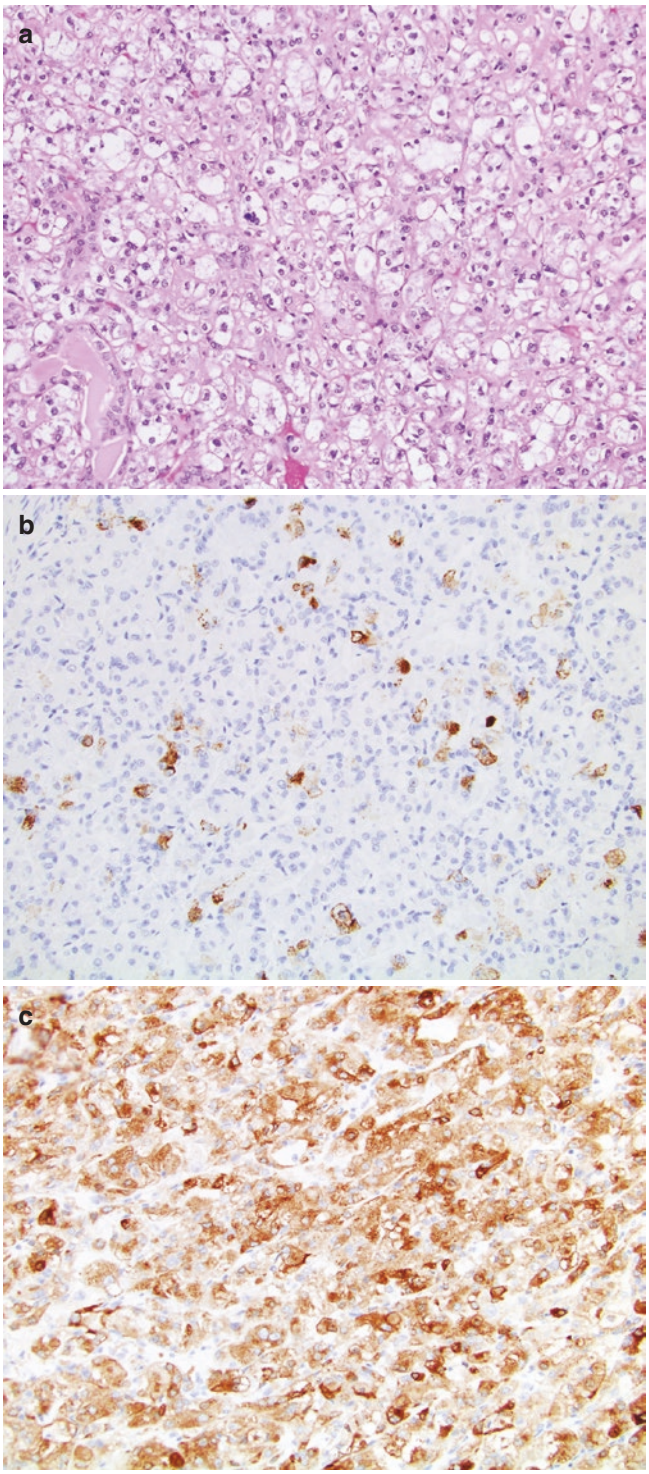

Fig. 1.45 (**a**) Histologically clear cell tumor composed of nests of epithelioid cells with sharp cell borders. (**b**) Immunohistochemistry demonstrates scattered HMB45 positivity. (**c**) Expression of another melanocytic marker Melan-A is more diffuse and uniform

Case 8

Learning Objectives

1. To become familiar with the histologic and immunohistochemical features of the tumor.
2. To generate the differential diagnosis.

Case History

The patient is a healthy 34-year-old female, former marathon-runner with two little children, who presented with acute flank pain and hematuria. Abdominal CT revealed a renal fatty mass with central density, consistent with hemorrhage.

Gross

Partial nephrectomy specimen with extrarenal 11.5 cm mass loosely attached to a portion of kidney parenchyma. On cut surface the mass has a central 7 cm hemorrhagic cavity surrounded by areas of brightly yellow discoloration.

Histologic Findings

At low power, this mass appears to be pure lipomatous neoplasm consisting of sheets of variably sized adipocytes with areas of hemorrhage (Fig. 1.46a). At higher power, the central portion of tumor shows extensive fat necrosis (Fig. 1.46b). At the periphery, tumor contains a few irregular thickened vessels and vascular channels surrounded by elongated plump smooth muscle cells (Fig. 1.46c). No obvious lipoblasts and pleomorphic atypical cells are identified. Renal parenchyma is unremarkable.

Differential Diagnosis

- Lipoma.
- Well-differentiated liposarcoma.
- Fat-rich angiomyolipoma.

Ancillary IHC Studies

- Positive immunostains: HMB45 (rare cells), Melan-A (focally positive).
- Negative immunostains: MDM2, CDK4.

Final Diagnosis

Lipomatous angiomyolipoma (AML).

Take-Home Messages

1. Angiomyolipomas can be fat-rich and predominantly extrarenal when arising from kidney capsule, thus mimicking retroperitoneal well-differentiated lipomatous tumors or even normal perinephric fat.
2. Presence of necrosis and hemorrhage raises concern for malignancy; however, vascular rupture and subsequent

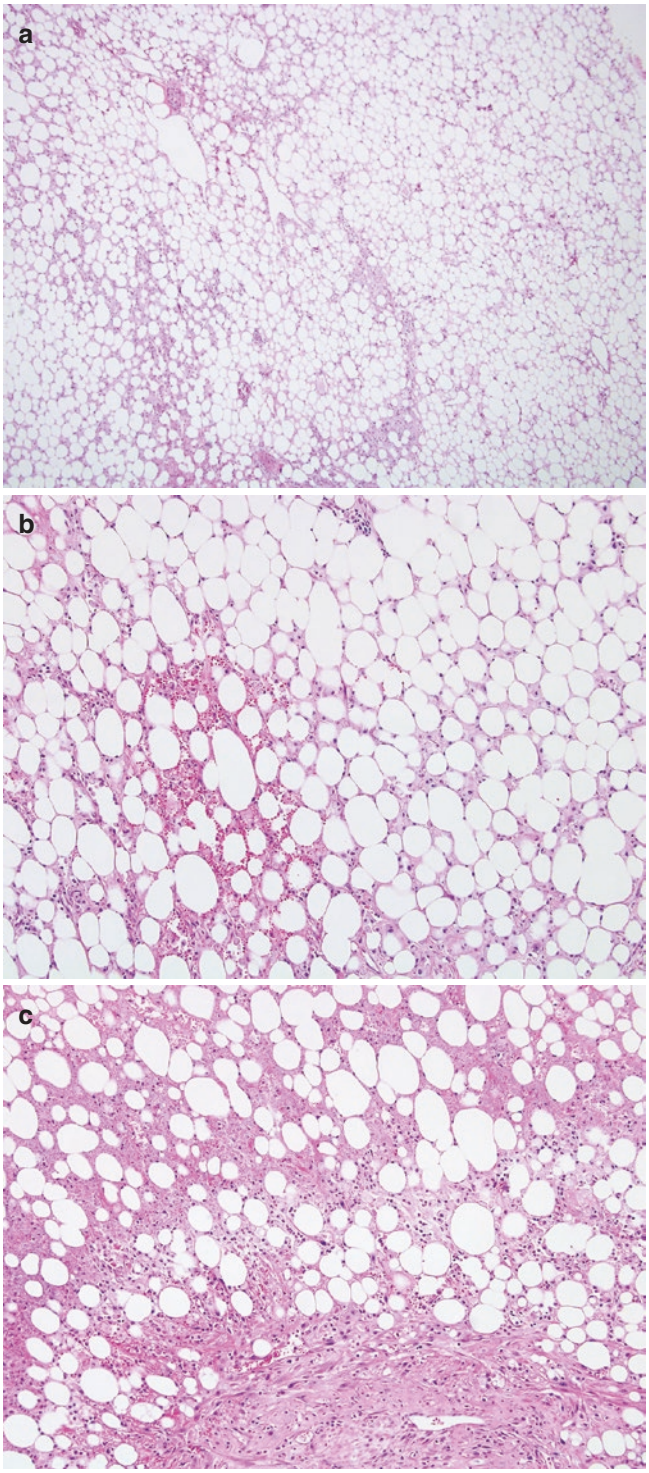

Fig. 1.46 (**a**) Large mass comprised of sheets of variably sized adipocytes. (**b**) Hemorrhage and fat necrosis were apparent at higher magnification. (**c**) Scant stroma represented by spindled plump eosinophilic cells surrounding dysmorphic vessels

ischemic necrosis are well-known complications in larger AMLs.
3. Expression of melanocytic markers and presence of dysmorphic vessels are critical in making a diagnosis of fat-rich AML, whereas smooth muscle actin and MDM2 could be nonspecific (expressed in both AML and well-differentiated liposarcoma).

References: [191, 192].

Case 9

Learning Objectives

1. To become familiar with the histologic and immunohistochemical features of the tumor.
2. To generate the differential diagnosis.

Case History

The patient is a 55-year-old female presented with a left upper quadrant pain after a mild body injury. Radiologic examination revealed a 2.1 cm solid mass with focal cystic change concerning for renal cell carcinoma, which was removed.

Gross

Partial nephrectomy specimen contains a 2.1 x 1.9 x 1.7 cm subcapsular mass with scattered cystic spaces and unremarkable adjacent renal parenchyma.

Histologic Findings

Low-grade mesenchymal neoplasm composed of fascicles and whorls of plump spindle cells surrounding small capillary channels and slit-like vascular spaces with nested, anastomosing pattern (Fig. 1.47a). Other histologic findings include a few cysts within a solid component lined by a single layer of flattened to cuboidal epithelium with hobnailing. These bland cells show eosinophilic cytoplasm, round nuclei, fine chromatin, and inconspicuous nucleoli (Fig. 1.47b).

Differential Diagnosis

- Leiomyoma with entrapped cystically dilated renal tubules.
- Angiomyolipoma with epithelial cysts (AMLEC).
- Mixed epithelial and stromal tumor (MEST).

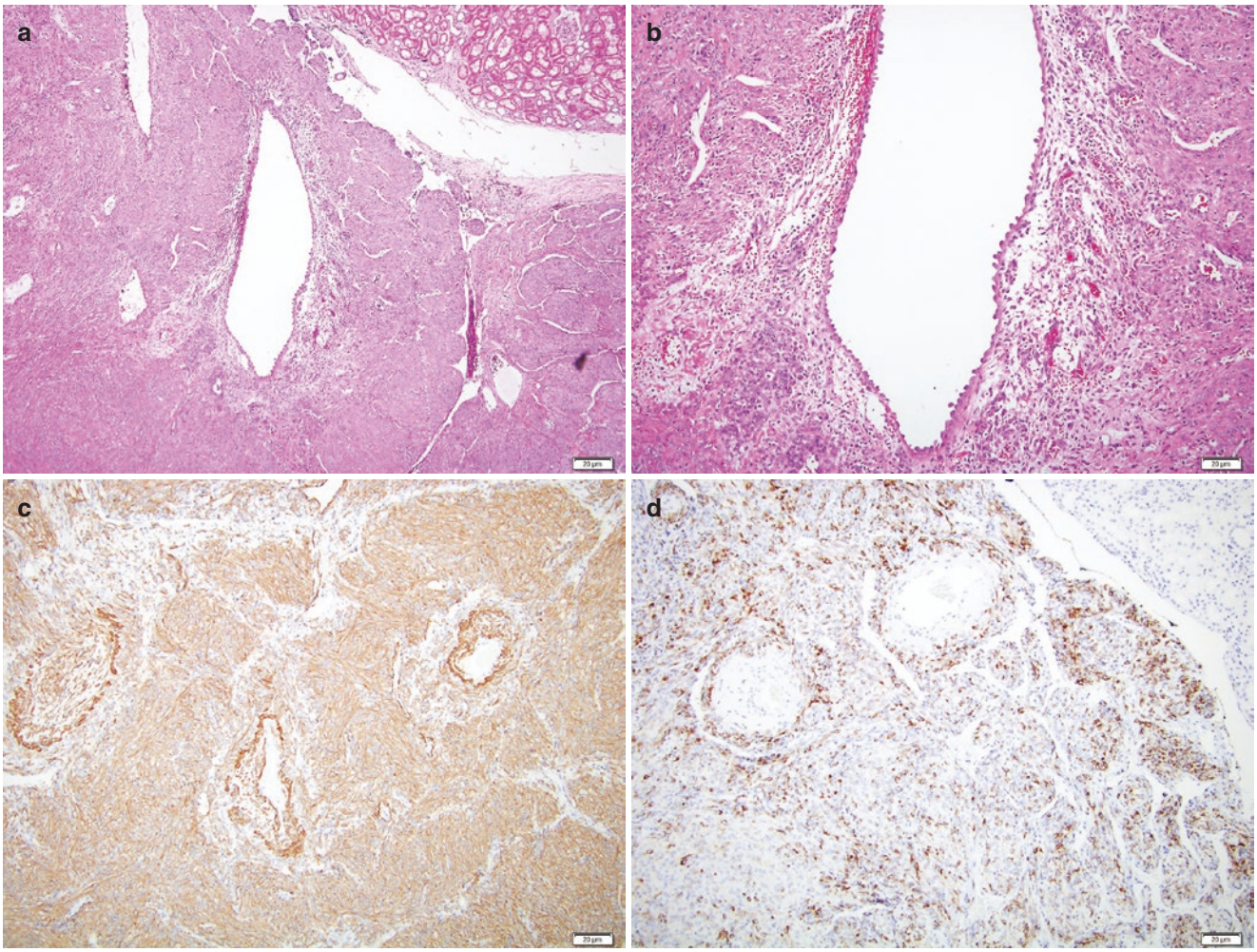

Fig. 1.47 (**a**) Histology demonstrated a smooth muscle neoplasm with scattered cystic spaces. (**b**) Cyst lined by a single layer of eosinophilic cells with hobnailing. (**c**) Immunohistochemistry shows diffuse expression of smooth muscle actin. (**d**) HMB45 expression is obvious in the majority of tumor cells

Ancillary IHC Studies

- Positive immunostains: stromal component positive for SMA (Fig. 1.47c) and HMB45 (Fig. 1.47d), as well as CD10, ER/PR, and vimentin; cyst lining positive for PAX8 and pan-cytokeratin.
- Negative immunostains: Melan-A, CD34, S100.

Final Diagnosis

AML with epithelial cysts (AMLEC).

Take-Home Messages

1. AMLEC is a rare variant of muscle-predominant AML mimicking MEST, but lacking ovarian-type stroma, stromal luteinization, and harboring abnormal vasculature.
2. Panel of melanocytic markers HMB45, Melan-A, and MITF is the most helpful ancillary study to diagnose AMLEC since other markers (SMA, caldesmon, CD10, ER/PR, vimentin) are shared by MEST.
3. AMLEC is a benign indolent tumor with excellent prognosis, whereas MEST could undergo malignant transformation.

References: [110, 113].

Case 10

Learning Objectives

1. To become familiar with the histologic and immunohistochemical features of the tumor.
2. To generate the differential diagnosis.

Case History

The patient is a 55-year-old male who presented with hematuria and acute abdominal pain. He was found to have an extremely large mass in the left kidney, small lesions in the

right kidney, and lymphadenopathy. The patient underwent left radical nephrectomy after embolization and regional lymph node dissection with a plan of subsequent potential second operation of right kidney exploration at a later date. His medical history is significant for pigmented cutaneous lesions, recent acute heart attack, aortic stenosis, and aortic valve replacement.

Gross

Radical nephrectomy specimen weighing 2813 gm is sectioned revealing a 14 × 13.5 × 10 cm tumor extending from the interpolar region into the pelvic fat. The tumor is 60% necrotic with large areas of hemorrhage. A second mass, measuring 5.0 × 4.0 × 2.5 cm, extends from the cortex of the superior pole anteriorly. This smaller mass is firm, tan, and somewhat fleshy. There is marked hydronephrosis. Additionally, a large aggregate of at least eight lymph node candidates was submitted.

Histologic Findings

The dominant tumor mass widely invasive into the hilar fat has variable morphology including intimately admixed epithelioid and mesenchymal areas with hemorrhagic background (Fig. 1.48a). The epithelioid component is composed of nests and sheets of round-to-cuboidal uniform cells with eosinophilic and vacuolated cytoplasm. These tumor nests are separated by abundant stroma with clusters of vessels with eccentrically thickened walls, adipocytes, and plump spindle cells (Fig. 1.48b). In some areas, tumor cells are forming large sheets of clear cells with prominent plant-like membranes, irregular wrinkled nuclei, and prominent perinuclear halos (Fig. 1.48c). Regional lymph nodes contain several areas of extensive spindle cell proliferations (Fig. 1.48d) splitting and invading into the sinusoidal spaces (Fig. 1.48e).

Differential Diagnosis

- Multifocal chromophobe renal cell carcinoma (RCC), suspicious for Birt-Hogg-Dube syndrome.
- Chromophobe RCC with sarcomatoid dedifferentiation and lymph node metastases.
- Multiple angiomyolipomas (AML) and RCC, suggestive of tuberous sclerosis syndrome.
- Clear cell RCC with abundant smooth muscle stroma.

Ancillary Studies

- Positive immunostains: PAX8 and CK7 in epithelioid areas (spindle cell areas negative).
- Negative immunostains: CAIX, AMACR, CD10.

Final Diagnosis

Chromophobe-like RCC and multiple angiomyolipomas (AMLs) involving kidney and lymph nodes, suggestive of tuberous sclerosis (later confirmed clinically).

Take-Home Messages

1. Multiple bilateral tumors including AML and RCC with AML-like stroma (Fig. 1.48a–c) are hallmark features of tuberous sclerosis complex.
2. Rare metastasis of RCC to regional lymph nodes has been reported, but death from RCC in patients with tuberous sclerosis is extremely uncommon.
3. Presence of AML in the lymph node is not considered a metastasis.

References: [188, 193].

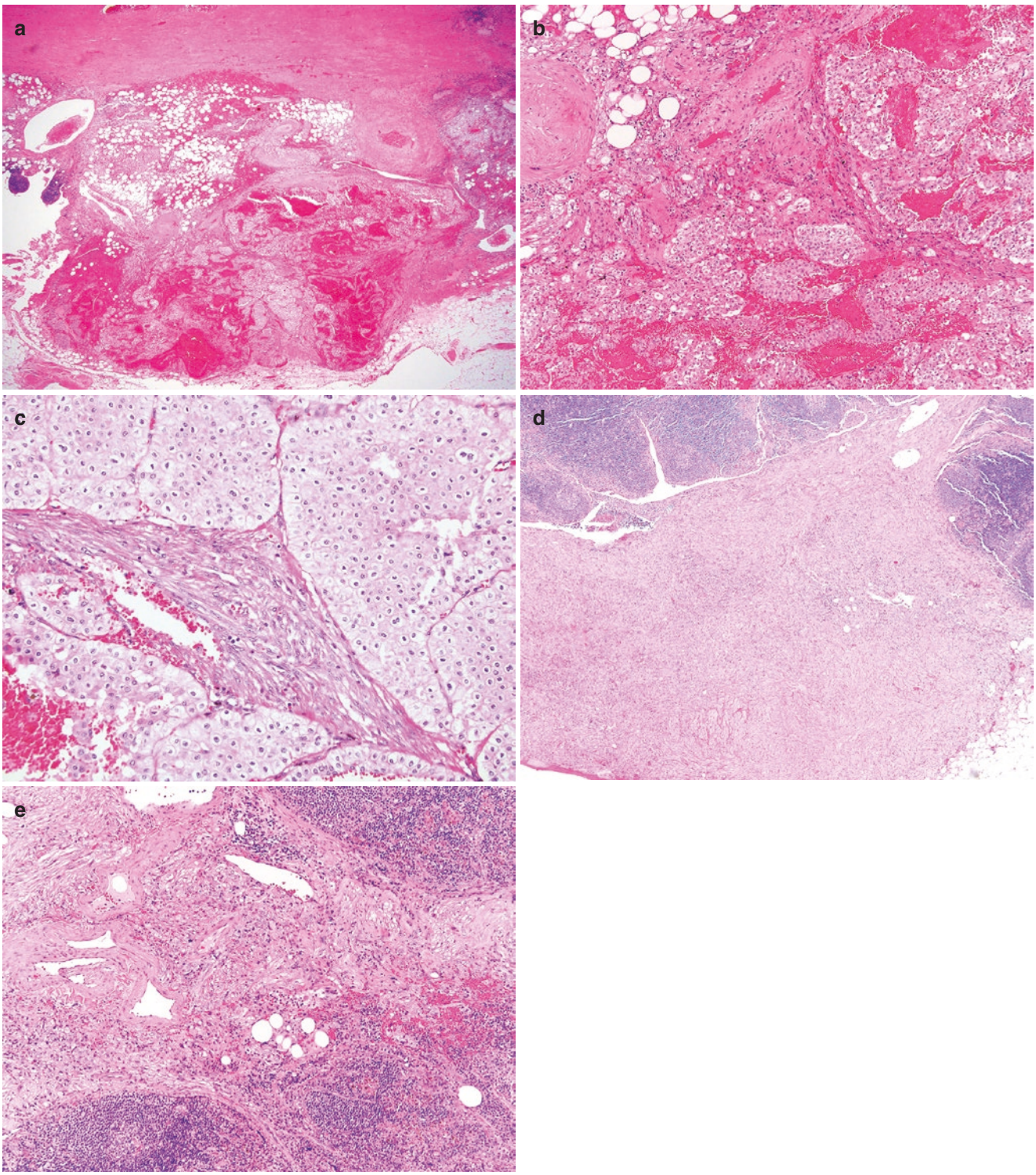

Fig. 1.48 (**a**) Renal hilum contains hemorrhagic tumor. (**b**) Clusters of clear to eosinophilic tumor cells infiltrate hilar fat and stroma. (**c**) Large confluent solid sheets are composed of cells with sharp borders and hyperchromatic raisinoid nuclei surrounded by clear halos. (**d**) Lymph node histology demonstrates pink area of spindle cell proliferation arising from capsule and extending into the extranodal adipose tissue. (**e**) Spindle cells with plump eosinophilic cytoplasm expand sinusoidal spaces of the lymph node

References

1. Halverson SJ, Kunju LP, Bhalla R, Gadzinski AJ, Alderman M, Miller DC, et al. Accuracy of determining small renal mass management with risk stratified biopsies: confirmation by final pathology. J Urol. 2013;189:441–6.
2. Evans AJ, Delahunt B, Srigley JR. Issues and challenges associated with classifying neoplasms in percutaneous needle biopsies of incidentally found small renal masses. Semin Diagn Pathol. 2015;32:184–95.
3. Richard PO, Jewett MA, Bhatt JR, Evans AJ, Timilsina N, Finelli A. Active surveillance for renal neoplasms with oncocytic features is safe. J Urol. 2016;195:581–6.
4. Williamson SR, Eble JN, Cheng L, Grignon DJ. Clear cell papillary renal cell carcinoma: differential diagnosis and extended immunohistochemical profile. Mod Pathol. 2013;26:697–708.
5. Kuroda N, Agatsuma Y, Tamura M, Martinek P, Hes O, Michal M. Sporadic renal hemangioblastoma with CA9, PAX2 and PAX8 expression: diagnostic pitfall in the differential diagnosis from clear cell renal cell carcinoma. Int J Clin Exp Pathol. 2015;8:2131–8.
6. Ohe C, Smith SC, Sirohi D, Divatia M, de Peralta-Venturina M, Paner GP, et al. Reappraisal of morphologic differences between renal medullary carcinoma, collecting duct carcinoma, and fumarate hydratase-deficient renal cell carcinoma. Am J Surg Pathol. 2018;42:279–92.
7. Wu AJ, Mehra R, Hafez K, Wolf JS Jr, Kunju LP. Metastases to the kidney: a clinicopathological study of 43 cases with an emphasis on deceptive features. Histopathology. 2015;66:587–97.
8. Chang A, Brimo F, Montgomery EA, Epstein JI. Use of PAX8 and GATA3 in diagnosing sarcomatoid renal cell carcinoma and sarcomatoid urothelial carcinoma. Hum Pathol. 2013;44:1563–8.
9. Klatte T, Said JW, Seligson DB, Rao PN, de Martino M, Shuch B, et al. Pathological, immunohistochemical and cytogenetic features of papillary renal cell carcinoma with clear cell features. J Urol. 2011;185:30–5.
10. Trpkov K, Grignon DJ, Bonsib SM, Amin MB, Billis A, Lopez-Beltran A, et al. Handling and staging of renal cell carcinoma: the International Society of Urological Pathology Consensus (ISUP) conference recommendations. Am J Surg Pathol. 2013;37:1505–17.
11. Bonsib SM. The renal sinus is the principal invasive pathway: a prospective study of 100 renal cell carcinomas. Am J Surg Pathol. 2004;28:1594–600.
12. Bonsib SM. T2 clear cell renal cell carcinoma is a rare entity: a study of 120 clear cell renal cell carcinomas. J Urol. 2005;174:1199–202; discussion 202
13. Bonsib SM. Renal lymphatics, and lymphatic involvement in sinus vein invasive (pT3b) clear cell renal cell carcinoma: a study of 40 cases. Mod Pathol. 2006;19:746–53.
14. Williamson SR, Rao P, Hes O, Epstein JI, Smith SC, Picken MM, et al. Challenges in pathologic staging of renal cell carcinoma: a study of interobserver variability among urologic pathologists. Am J Surg Pathol. 2018;42:1253–61.
15. Taneja K, Arora S, Rogers CG, Gupta NS, Williamson SR. Pathological staging of renal cell carcinoma: a review of 300 consecutive cases with emphasis on retrograde venous invasion. Histopathology. 2018;73:681–91.
16. Thompson RH, Blute ML, Krambeck AE, Lohse CM, Magera JS, Leibovich BC, et al. Patients with pT1 renal cell carcinoma who die from disease after nephrectomy may have unrecognized renal sinus fat invasion. Am J Surg Pathol. 2007;31:1089–93.
17. Srigley JR, Delahunt B, Eble JN, Egevad L, Epstein JI, Grignon D, et al. The International Society of Urological Pathology (ISUP) Vancouver classification of renal neoplasia. Am J Surg Pathol. 2013;37:1469–89.
18. Amin MB, Crotty TB, Tickoo SK, Farrow GM. Renal oncocytoma: a reappraisal of morphologic features with clinicopathologic findings in 80 cases. Am J Surg Pathol. 1997;21:1–12.
19. Perez-Ordonez B, Hamed G, Campbell S, Erlandson RA, Russo P, Gaudin PB, et al. Renal oncocytoma: a clinicopathologic study of 70 cases. Am J Surg Pathol. 1997;21:871–83.
20. Trpkov K, Yilmaz A, Uzer D, Dishongh KM, Quick CM, Bismar TA, et al. Renal oncocytoma revisited: a clinicopathological study of 109 cases with emphasis on problematic diagnostic features. Histopathology. 2010;57:893–906.
21. Wobker SE, Williamson SR. Modern pathologic diagnosis of renal Oncocytoma. J Kidney Cancer VHL. 2017;4:1–12.
22. Hes O, Michal M, Sima R, Vanecek T, Brunelli M, Martignoni G, et al. Renal oncocytoma with and without intravascular extension into the branches of renal vein have the same morphological, immunohistochemical, and genetic features. Virchows Arch. 2008;452:193–200.
23. Wobker SE, Przybycin CG, Sircar K, Epstein JI. Renal oncocytoma with vascular invasion: a series of 22 cases. Hum Pathol. 2016;58:1–6.
24. Xiao GQ, Ko HB, Unger P. Telangiectatic oncocytoma: a previously undescribed variant of renal oncocytoma. Am J Clin Pathol. 2013;140:103–8.
25. Williamson SR, Halat S, Eble JN, Grignon DJ, Lopez-Beltran A, Montironi R, et al. Multilocular cystic renal cell carcinoma: similarities and differences in immunoprofile compared with clear cell renal cell carcinoma. Am J Surg Pathol. 2012;36:1425–33.
26. Tran T, Jones CL, Williamson SR, Eble JN, Grignon DJ, Zhang S, et al. Tubulocystic renal cell carcinoma is an entity that is immunohistochemically and genetically distinct from papillary renal cell carcinoma. Histopathology. 2016;68:850–7.
27. Calio A, Eble JN, Grignon DJ, Delahunt B. Mixed epithelial and stromal tumor of the kidney: a clinicopathologic study of 53 cases. Am J Surg Pathol. 2016;40:1538–49.
28. Park HS, Lee K, Moon KC. Determination of the cutoff value of the proportion of cystic change for prognostic stratification of clear cell renal cell carcinoma. J Urol. 2011;186:423–9.
29. Mantilla JG, Antic T, Tretiakova M. GATA3 as a valuable marker to distinguish clear cell papillary renal cell carcinomas from morphologic mimics. Hum Pathol. 2017;66:152–8.
30. Park JJ, Jeong BC, Kim CK, Seo SI, Carriere KC, Kim M, et al. Postoperative outcome of cystic renal cell carcinoma defined on preoperative imaging: a retrospective study. J Urol. 2017;197:991–7.
31. Hartman DS, Davis CJ Jr, Johns T, Goldman SM. Cystic renal cell carcinoma. Urology. 1986;28:145–53.
32. Liu L, Qian J, Singh H, Meiers I, Zhou X, Bostwick DG. Immunohistochemical analysis of chromophobe renal cell carcinoma, renal oncocytoma, and clear cell carcinoma: an optimal and practical panel for differential diagnosis. Arch Pathol Lab Med. 2007;131:1290–7.
33. Miettinen M, McCue PA, Sarlomo-Rikala M, Rys J, Czapiewski P, Wazny K, et al. GATA3: a multispecific but potentially useful marker in surgical pathology: a systematic analysis of 2500 epithelial and nonepithelial tumors. Am J Surg Pathol. 2014;38:13–22.
34. Gonzalez-Roibon N, Faraj SF, Munari E, Bezerra SM, Albadine R, Sharma R, et al. Comprehensive profile of GATA binding protein 3 immunohistochemical expression in primary and metastatic renal neoplasms. Hum Pathol. 2014;45:244–8.
35. Camparo P, Vasiliu V, Molinie V, Couturier J, Dykema KJ, Petillo D, et al. Renal translocation carcinomas: clinicopathologic, immunohistochemical, and gene expression profiling analysis of 31 cases with a review of the literature. Am J Surg Pathol. 2008;32:656–70.

36. Williamson SR, Gadde R, Trpkov K, Hirsch MS, Srigley JR, Reuter VE, et al. Diagnostic criteria for oncocytic renal neoplasms: a survey of urologic pathologists. Hum Pathol. 2017;63:149–56.
37. Brugarolas J. Molecular genetics of clear-cell renal cell carcinoma. J Clin Oncol. 2014;32:1968–76.
38. Favazza L, Chitale DA, Barod R, Rogers CG, Kalyana-Sundaram S, Palanisamy N, et al. Renal cell tumors with clear cell histology and intact VHL and chromosome 3p: a histological review of tumors from the Cancer genome atlas database. Mod Pathol. 2017;30:1603–12.
39. Cancer Genome Atlas Research Network. Comprehensive molecular characterization of clear cell renal cell carcinoma. Nature. 2013;499:43–9.
40. Sato Y, Yoshizato T, Shiraishi Y, Maekawa S, Okuno Y, Kamura T, et al. Integrated molecular analysis of clear-cell renal cell carcinoma. Nat Genet. 2013;45:860–7.
41. Green WM, Yonescu R, Morsberger L, Morris K, Netto GJ, Epstein JI, et al. Utilization of a TFE3 break-apart FISH assay in a renal tumor consultation service. Am J Surg Pathol. 2013;37:1150–63.
42. Rao Q, Williamson SR, Zhang S, Eble JN, Grignon DJ, Wang M, et al. TFE3 break-apart FISH has a higher sensitivity for Xp11.2 translocation-associated renal cell carcinoma compared with TFE3 or cathepsin K immunohistochemical staining alone: expanding the morphologic spectrum. Am J Surg Pathol. 2013;37:804–15.
43. Williamson SR, Grignon DJ, Cheng L, Favazza L, Gondim DD, Carskadon S, et al. Renal cell carcinoma with chromosome 6p amplification including the TFEB gene: a novel mechanism of tumor pathogenesis? Am J Surg Pathol. 2017;41:287–98.
44. Argani P, Reuter VE, Zhang L, Sung YS, Ning Y, Epstein JI, et al. TFEB-amplified renal cell carcinomas: an aggressive molecular subset demonstrating variable melanocytic marker expression and morphologic heterogeneity. Am J Surg Pathol. 2016;40:1484–95.
45. Gupta S, Johnson SH, Vasmatzis G, Porath B, Rustin JG, Rao P, et al. TFEB-VEGFA (6p21.1) co-amplified renal cell carcinoma: a distinct entity with potential implications for clinical management. Mod Pathol. 2017;30:998–1012.
46. Sukov WR, Ketterling RP, Lager DJ, Carlson AW, Sinnwell JP, Chow GK, et al. CCND1 rearrangements and cyclin D1 overexpression in renal oncocytomas: frequency, clinicopathologic features, and utility in differentiation from chromophobe renal cell carcinoma. Hum Pathol. 2009;40:1296–303.
47. Argani P, Zhang L, Reuter VE, Tickoo SK, Antonescu CR. RBM10-TFE3 renal cell carcinoma: a potential diagnostic pitfall due to cryptic intrachromosomal Xp11.2 inversion resulting in false-negative TFE3 FISH. Am J Surg Pathol. 2017;41:655–62.
48. Xia QY, Wang XT, Zhan XM, Tan X, Chen H, Liu Y, et al. Xp11 translocation renal cell carcinomas (RCCs) with RBM10-TFE3 gene fusion demonstrating melanotic features and overlapping morphology with t(6;11) RCC: interest and diagnostic pitfall in detecting a paracentric inversion of TFE3. Am J Surg Pathol. 2017;41:663–76.
49. Xia QY, Wang Z, Chen N, Gan HL, Teng XD, Shi SS, et al. Xp11.2 translocation renal cell carcinoma with NONO-TFE3 gene fusion: morphology, prognosis, and potential pitfall in detecting TFE3 gene rearrangement. Mod Pathol. 2017;30:416–26.
50. Delahunt B, Cheville JC, Martignoni G, Humphrey PA, Magi-Galluzzi C, McKenney J, et al. The International Society of Urological Pathology (ISUP) grading system for renal cell carcinoma and other prognostic parameters. Am J Surg Pathol. 2013;37:1490–504.
51. Delahunt B, McKenney JK, Lohse CM, Leibovich BC, Thompson RH, Boorjian SA, et al. A novel grading system for clear cell renal cell carcinoma incorporating tumor necrosis. Am J Surg Pathol. 2013;37:311–22.
52. Delahunt B, Sika-Paotonu D, Bethwaite PB, William Jordan T, Magi-Galluzzi C, Zhou M, et al. Grading of clear cell renal cell carcinoma should be based on nucleolar prominence. Am J Surg Pathol. 2011;35:1134–9.
53. Paner GP, Amin MB, Alvarado-Cabrero I, Young AN, Stricker HJ, Moch H, et al. A novel tumor grading scheme for chromophobe renal cell carcinoma: prognostic utility and comparison with Fuhrman nuclear grade. Am J Surg Pathol. 2010;34:1233–40.
54. Renshaw AA, Cheville JC. Quantitative tumour necrosis is an independent predictor of overall survival in clear cell renal cell carcinoma. Pathology. 2015;47:34–7.
55. Sengupta S, Lohse CM, Leibovich BC, Frank I, Thompson RH, Webster WS, et al. Histologic coagulative tumor necrosis as a prognostic indicator of renal cell carcinoma aggressiveness. Cancer. 2005;104:511–20.
56. Williamson SR, MacLennan GT, Lopez-Beltran A, Montironi R, Tan PH, Martignoni G, et al. Cystic partially regressed clear cell renal cell carcinoma: a potential mimic of multilocular cystic renal cell carcinoma. Histopathology. 2013;63:767–79.
57. Kryvenko ON, Jorda M, Argani P, Epstein JI. Diagnostic approach to eosinophilic renal neoplasms. Arch Pathol Lab Med. 2014;138:1531–41.
58. Kryvenko ON, Roquero L, Gupta NS, Lee MW, Epstein JI. Low-grade clear cell renal cell carcinoma mimicking hemangioma of the kidney: a series of 4 cases. Arch Pathol Lab Med. 2013;137:251–4.
59. Williamson SR, Kum JB, Goheen MP, Cheng L, Grignon DJ, Idrees MT. Clear cell renal cell carcinoma with a syncytial-type multinucleated giant tumor cell component: implications for differential diagnosis. Hum Pathol. 2014;45:735–44.
60. Dhakal HP, McKenney JK, Khor LY, Reynolds JP, Magi-Galluzzi C, Przybycin CG. Renal neoplasms with overlapping features of clear cell renal cell carcinoma and clear cell papillary renal cell carcinoma: a clinicopathologic study of 37 cases from a single institution. Am J Surg Pathol. 2016;40:141–54.
61. Williamson SR, Gupta NS, Eble JN, Rogers CG, Michalowski S, Zhang S, et al. Clear cell renal cell carcinoma with borderline features of clear cell papillary renal cell carcinoma: combined morphologic, immunohistochemical, and cytogenetic analysis. Am J Surg Pathol. 2015;39:1502–10.
62. Williamson SR, Zhang S, Eble JN, Grignon DJ, Martignoni G, Brunelli M, et al. Clear cell papillary renal cell carcinoma-like tumors in patients with von Hippel-Lindau disease are unrelated to sporadic clear cell papillary renal cell carcinoma. Am J Surg Pathol. 2013;37:1131–9.
63. Gobbo S, Eble JN, Maclennan GT, Grignon DJ, Shah RB, Zhang S, et al. Renal cell carcinomas with papillary architecture and clear cell components: the utility of immunohistochemical and cytogenetical analyses in differential diagnosis. Am J Surg Pathol. 2008;32:1780–6.
64. Tickoo SK, Amin MB, Zarbo RJ. Colloidal iron staining in renal epithelial neoplasms, including chromophobe renal cell carcinoma: emphasis on technique and patterns of staining. Am J Surg Pathol. 1998;22:419–24.
65. Li L, Parwani AV. Xanthogranulomatous pyelonephritis. Arch Pathol Lab Med. 2011;135:671–4.
66. Eble JN, Moch H, Amin MB, Argani P, Cheville J, Delahunt B, et al. Papillary adenoma. In: Moch H, Humphrey PA, Ulbright TM, Reuter VE, editors. WHO classification of tumours of the urinary system and male genital organs. 4th ed. Lyon: International Agency for Research on Cancer; 2016. p. 42–3.
67. Umbreit EC, Shimko MS, Childs MA, Lohse CM, Cheville JC, Leibovich BC, et al. Metastatic potential of a renal mass according to original tumour size at presentation. BJU Int. 2012;109:190–4; discussion 4
68. Kinney SN, Eble JN, Hes O, Williamson SR, Grignon DJ, Wang M, et al. Metanephric adenoma: the utility of immunohistochemical and cytogenetic analyses in differential diagnosis, including solid

variant papillary renal cell carcinoma and epithelial-predominant nephroblastoma. Mod Pathol. 2015;28:1236–48.
69. Choueiri TK, Cheville J, Palescandolo E, Fay AP, Kantoff PW, Atkins MB, et al. BRAF mutations in metanephric adenoma of the kidney. Eur Urol. 2012;62:917–22.
70. Udager AM, Pan J, Magers MJ, Palapattu GS, Morgan TM, Montgomery JS, et al. Molecular and immunohistochemical characterization reveals novel BRAF mutations in metanephric adenoma. Am J Surg Pathol. 2015;39:549–57.
71. Delahunt B, Eble JN. Papillary renal cell carcinoma: a clinicopathologic and immunohistochemical study of 105 tumors. Mod Pathol. 1997;10:537–44.
72. Trpkov K, Hes O, Agaimy A, Bonert M, Martinek P, Magi-Galluzzi C, et al. Fumarate hydratase-deficient renal cell carcinoma is strongly correlated with fumarate hydratase mutation and hereditary leiomyomatosis and renal cell carcinoma syndrome. Am J Surg Pathol. 2016;40:865–75.
73. Cancer Genome Atlas Research Network, Linehan WM, Spellman PT, Ricketts CJ, Creighton CJ, Fei SS, et al. Comprehensive molecular characterization of papillary renal-cell carcinoma. N Engl J Med. 2016;374:135–45.
74. Cossu-Rocca P, Eble JN, Delahunt B, Zhang S, Martignoni G, Brunelli M, et al. Renal mucinous tubular and spindle carcinoma lacks the gains of chromosomes 7 and 17 and losses of chromosome Y that are prevalent in papillary renal cell carcinoma. Mod Pathol. 2006;19:488–93.
75. Eble JN. Mucinous tubular and spindle cell carcinoma and postneuroblastoma carcinoma: newly recognised entities in the renal cell carcinoma family. Pathology. 2003;35:499–504.
76. Fine SW, Argani P, DeMarzo AM, Delahunt B, Sebo TJ, Reuter VE, et al. Expanding the histologic spectrum of mucinous tubular and spindle cell carcinoma of the kidney. Am J Surg Pathol. 2006;30:1554–60.
77. Mehra R, Vats P, Cieslik M, Cao X, Su F, Shukla S, et al. Biallelic alteration and dysregulation of the Hippo pathway in mucinous tubular and spindle cell carcinoma of the kidney. Cancer Discov. 2016;6:1258–66.
78. Peckova K, Martinek P, Sperga M, Montiel DP, Daum O, Rotterova P, et al. Mucinous spindle and tubular renal cell carcinoma: analysis of chromosomal aberration pattern of low-grade, high-grade, and overlapping morphologic variant with papillary renal cell carcinoma. Ann Diagn Pathol. 2015;19:226–31.
79. Ren Q, Wang L, Al-Ahmadie HA, Fine SW, Gopalan A, Sirintrapun SJ, et al. Distinct genomic copy number alterations distinguish mucinous tubular and spindle cell carcinoma of the kidney from papillary renal cell carcinoma with overlapping histologic features. Am J Surg Pathol. 2018;42:767–77.
80. Wang L, Zhang Y, Chen YB, Skala SL, Al-Ahmadie HA, Wang X, et al. VSTM2A overexpression is a sensitive and specific biomarker for mucinous tubular and spindle cell carcinoma (MTSCC) of the kidney. Am J Surg Pathol. 2018;42(12):1571–84.
81. Gunia S, Erbersdobler A, Koch S, Otto W, Staibano S, D'Alterio C, et al. Protein gene product 9.5 is diagnostically helpful in delineating high-grade renal cell cancer involving the renal medullary/sinus region from invasive urothelial cell carcinoma of the renal pelvis. Hum Pathol. 2013;44:712–7.
82. Davis CF, Ricketts CJ, Wang M, Yang L, Cherniack AD, Shen H, et al. The somatic genomic landscape of chromophobe renal cell carcinoma. Cancer Cell. 2014;26:319–30.
83. Sperga M, Martinek P, Vanecek T, Grossmann P, Bauleth K, Perez-Montiel D, et al. Chromophobe renal cell carcinoma--chromosomal aberration variability and its relation to Paner grading system: an array CGH and FISH analysis of 37 cases. Virchows Arch. 2013;463:563–73.
84. Ng KL, Morais C, Bernard A, Saunders N, Samaratunga H, Gobe G, et al. A systematic review and meta-analysis of immunohistochemical biomarkers that differentiate chromophobe renal cell carcinoma from renal oncocytoma. J Clin Pathol. 2016;69:661–71.
85. Ng KL, Rajandram R, Morais C, Yap NY, Samaratunga H, Gobe GC, et al. Differentiation of oncocytoma from chromophobe renal cell carcinoma (RCC): can novel molecular biomarkers help solve an old problem? J Clin Pathol. 2014;67:97–104.
86. Zhou C, Urbauer DL, Fellman BM, Tamboli P, Zhang M, Matin SF, et al. Metastases to the kidney: a comprehensive analysis of 151 patients from a tertiary referral centre. BJU Int. 2016;117:775–82.
87. Pal SK, Choueiri TK, Wang K, Khaira D, Karam JA, Van Allen E, et al. Characterization of clinical cases of collecting duct carcinoma of the kidney assessed by comprehensive genomic profiling. Eur Urol. 2016;70:516–21.
88. Amin MB, Smith SC, Agaimy A, Argani P, Comperat EM, Delahunt B, et al. Collecting duct carcinoma versus renal medullary carcinoma: an appeal for nosologic and biological clarity. Am J Surg Pathol. 2014;38:871–4.
89. Calderaro J, Masliah-Planchon J, Richer W, Maillot L, Maille P, Mansuy L, et al. Balanced translocations disrupting SMARCB1 are hallmark recurrent genetic alterations in renal medullary carcinomas. Eur Urol. 2016;69:1055–61.
90. Calderaro J, Moroch J, Pierron G, Pedeutour F, Grison C, Maille P, et al. SMARCB1/INI1 inactivation in renal medullary carcinoma. Histopathology. 2012;61:428–35.
91. Carlo MI, Chaim J, Patil S, Kemel Y, Schram AM, Woo K, et al. Genomic characterization of renal medullary carcinoma and treatment outcomes. Clin Genitourin Cancer. 2017;15:e987–e94.
92. Liu Q, Galli S, Srinivasan R, Linehan WM, Tsokos M, Merino MJ. Renal medullary carcinoma: molecular, immunohistochemistry, and morphologic correlation. Am J Surg Pathol. 2013;37:368–74.
93. Shuch B, Bratslavsky G, Linehan WM, Srinivasan R. Sarcomatoid renal cell carcinoma: a comprehensive review of the biology and current treatment strategies. Oncologist. 2012;17:46–54.
94. Merrill MM, Wood CG, Tannir NM, Slack RS, Babaian KN, Jonasch E, et al. Clinically nonmetastatic renal cell carcinoma with sarcomatoid dedifferentiation: natural history and outcomes after surgical resection with curative intent. Urol Oncol. 2015;33:166.e21–9.
95. Zhang L, Wu B, Zha Z, Zhao H, Feng Y. The prognostic value and clinicopathological features of sarcomatoid differentiation in patients with renal cell carcinoma: a systematic review and meta-analysis. Cancer Manag Res. 2018;10:1687–703.
96. Wang Z, Kim TB, Peng B, Karam J, Creighton C, Joon A, et al. Sarcomatoid renal cell carcinoma has a distinct molecular pathogenesis, driver mutation profile, and transcriptional landscape. Clin Cancer Res. 2017;23:6686–96.
97. Dotan ZA, Tal R, Golijanin D, Snyder ME, Antonescu C, Brennan MF, et al. Adult genitourinary sarcoma: the 25-year memorial Sloan-Kettering experience. J Urol. 2006;176:2033–8; discussion 8–9
98. Shuch B, Bratslavsky G, Shih J, Vourganti S, Finley D, Castor B, et al. Impact of pathological tumour characteristics in patients with sarcomatoid renal cell carcinoma. BJU Int. 2012;109:1600–6.
99. Tan PH, Cheng L, Rioux-Leclercq N, Merino MJ, Netto G, Reuter VE, et al. Renal tumors: diagnostic and prognostic biomarkers. Am J Surg Pathol. 2013;37:1518–31.
100. Fatima N, Canter DJ, Carthon BC, Kucuk O, Master VA, Nieh PT, et al. Sarcomatoid urothelial carcinoma of the bladder: a contemporary clinicopathologic analysis of 37 cases. Can J Urol. 2015;22:7783–7.
101. Fatima N, Osunkoya AO. GATA3 expression in sarcomatoid urothelial carcinoma of the bladder. Hum Pathol. 2014;45:1625–9.
102. Martignoni G, Pea M, Zampini C, Brunelli M, Segala D, Zamboni G, et al. PEComas of the kidney and of the genitourinary tract. Semin Diagn Pathol. 2015;32:140–59.

103. Lane BR, Aydin H, Danforth TL, Zhou M, Remer EM, Novick AC, et al. Clinical correlates of renal angiomyolipoma subtypes in 209 patients: classic, fat poor, tuberous sclerosis associated and epithelioid. J Urol. 2008;180:836–43.
104. Fine SW, Reuter VE, Epstein JI, Argani P. Angiomyolipoma with epithelial cysts (AMLEC): a distinct cystic variant of angiomyolipoma. Am J Surg Pathol. 2006;30:593–9.
105. Martignoni G, Pea M, Bonetti F, Brunelli M, Eble JN. Oncocytoma-like angiomyolipoma. A clinicopathologic and immunohistochemical study of 2 cases. Arch Pathol Lab Med. 2002;126:610–2.
106. Matsuyama A, Hisaoka M, Ichikawa K, Fujimori T, Udo K, Uchihashi K, et al. Sclerosing variant of epithelioid angiomyolipoma. Pathol Int. 2008;58:306–10.
107. Chowdhury PR, Tsuda N, Anami M, Hayashi T, Iseki M, Kishikawa M, et al. A histopathologic and immunohistochemical study of small nodules of renal angiomyolipoma: a comparison of small nodules with angiomyolipoma. Mod Pathol. 1996;9:1081–8.
108. Calio A, Warfel KA, Eble JN. Renomedullary interstitial cell tumors: pathologic features and clinical correlations. Am J Surg Pathol. 2016;40:1693–701.
109. Gatalica Z, Lilleberg SL, Koul MS, Vanecek T, Hes O, Wang B, et al. COX-2 gene polymorphisms and protein expression in renomedullary interstitial cell tumors. Hum Pathol. 2008;39:1495–504.
110. Wei J, Li Y, Wen Y, Li L, Zhang R. Renal angiomyolipoma with epithelial cysts: a rare entity and review of literature. Int J Clin Exp Pathol. 2015;8:11760–5.
111. Zhou M, Kort E, Hoekstra P, Westphal M, Magi-Galluzzi C, Sercia L, et al. Adult cystic nephroma and mixed epithelial and stromal tumor of the kidney are the same disease entity: molecular and histologic evidence. Am J Surg Pathol. 2009;33:72–80.
112. Lane BR, Campbell SC, Remer EM, Fergany AF, Williams SB, Novick AC, et al. Adult cystic nephroma and mixed epithelial and stromal tumor of the kidney: clinical, radiographic, and pathologic characteristics. Urology. 2008;71:1142–8.
113. Michal M, Hes O, Bisceglia M, Simpson RH, Spagnolo DV, Parma A, et al. Mixed epithelial and stromal tumors of the kidney. A report of 22 cases. Virchows Arch. 2004;445:359–67.
114. Jung SJ, Shen SS, Tran T, Jun SY, Truong L, Ayala AG, et al. Mixed epithelial and stromal tumor of kidney with malignant transformation: report of two cases and review of literature. Hum Pathol. 2008;39:463–8.
115. Aydin H, Magi-Galluzzi C, Lane BR, Sercia L, Lopez JI, Rini BI, et al. Renal angiomyolipoma: clinicopathologic study of 194 cases with emphasis on the epithelioid histology and tuberous sclerosis association. Am J Surg Pathol. 2009;33:289–97.
116. Aron M, Aydin H, Sercia L, Magi-Galluzzi C, Zhou M. Renal cell carcinomas with intratumoral fat and concomitant angiomyolipoma: potential pitfalls in staging and diagnosis. Am J Clin Pathol. 2010;134:807–12.
117. He W, Cheville JC, Sadow PM, Gopalan A, Fine SW, Al-Ahmadie HA, et al. Epithelioid angiomyolipoma of the kidney: pathological features and clinical outcome in a series of consecutively resected tumors. Mod Pathol. 2013;26:1355–64.
118. Martignoni G, Cheville J, Fletcher CDM, Pea M, Reuter VE, Ro JY, et al. Epithelioid angiomyolipoma. In: Moch A, Humphrey PA, Ulbright TM, Reuter VE, editors. World Health Organization classification of tumours the urinary system and male genital organs. 4th ed. Lyon: IARC Press; 2016. p. 65–6.
119. Brimo F, Robinson B, Guo C, Zhou M, Latour M, Epstein JI. Renal epithelioid angiomyolipoma with atypia: a series of 40 cases with emphasis on clinicopathologic prognostic indicators of malignancy. Am J Surg Pathol. 2010;34:715–22.
120. Nese N, Martignoni G, Fletcher CD, Gupta R, Pan CC, Kim H, et al. Pure epithelioid PEComas (so-called epithelioid angiomyolipoma) of the kidney: a clinicopathologic study of 41 cases: detailed assessment of morphology and risk stratification. Am J Surg Pathol. 2011;35:161–76.
121. Varma S, Gupta S, Talwar J, Forte F, Dhar M. Renal epithelioid angiomyolipoma: a malignant disease. J Nephrol. 2011;24:18–22.
122. Konosu-Fukaya S, Nakamura Y, Fujishima F, Kasajima A, McNamara KM, Takahashi Y, et al. Renal epithelioid angiomyolipoma with malignant features: histological evaluation and novel immunohistochemical findings. Pathol Int. 2014;64:133–41.
123. Zheng S, Bi XG, Song QK, Yuan Z, Guo L, Zhang H, et al. A suggestion for pathological grossing and reporting based on prognostic indicators of malignancies from a pooled analysis of renal epithelioid angiomyolipoma. Int Urol Nephrol. 2015;47:1643–51.
124. Lei JH, Liu LR, Wei Q, Song TR, Yang L, Yuan HC, et al. A four-year follow-up study of renal epithelioid angiomyolipoma: a multicenter experience and literature review. Sci Rep. 2015;5:10030.
125. Park JH, Lee C, Suh JH, Kim G, Song B, Moon KC. Renal epithelioid angiomyolipoma: histopathologic review, immunohistochemical evaluation and prognostic significance. Pathol Int. 2016;66:571–7.
126. Miller JS, Zhou M, Brimo F, Guo CC, Epstein JI. Primary leiomyosarcoma of the kidney: a clinicopathologic study of 27 cases. Am J Surg Pathol. 2010;34:238–42.
127. Mayes DC, Fechner RE, Gillenwater JY. Renal liposarcoma. Am J Surg Pathol. 1990;14:268–73.
128. Matsushita M, Ito A, Ishidoya S, Endoh M, Moriya T, Arai Y. Intravenous extended liposarcoma arising from renal sinus. Int J Urol. 2007;14:769–70.
129. Olgac S, Mazumdar M, Dalbagni G, Reuter VE. Urothelial carcinoma of the renal pelvis: a clinicopathologic study of 130 cases. Am J Surg Pathol. 2004;28:1545–52.
130. Gupta R, Paner GP, Amin MB. Neoplasms of the upper urinary tract: a review with focus on urothelial carcinoma of the pelvicalyceal system and aspects related to its diagnosis and reporting. Adv Anat Pathol. 2008;15:127–39.
131. Lughezzani G, Jeldres C, Isbarn H, Sun M, Shariat SF, Alasker A, et al. Nephroureterectomy and segmental ureterectomy in the treatment of invasive upper tract urothelial carcinoma: a population-based study of 2299 patients. Eur J Cancer. 2009;45:3291–7.
132. Cha EK, Shariat SF, Kormaksson M, Novara G, Chromecki TF, Scherr DS, et al. Predicting clinical outcomes after radical nephroureterectomy for upper tract urothelial carcinoma. Eur Urol. 2012;61:818–25.
133. Gupta R, Billis A, Shah RB, Moch H, Osunkoya AO, Jochum W, et al. Carcinoma of the collecting ducts of Bellini and renal medullary carcinoma: clinicopathologic analysis of 52 cases of rare aggressive subtypes of renal cell carcinoma with a focus on their interrelationship. Am J Surg Pathol. 2012;36:1265–78.
134. Higgins JP, Kaygusuz G, Wang L, Montgomery K, Mason V, Zhu SX, et al. Placental S100 (S100P) and GATA3: markers for transitional epithelium and urothelial carcinoma discovered by complementary DNA microarray. Am J Surg Pathol. 2007;31:673–80.
135. Albadine R, Schultz L, Illei P, Ertoy D, Hicks J, Sharma R, et al. PAX8 (+)/p63 (−) immunostaining pattern in renal collecting duct carcinoma (CDC): a useful immunoprofile in the differential diagnosis of CDC versus urothelial carcinoma of upper urinary tract. Am J Surg Pathol. 2010;34:965–9.
136. Williams PA, Mai KT. Primary carcinoma of renal calyx. Pathol Res Pract. 2013;209:654–61.
137. Perlman EJ. Pediatric renal tumors: practical updates for the pathologist. Pediatr Dev Pathol. 2005;8:320–38.
138. Parham DM, Roloson GJ, Feely M, Green DM, Bridge JA, Beckwith JB. Primary malignant neuroepithelial tumors of the kidney: a clinicopathologic analysis of 146 adult and pediatric cases from the National Wilms' Tumor Study Group Pathology Center. Am J Surg Pathol. 2001;25:133–46.

139. Ellison DA, Parham DM, Bridge J, Beckwith JB. Immunohistochemistry of primary malignant neuroepithelial tumors of the kidney: a potential source of confusion? A study of 30 cases from the National Wilms Tumor Study Pathology Center. Hum Pathol. 2007;38:205–11.
140. Argani P, Faria PA, Epstein JI, Reuter VE, Perlman EJ, Beckwith JB, et al. Primary renal synovial sarcoma: molecular and morphologic delineation of an entity previously included among embryonal sarcomas of the kidney. Am J Surg Pathol. 2000;24:1087–96.
141. Arnold MA, Schoenfield L, Limketkai BN, Arnold CA. Diagnostic pitfalls of differentiating desmoplastic small round cell tumor (DSRCT) from Wilms tumor (WT): overlapping morphologic and immunohistochemical features. Am J Surg Pathol. 2014;38:1220–6.
142. Magro G, Longo FR, Angelico G, Spadola S, Amore FF, Salvatorelli L. Immunohistochemistry as potential diagnostic pitfall in the most common solid tumors of children and adolescents. Acta Histochem. 2015;117:397–414.
143. da Silva RC, Medeiros Filho P, Chioato L, Silva TR, Ribeiro SM, Bacchi CE. Desmoplastic small round cell tumor of the kidney mimicking Wilms tumor: a case report and review of the literature. Appl Immunohistochem Mol Morphol. 2009;17:557–62.
144. Gustafson S, Medeiros LJ, Kalhor N, Bueso-Ramos CE. Anaplastic large cell lymphoma: another entity in the differential diagnosis of small round blue cell tumors. Ann Diagn Pathol. 2009;13:413–27.
145. Thyavihally YB, Tongaonkar HB, Gupta S, Kurkure PA, Amare P, Muckaden MA, et al. Primitive neuroectodermal tumor of the kidney: a single institute series of 16 patients. Urology. 2008;71:292–6.
146. Lane BR, Chery F, Jour G, Sercia L, Magi-Galluzzi C, Novick AC, et al. Renal neuroendocrine tumours: a clinicopathological study. BJU Int. 2007;100:1030–5.
147. Argani P, Perlman EJ, Breslow NE, Browning NG, Green DM, D'Angio GJ, et al. Clear cell sarcoma of the kidney: a review of 351 cases from the National Wilms Tumor Study Group Pathology Center. Am J Surg Pathol. 2000;24:4–18.
148. Dumba M, Jawad N, McHugh K. Neuroblastoma and nephroblastoma: a radiological review. Cancer Imaging. 2015;15:5.
149. Shimada H. The international neuroblastoma pathology classification. Pathologica. 2003;95:240–1.
150. Campbell K, Gastier-Foster JM, Mann M, Naranjo AH, Van Ryn C, Bagatell R, et al. Association of MYCN copy number with clinical features, tumor biology, and outcomes in neuroblastoma: a report from the Children's Oncology Group. Cancer. 2017;123:4224–35.
151. Sharma S, Kamala R, Nair D, Ragavendra TR, Mhatre S, Sabharwal R, et al. Round cell tumors: classification and immunohistochemistry. Indian J Med Paediatr Oncol. 2017;38:349–53.
152. Morgenstern BZ, Krivoshik AP, Rodriguez V, Anderson PM. Wilms' tumor and neuroblastoma. Acta Paediatr Suppl. 2004;93:78–84; discussion -5
153. Dome SJ, Millen EM, Argani P. Pediatric renal tumors. In: Orkin SH, Nathan DG, Ginsburg D, Look AT, Fisher DE, Lux SE, editors. Nathan and Oski's hematology and oncology of infancy and childhood. 8th ed. Philadelphia: Elsevier/Saunders; 2015. p. 1714–46.
154. Al-Hussain T, Ali A, Akhtar M. Wilms tumor: an update. Adv Anat Pathol. 2014;21:166–73.
155. Jet Aw S, Hong Kuick C, Hwee Yong M, Wen Quan Lian D, Wang S, Liang Loh AH, et al. Novel karyotypes and cyclin D1 immunoreactivity in clear cell sarcoma of the kidney. Pediatr Dev Pathol. 2015;18:297–304.
156. Karlsson J, Valind A, Gisselsson D. BCOR internal tandem duplication and YWHAE-NUTM2B/E fusion are mutually exclusive events in clear cell sarcoma of the kidney. Genes Chromosomes Cancer. 2016;55:120–3.
157. Franckevica I, Kleina R, Voika O. Originally misdiagnosed rhabdoid tumour of the kidney. A case report and differential diagnosis. Pol J Pathol. 2011;62:163–7.
158. Lee JS, Sanchez TR, Wootton-Gorges S. Malignant renal tumors in children. J Kidney Cancer VHL. 2015;2:84–9.
159. Goyal S, Mishra K, Sarkar U, Sharma S, Kumari A. Diagnostic utility of Wilms' tumour-1 protein (WT-1) immunostaining in paediatric renal tumours. Indian J Med Res. 2016;143:S59–s67.
160. Hong CR, Kang HJ, Ju HY, Lee JW, Kim H, Park SH, et al. Extracranial malignant rhabdoid tumor in children: a single institute experience. Cancer Res Treat. 2015;47:889–96.
161. Geller JI, Roth JJ, Biegel JA. Biology and treatment of Rhabdoid tumor. Crit Rev Oncog. 2015;20:199–216.
162. Delahunt B, Thomson KJ, Ferguson AF, Neale TJ, Meffan PJ, Nacey JN. Familial cystic nephroma and pleuropulmonary blastoma. Cancer. 1993;71:1338–42.
163. Eble JN, Bonsib SM. Extensively cystic renal neoplasms: cystic nephroma, cystic partially differentiated nephroblastoma, multilocular cystic renal cell carcinoma, and cystic hamartoma of renal pelvis. Semin Diagn Pathol. 1998;15:2–20.
164. van den Hoek J, de Krijger R, van de Ven K, Lequin M, van den Heuvel-Eibrink MM. Cystic nephroma, cystic partially differentiated nephroblastoma and cystic Wilms' tumor in children: a spectrum with therapeutic dilemmas. Urol Int. 2009;82:65–70.
165. Bahubeshi A, Bal N, Rio Frio T, Hamel N, Pouchet C, Yilmaz A, et al. Germline DICER1 mutations and familial cystic nephroma. J Med Genet. 2010;47:863–6.
166. Doros LA, Rossi CT, Yang J, Field A, Williams GM, Messinger Y, et al. DICER1 mutations in childhood cystic nephroma and its relationship to DICER1-renal sarcoma. Mod Pathol. 2014;27:1267–80.
167. Stout TE, Au JK, Hicks JM, Gargollo PC. A case of bilateral cystic partially differentiated nephroblastoma vs cystic Wilms' tumor: highlighting a diagnostic dilemma. Urology. 2016;92:106–9.
168. Irtan S, Ehrlich PF, Pritchard-Jones K. Wilms tumor: "state-of-the-art" update, 2016. Semin Pediatr Surg. 2016;25:250–6.
169. Faure A, Atkinson J, Bouty A, O'Brien M, Levard G, Hutson J, et al. DICER1 pleuropulmonary blastoma familial tumour predisposition syndrome: what the paediatric urologist needs to know. J Pediatr Urol. 2016;12:5–10.
170. Schultz KAP, Williams GM, Kamihara J, Stewart DR, Harris AK, Bauer AJ, et al. DICER1 and associated conditions: identification of at-risk individuals and recommended surveillance strategies. Clin Cancer Res. 2018;24:2251–61.
171. Haas JE, Palmer NF, Weinberg AG, Beckwith JB. Ultrastructure of malignant rhabdoid tumor of the kidney. A distinctive renal tumor of children. Hum Pathol. 1981;12:646–57.
172. Hoot AC, Russo P, Judkins AR, Perlman EJ, Biegel JA. Immunohistochemical analysis of hSNF5/INI1 distinguishes renal and extra-renal malignant rhabdoid tumors from other pediatric soft tissue tumors. Am J Surg Pathol. 2004;28:1485–91.
173. Egas-Bejar D, Huh WW. Rhabdomyosarcoma in adolescent and young adult patients: current perspectives. Adolesc Health Med Ther. 2014;5:115–25.
174. Keller C, Guttridge DC. Mechanisms of impaired differentiation in rhabdomyosarcoma. FEBS J. 2013;280:4323–34.
175. Bolande RP, Brough AJ, Izant RJ Jr. Congenital mesoblastic nephroma of infancy. A report of eight cases and the relationship to Wilms' tumor. Pediatrics. 1967;40:272–8.
176. Glick RD, Hicks MJ, Nuchtern JG, Wesson DE, Olutoye OO, Cass DL. Renal tumors in infants less than 6 months of age. J Pediatr Surg. 2004;39:522–5.
177. Sebire NJ, Vujanic GM. Paediatric renal tumours: recent developments, new entities and pathological features. Histopathology. 2009;54:516–28.

178. Ranganathan S. Pediatric renal neoplasms. Surg Pathol Clin. 2009;2:27–60.
179. England RJ, Haider N, Vujanic GM, Kelsey A, Stiller CA, Pritchard-Jones K, et al. Mesoblastic nephroma: a report of the United Kingdom Children's Cancer and Leukaemia Group (CCLG). Pediatr Blood Cancer. 2011;56:744–8.
180. Wang ZP, Li K, Dong KR, Xiao XM, Zheng S. Congenital mesoblastic nephroma: clinical analysis of eight cases and a review of the literature. Oncol Lett. 2014;8:2007–11.
181. Davis CJ Jr, Barton JH, Sesterhenn IA, Mostofi FK. Metanephric adenoma. Clinicopathological study of fifty patients. Am J Surg Pathol. 1995;19:1101–14.
182. Chami R, Yin M, Marrano P, Teerapakpinyo C, Shuangshoti S, Thorner PS. BRAF mutations in pediatric metanephric tumors. Hum Pathol. 2015;46:1153–61.
183. Adeniran AJ, Shuch B, Humphrey PA. Hereditary renal cell carcinoma syndromes: clinical, pathologic, and genetic features. Am J Surg Pathol. 2015;39:e1–e18.
184. Przybycin CG, Magi-Galluzzi C, McKenney JK. Hereditary syndromes with associated renal neoplasia: a practical guide to histologic recognition in renal tumor resection specimens. Adv Anat Pathol. 2013;20:245–63.
185. Kim E, Zschiedrich S. Renal cell carcinoma in von Hippel-Lindau disease-from tumor genetics to novel therapeutic strategies. Front Pediatr. 2018;6:16.
186. Wadt KA, Gerdes AM, Hansen TV, Toft BG, Friis-Hansen L, Andersen MK. Novel germline c-MET mutation in a family with hereditary papillary renal carcinoma. Familial Cancer. 2012;11:535–7.
187. Chen YB, Brannon AR, Toubaji A, Dudas ME, Won HH, Al-Ahmadie HA, et al. Hereditary leiomyomatosis and renal cell carcinoma syndrome-associated renal cancer: recognition of the syndrome by pathologic features and the utility of detecting aberrant succination by immunohistochemistry. Am J Surg Pathol. 2014;38:627–37.
188. Guo J, Tretiakova MS, Troxell ML, Osunkoya AO, Fadare O, Sangoi AR, et al. Tuberous sclerosis-associated renal cell carcinoma: a clinicopathologic study of 57 separate carcinomas in 18 patients. Am J Surg Pathol. 2014;38:1457–67.
189. Gill AJ. Succinate dehydrogenase (SDH)-deficient neoplasia. Histopathology. 2018;72:106–16.
190. Argani P, Zhong M, Reuter VE, Fallon JT, Epstein JI, Netto GJ, et al. TFE3-fusion variant analysis defines specific Clinicopathologic associations among Xp11 translocation cancers. Am J Surg Pathol. 2016;40:723–37.
191. Asch-Kendrick RJ, Shetty S, Goldblum JR, Sharma R, Epstein JI, Argani P, et al. A subset of fat-predominant angiomyolipomas label for MDM2: a potential diagnostic pitfall. Hum Pathol. 2016;57:7–12.
192. Seyam RM, Alkhudair WK, Kattan SA, Alotaibi MF, Alzahrani HM, Altaweel WM. The risks of renal angiomyolipoma: reviewing the evidence. J Kidney Cancer VHL. 2017;4:13–25.
193. Yang P, Cornejo KM, Sadow PM, Cheng L, Wang M, Xiao Y, et al. Renal cell carcinoma in tuberous sclerosis complex. Am J Surg Pathol. 2014;38:895–909.